2019

WHY THE WEIRD WINGS? Investigating the morphology, function, and evolution of unusual feathers in pigeons and doves (Columbidae)

Robert Lawrence Niese
University of Montana, Missoula

Recommended Citation

Niese, Robert Lawrence, "WHY THE WEIRD WINGS? Investigating the morphology, function, and evolution of unusual feathers in pigeons and doves (Columbidae)" (2019). *Graduate Student Theses, Dissertations, & Professional Papers*. 11406.
https://scholarworks.umt.edu/etd/11406

WHY THE WEIRD WINGS?
Investigating the morphology, function, and evolution of unusual feathers in pigeons and doves (Columbidae)

By

ROBERT LAWRENCE NIESE
B.Sc. Biology, University of Puget Sound, Tacoma, WA, 2011

Dissertation
presented in partial fulfillment of the requirements
for the degree of

Doctor of Philosophy
in Organismal Biology, Ecology, and Evolution

The University of Montana
Missoula, MT

Approved by:

Dr. Bret W. Tobalske, Chairperson
Division of Biological Sciences, University of Montana

Dr. Christopher J. Clark
Department of Biology, University of California - Riverside

Dr. Erick Greene
Division of Biological Sciences, University of Montana

Dr. Douglas J. Emlen
Division of Biological Sciences, University of Montana

Dr. H. Arthur Woods
Division of Biological Sciences, University of Montana

Dr. Scott Whittenburg,
Graduate School Dean, University of Montana

TABLE OF CONTENTS

OVERVIEW

Feathers are the most phenotypically diverse (Prum and Brush, 2002; Stoddard and Prum, 2011) and structurally complex (Feo et al., 2015; Prum and Williamson, 2001) integumentary structures in vertebrates. They vary in size, shape, color, structure, and chemical composition between species, between locations on the body, and even within a single feather follicle across an individual's lifetime (Lucas and Stettenheim, 1972). However, some feathers are morphologically conserved and show comparatively little variation across disparate taxa, individual lifespans, and evolutionary time. Remiges, the feathers that make up the majority of the surface area of a wing, are constrained and consequently morphologically stereotyped by the physical demands of flight. This morphological stereotyping by selection on flight ability has shaped the avian Bauplan since the Jurassic, and paleornithologists have used the presence of these specialized, asymmetrical feathers to define the origins of flight in the fossil record (Feduccia and Tordoff, 1979). In modern birds, this morphology is required for effective and efficient flight (Hedenström, 2003), and birds go to great lengths to compensate for, and recover from the impacts of a reduction in overall wing surface area caused by feather damage or loss (DesRochers et al., 2009; Echeverry-Galvis and Hau, 2013; Hedenström, 2003; Swaddle et al., 1996).

In comparison, the feathers of the tail (the rectrices), which are also typically aerodynamically specialized and asymmetrical, are released from the constraints of locomotion by "hiding in the wake" of the flying bird (Askew, 2014; Clark, 2010; Clark and Dudley, 2009). This has allowed rectrices to evolve atypical and extreme morphologies dozens, if not hundreds of times (Clark and Dudley, 2009) that function as sexually selected visual signals (e.g.

widowbirds, *Euplectes*; pheasants, Phasianinae; hummingbirds, Trochilidae; etc.; Andersson, 1992; Clark and Dudley, 2009). In the feathers of the wing, conversely, remex morphologies have been modified for sexually selected visual signals in only three species, where, in the Great Argus (*Argusianus argus*) for example, these dramatically elongated feathers “almost entirely deprive the bird of flight” (Darwin, 1871, 259).

Yet, in spite of this morphological and functional stereotyping for flight ability among the feathers of the wing, some species do possess remiges that deviate from typical aerodynamic forms (Fig. 1). Historically, this variation in remex morphology has been attributed to unique aerodynamic specializations of the wing such as those that increase soaring efficiency or take-off efficacy (Fig. 1A,B; Averill, 1927; Drovetski, 1996). These morphologies are rarely considered “extreme” and can be found in hundreds of disparate taxa (Klaassen van Oorschot et al., 2017) and are, perhaps, not “specialized morphologies”. More rarely, birds can also possess morphologies that are striking, sexually dimorphic, and, often, unique to a species or clade (Fig. 1C). Recent research suggests that these particular morphologies are the result of selection for locomotion-induced acoustic signals, or sonations, that are produced in sexually selected displays (Clark and Prum, 2015). In some species, however, conspicuous atypical remex morphologies exist in both sexes and do not appear to play an obvious role in sexually selected displays (Fig. 1D,E). These morphologies are not subtle and have captured the attention of naturalists for centuries (Cuvier, 1817a; Selby, 1850; Swainson, 1825), and yet, outside of this dissertation, only one such feather has been rigorously tested to determine the function of its unusual morphology (Murray et al., 2017).

Atypical remiges that are sexually monomorphic, especially those in an otherwise sexually dimorphic or ornamented species, are likely shaped by natural selection and two hypotheses exist to explain their evolution. First, an aerodynamic hypothesis suggests that morphologies evolve as specialized devices that improve aerodynamic performance during specific modes of flight. The alula, for example, acts as a high-lift device, generating vortices over the wing to prevent flow separation during low advance ratio flight such as take-off or landing (Lee et al., 2015). Alternatively, atypical feathers may serve an aeroacoustic signaling function, producing sonations. Naturally selected sonations are only known to occur in one species (Crested Pigeon, *Ocyphaps lophotes*; Murray et al., 2017) but have been hypothesized to exist in dozens (e.g. Barrera et al., 2011; Coleman, 2008; Craig, 1911a; Craig, 1911b; Johnston, 1960; Johnston, 1961; Townsend, 1915; Wetmore, 1920). Finally, atypical remex morphologies may have evolved through a complex interplay between selection on aerodynamic performance as well as a non-aerodynamic function, as is known to have occurred in Hirundinae swallows where both natural and sexual selection influence rectrix length (Rowe et al., 2001).

Similarly, many species lack dramatic feather modifications, but are known to produce peculiar sounds during locomotion – sounds that are involved in sexually selected displays (e.g. Barrow's Goldeneye, Bucephala islandica, Anatidae; Clark and Prum, 2015; African broadbills, *Smithornis spp.*, Eurylaimidae; Clark et al., 2016) or are otherwise hypothesized to be communicative (e.g. Mourning Doves, *Zenaida macroura*, Columbidae; Coleman, 2008). These cryptically sonating feathers may provide insight regarding the evolutionary steps by which typical, aerodynamically optimized feathers become atypical signaling structures.

Given the powerful and constraining nature of aerial locomotion, my dissertation seeks to address how and why remiges evolve away from an aerodynamically stereotyped function and morphology. Specifically, I investigate the link between morphology, sound production, and aerodynamic performance in the primary feathers of a diverse, but closely related clade – the Columbidae – and test feathers according to the two hypotheses outlined above.

In Chapter 1, I examine atypical remiges unique to a small, evolutionarily distinct group of New World ground doves, the Peristerinae, and test their function as specialized acoustic signaling structures. I utilize publicly available, citizen scientist-curated collections of audio recordings to compare wing sounds produced experimentally by museum specimens to those produced by live birds in the wild. My findings in this Chapter indicate that these unique remiges are specialized, sonating structures that likely function as alarm signals or as mutually-selected sexual signals. These experiments provide robust support for the aeroacoustic signaling hypothesis of remex shape evolution.

In Chapter 2, I investigate an atypical remex morphology found in many, distantly related groups of pigeons and doves which has been the subject of two centuries of speculation. Here, I test its function as a specialized acoustic signaling structure and a specialized aerodynamic device and evaluate its evolution across the entire family in its relation to foraging habits, determining that the feather does not sonate, but instead improves aerodynamic performance. The performance benefits conferred by this specialized remex are particularly dramatic in emulated low advance-ratio flapping (i.e. take-off and landing), but also improve efficiency in emulated gliding or low wingbeat-amplitude cruising. This work provides robust support for the specialized aerodynamic device hypothesis of remex shape evolution.

Lastly, in Chapter 3, I focus on a species that has long been hypothesized to sonate with its wings (the Rock Pigeon, *Columba livia*), but which lacks obviously specialized remex morphologies. In this chapter, I analyze over 2000 morphometric data points and perform experiments on individual feathers and live birds to determine that a small change to the trailing vane of the outermost remex produces feathers that reliably sonate, but at a cost to aerodynamic performance. The aerodynamic and aeroacoustic behavior of this subtle remex morphology and the trade-off between the two may inform our understanding of how feathers transition from aerodynamically stereotyped forms to specialized acoustic signaling structures.

Asymmetrical feathers specialized for aerial locomotion were a critical evolutionary transition in the avian lineage. The selective pressures that stereotype these morphologies are so powerful that, even in taxa separated by nearly 80 million years of evolution (Jetz et al., 2012) and three orders of magnitude in body mass, primary feathers differ only in size (Fig. 2A,B). Understanding how and why some taxa evolve feathers that deviate from, or entirely circumvent this constraint on remex morphology (Fig. 2C,D) elucidates the mechanisms by which Aves has diversified. Furthermore, through investigating the mechanisms by which "occasional and accidental sounds" (e.g. the sounds of feathers flapping) become communicative signals I am probing the evolutionary origins of acoustic communication (Darwin, 1871), an endeavor which may even influence our understanding of the evolution of human language (Larsson, 2014).

Overall, this work combines centuries-old hypotheses, modern aerodyanimcs, and new signaling theories using innovative techniques that utilize recently developed and underappreciated scientific data resources (e.g. public animal sound archives, spread wing collections). Studies with a suite of characteristics such as these have the potential to garner broader public appreciation, and, in this case, may highlight a charismatic, but poorly known clade of birds, many of which are endemic and/or endangered. And lastly, this study finally addresses a research recommendation from William Swainson in which, upon discovering that pigeon species in Brazil, Africa, and Australia all possessed the same strange P10 feathers, he states “these quill feathers, which in some are very peculiar and [are] connected with the powers of loco-motion, deserve our attention,” (1825, 473).

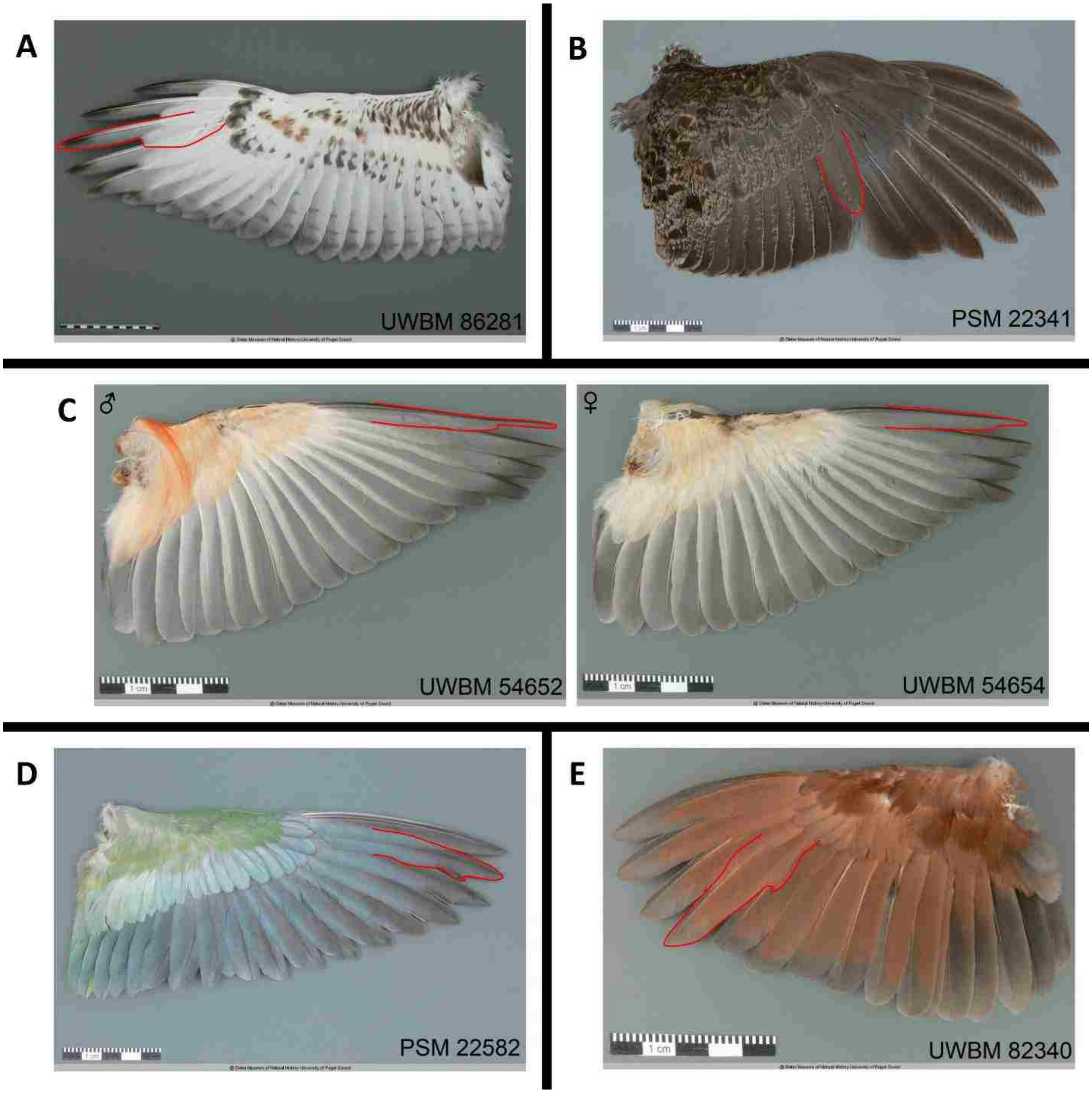

FIGURE 1. Spread wing specimens from the Slater Museum of Natural History's Digital Wing and Tail Image Collection. (A) Ferruginous Hawk (*Buteo regalis*; Falconiformes, Accipitridae) with prominent wing slotting (i.e. feather emargination) which improves aerodynamic efficiency in gliding and flapping. (B) Spruce Grouse (*Falcipennis canadensis*; Galliformes, Phasianidae) with a "notch" created by a modified S1 (shortened) that improves take-off performance in most galliforms. (C) Scissor-tailed Flycatchers (*Tyrannus forficatus*; Passeriformes, Tyrannidae;

male left, female right) with sexually dimorphic outermost primaries that produce tones during male display flights. (D) Monk Parakeet (*Myiopsitta monachus*; Psittaciformes, Psittacidae) with modified outer primary tips that are apparently sexually monomorphic, but have never been investigated. Similar morphologies can be found throughout Psittacidae. (E) Common Ground Dove (*Columbina passerina*; Columbiformes, Columbidae) with a modified P7 characteristic of members of this genus (see Chapter 2). High resolution images of all wings are available online <http://digitalcollections.pugetsound.edu/cdm/search/collection/slaterwing>.

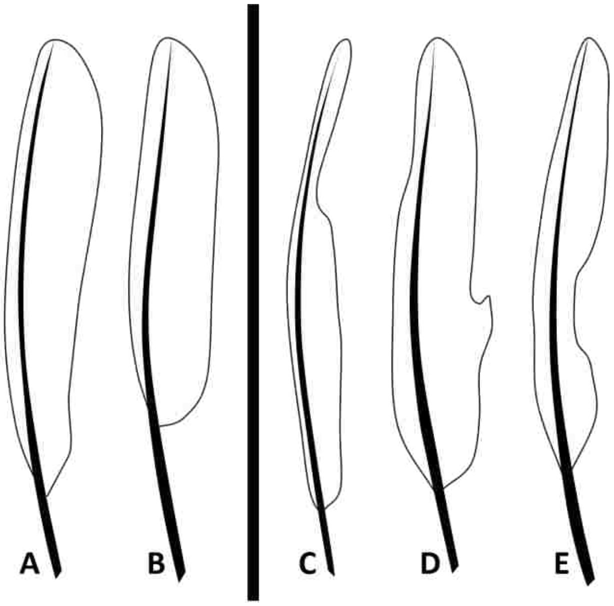

FIGURE 2. Primary feathers can be aerodynamically stereotyped (A, B), but occasionally display unique morphologies (C, D, E). (A) P6 feather in the House Finch (*Haemorhous mexicanus*; Passeriformes, Fringillidae). (B) P6 feather in the Trumpeter Swan (*Cygnus buccinator*; Anseriformes, Anatidae). (C) P10 feather in the Yungas Dove (*Leptotila megalura*; Columbiformes, Columbidae). (D) P7 feather in the Common Ground Dove (*Columbina passerina*; Columbiformes, Columbidae). (E) P8 feather in the Pink-necked Green Pigeon (*Treron verans*; Columbiformes, Columbidae). All feathers scaled to be similar heights.

REFERENCES

Andersson, S. (1992). Female preference for long tails in lekking Jackson's widowbirds: experimental evidence. *Anim. Behav.* **43**, 379–388.

Askew, G. N. (2014). The elaborate plumage in peacocks is not such a drag. *J. Exp. Biol.* **217**, 3237–3241.

Averill, C. K. (1927). Emargination of the Long Primaries in Relation to Power of Flight and Migration. *Condor* **29**, 17–18.

Barrera, J. P., Chong, L., Judy, K. N. and Blumstein, D. T. (2011). Reliability of public information: Predators provide more information about risk than conspecifics. *Anim. Behav.* **81**, 779–787.

Clark, C. J. (2010). Effects of tail length on an escape maneuver of the Red-billed Streamertail. *J. Ornithol.* **152**, 397–408.

Clark, C. J. and Dudley, R. (2009). Flight costs of long, sexually selected tails in hummingbirds. *Proc. R. Soc. B Biol. Sci.* **276**, 2109–15.

Clark, C. J. and Prum, R. O. (2015). Aeroelastic flutter of feathers, flight, and the evolution of nonvocal communication in birds. *J. Exp. Biol.* **218**, 3520–3527.

Clark, C. J., Kirschel, A. N. G., Hadjioannou, L. and Prum, R. O. (2016). Smithornis broadbills produce loud wing song by aeroelastic flutter of medial primary wing feathers. *J. Exp. Biol.* **219**, 1069–1075.

Coleman, S. W. (2008). Mourning dove (Zenaida macroura) wing-whistles may contain threat-related information for con- and hetero-specifics. *Naturwissenschaften* **95**, 981–6.

Craig, W. (1911a). The Expressions of Emotion in the Pigeons. III. The Passenger Pigeon (Ectopistes migratorius Linn.). *Auk* **28**, 408–427.

Craig, W. (1911b). The Expressions of Emotion in the Pigeons. II. The Mourning Dove (Zenaidura macroura Linn.). *Auk* **28**, 398–407.

Cuvier, G. (1817). *The Animal Kingdom: Arranged According to Its Organisation*. Paris: Wm. S. Orr and Company.

Darwin, C. (1871). *The Descent of Man and Selection in Relation to Sex*.

DesRochers, D. W., Reed, J. M., Awerman, J., Kluge, J. A., Wilkinson, J., van Griethuijsen, L. I., Aman, J. and Romero, L. M. (2009). Exogenous and endogenous corticosterone alter feather quality. *Comp. Biochem. Physiol. - A Mol. Integr. Physiol.* **152**, 46–52.

Drovetski, S. (1996). Influence of the trailing-edge notch on flight performance of galliforms. *Auk* **113**, 802–810.

Echeverry-Galvis, M. A. and Hau, M. (2013). Flight Performance and Feather Quality: Paying the Price of Overlapping Moult and Breeding in a Tropical Highland Bird. *PLoS One* **8**,.

Feduccia, A. and Tordoff, H. B. (1979). Feathers of archaeopteryx: Asymmetric vanes indicate aerodynamic function. *Science (80-.).* **203**, 1021–1022.

Feo, T. J., Field, D. J. and Prum, R. O. (2015). Barb geometry of asymmetrical feathers reveals a transitional morphology in the evolution of avian flight. *Proc. R. Soc. B Biol. Sci.* **282**, 20142864.

Hedenström, A. (2003). Flying with holey wings. *J. Avian Biol.* **34**, 324–327.

Jetz, W., Thomas, G. H. H., Joy, J. B. B., Hartmann, K. and Mooers, a. O. O. (2012). The global diversity of birds in space and time. *Nature* **491**, 1–5.

Johnston, R. F. (1960). Behavior of the Inca dove. *Condor* **62**, 7–24.

Johnston, R. F. (1961). The genera of American ground doves. *Auk* **78**, 372–378.

Klaassen van Oorschot, B., Tang, H. K. and Tobalske, B. W. (2017). Phylogenetics and ecomorphology of emarginate primary feathers. *J. Morphol.* **278**, 936–947.

Larsson, M. (2014). Self-generated sounds of locomotion and ventilation and the evolution of human rhythmic abilities. *Anim. Cogn.* **17**, 1–14.

Lee, S., Kim, J., Park, H., Jabłoński, P. G. and Choi, H. (2015). The Function of the Alula in Avian Flight. *Sci. Rep.* **5**, 9914.

Lucas, A. M. and Stettenheim, P. R. (1972). *Avian anatomy: integument*. Washington D.C.: United States Department of Agriculture; Agriculture handbook, no. 362.

Murray, T. G., Zeil, J. and Magrath, R. D. (2017). Sounds of Modified Flight Feathers Reliably Signal Danger in a Pigeon. *Curr. Biol.* **27**, 3520–3525.e4.

Prum, R. O. and Brush, A. H. (2002). The evolutionary origin and diversification of feathers. *Q. Rev. Biol.* **78**, 275–301.

Prum, R. O. and Williamson, S. (2001). Theory of the growth and evolution of feather shape. *J. Exp. Zool.* **291**, 30–57.

Rowe, L. V., Evans, M. R. and Buchanan, K. L. (2001). The function and evolution of the tail streamer in hirundines. *Behav. Ecol.* **12**, 157–163.

Selby, P. J. (1850). The Natural History of Gallinaceous Birds: Columbidae or Pigeons. In *The Naturalist's Library: Ornithology* (ed. Jardine, W.), Lizars, W. H.), Smith, C. H.), and Stewart, J.), p. London: W. H. Lizars.

Stoddard, M. C. and Prum, R. O. (2011). How colorful are birds? Evolution of the avian plumage color gamut. *Behav. Ecol.* **22**, 1042–1052.

Swaddle, J. P., Witter, M. S., Cuthill, I. C., Budden, A. and McCowen, P. (1996). Plumage Condition Affects Flight Performance in Common Starlings: Implications for Developmental Homeostasis, Abrasion and Moult. *J. Avian Biol.* **27**, 103–111.

Swainson, W. (1825). On the characters and natural affinities of several birds from Australia; including some observations on the Colulmbidae. *Zool. J.* **1**, 463–484.

Townsend, C. W. (1915). Notes on the Rock Dove (Columba domestica). *Auk* **32**, 306–316.

Wetmore, A. (1920). Observations on the Habits of the White-Winged Dove. *Condor* **22**, 140–146.

CHAPTER 1

Unique feathers produce sonations during flight in *Columbina* ground doves

Robert L. Niese[1], Christopher J. Clark[2], and Bret W. Tobalske[1]

[1] Field Research Station at Fort Missoula, Division of Biological Sciences, University of Montana, Missoula, MT 59812, USA

[2] Department of Evolution, Ecology, and Organismal Biology, University of California Riverside, CA 92521, USA

ABSTRACT

Primary feather morphology is constrained by the physical demands of flight, yet is strikingly diverse within a subfamily of New World ground doves (Peristerinae). Members of the genus *Columbina* specifically possess modified P7 feathers which have been hypothesized to serve a signaling function via sonations produced during flight. We test the sound-producing capabilities of P7 feathers from three species (*C. inca*, *C. passerina*, and *C. talpacoti*) in an aeroacoustic wind tunnel and find that they readily produce buzzing sounds that are similar to those observed in wild birds. Buzzes are produced as a modified region of barbs on P7 flutters and collides with the adjacent P6 at rates between 200 and 400Hz, producing broadband sounds in a rapid buzz. In *C. inca,* juvenile birds often lack the morphologies present in adults, producing significantly quieter buzzes. While we can only speculate as to the communicative

significance of these buzzes in *Columbina*, we can confidently conclude that they are indeed sonations due to the presence of a modified morphology in P7 that is specialized for sound production. This morphology is found in all members of the genus *Columbina*, to varying degrees, and may be involved in mutual mate choice or, as has been demonstrated for other pigeons and doves, may be a signal of alarm.

INTRODUCTION

Feathers are the most phenotypically diverse (Prum and Brush, 2002; Stoddard and Prum, 2011) and structurally complex (Feo et al., 2015; Prum and Williamson, 2001) integumentary structures in vertebrates. They vary in size, shape, color, structure, and chemical composition between species, between locations on the body, and even within a single feather follicle across an individual's lifetime (Lucas and Stettenheim, 1972). But not all feathers vary to the same degree across species. Remiges, for example, are morphologically conserved and show comparatively little variation across disparate taxa, individual lifespans, and evolutionary time (Feo et al., 2015; Heers and Dial, 2012; Prum and Brush, 2002). These feathers, which make up the majority of the surface area of a wing in volant species, are constrained and consequently morphologically stereotyped by the physical demands of flight (e.g. Bachmann et al., 2012; Ennos et al., 1995; Swaddle et al., 1996). Therefore, feathers that diverge from aerodynamically stereotyped forms may be evidence of functional specializations other than flight.

Primary and secondary feathers (collectively, the remiges) can dramatically deviate from aerodynamically stereotyped shapes in three ways: as sexually selected visual signals, as specialized sonation-producing structures, and as specialized aerodynamic devices. Remex shape has been modified to function in sexually selected visual signals in only three species of birds – the Great Argus (*Argusianus argus*, Phasianidae) and two species of nightjars (*Caprimulgus longipennis* and *C. vexillarius*, Caprimuligidae). Conversely, selection on the remiges to produce non-vocal acoustic signals, or sonations, is common (Clark and Prum, 2015) and has resulted in diverse, specialized morphologies such as those in the Club-winged Manakin

(*Machaeropteris deliciosus,* Pipridae; Bostwick et al., 2010), Crested Pigeon (*Ocyphaps lophotes*; Murray et al., 2017), American Woodcock (*Scolopax minor*, Scolopacidae; Clark and Prum, 2015), Scissor-tailed Flycatcher (*Tyrannus forficatus,* Tyrannidae; Clark and Prum, 2015), and others. Most sonations produced by remiges are part of sexually selected displays and their associated morphologies are often sexually dimorphic (Clark, 2018; Clark and Prum, 2015), but remiges can also be specialized for a naturally-selected sonation (alarm signals) that is performed by both sexes (e.g. Murray et al., 2017). Lastly, it has been hypothesized (Goodwin, 1983; Mahler and Tubaro, 2001) that remex morphology may become dramatically modified as a specialized aerodynamic device with functions akin to slotted primaries (KleinHeerenbrink et al., 2017) or the alula (Lee et al., 2015), but such morphologies have never been tested.

Modified remex morphologies are particularly common among the pigeons and doves (Columbidae) where birds known to produce naturally-selected sonations with unique remiges (Murray et al., 2017), and nearly a quarter of all species in the clade possess a modified outermost remex (P10) that could be a specialized aerodynamic device (Goodwin, 1983; Mahler and Tubaro, 2001). Unlike sonations among birds broadly, sexually selected sonations involving modified remiges are not known to exist among pigeons and doves, and remex modifications are not known to be sexually dimorphic. For more than two centuries, naturalists have speculated on the function of several particularly striking feather morphologies among the pigeons and doves (Cuvier, 1817b; Selby, 1850; Swainson, 1825), but, to date, feather function has only been tested in one species (Murray et al., 2017).

New World ground doves (Peristerinae; Pereira et al., 2007; Sweet et al., 2017) possess several unique remex morphologies, and species in the clade can have one, two, three, or even four modified feathers of different shapes. In some species, these feathers are thought to be specialized aerodynamic devices (Goodwin, 1983), while others, specifically in feathers that are more proximal on the wing (i.e. P7 and P6), have been hypothesized to produce sonations (Johnston, 1960; Johnston, 1961). The largest genus in this clade, *Columbina*, has eight members which possess several forms of a modified P7 feather, and, in some species, an additional modified P6. The critically endangered and phenotypically distinct *C. cyanopis* has traditionally been included in this genus, but due to its rarity and a lack of genetic and morphological data on the species, we have excluded it from this study. In several species, these modified feathers are striking and appear to be unique to the genus, but their function is unknown.

Columbina ground doves, like many other pigeons and doves, produce curious wing-sounds during flight. For centuries, columbid wing sounds have intrigued naturalists and many have hypothesized that they might serve a communicative function (Audubon, 1870; Craig, 1911a; Selby, 1850; Wetmore, 1920; Wilson, 1808). *Columbina* doves specifically produce a unique buzzing sound during flight (Audio 1). The physical cause of these sounds and their function (if any) are unknown, but the presence of highly modified primary feathers in the clade has led some to speculate that the two are linked (Johnston, 1960; Johnston, 1961). Here, we test these modified feathers in *Columbina* ground doves to determine their ability to produce such buzzing wing sounds. Using dried spread wing specimens from the University of Washington's Burke Museum, we recorded the acoustic and kinematic behavior of feathers as they produced sounds in an aeroacoustic wind tunnel (Clark and Mistick, 2018a). Then, we compared the acoustic qualities of sounds recorded in the wind tunnel to sounds produced by wild birds in flight using recordings from XenoCanto.org and the Macaulay Library of Sound. Lastly, we investigated the evolution and prevalence of these morphologies and inferred ancestral states of P7 shape across the genus.

MATERIALS AND METHODS

Dried spread wings in an aeroacoustic wind tunnel

We selected dried spread-wing specimens from the University of Washington’s Burke Museum to test in an aeroacoustic wind tunnel at the University of California – Riverside (for detailed specifications regarding the wind tunnel design and performance, see Clark and Mistick, 2018). All specimens were from adult birds, possessed intact and fully-grown outermost primary feathers (P10-P5), and were each from a different individual (*Columbina passerina* n=4; *Columbina talpacoti* n=7; *Columbina inca* n=4; Table S1). Morphologies were superficially similar between the sexes (as has been reported in greater detail for other related species; Murray et al., 2017; Niese and Tobalske, 2016), and we assumed them to be monomorphic for the remainder of the study. We additionally tested the sound-producing capabilities of four wings from juvenile Inca Doves (aged according to the degree of atrophy in the bursa of Fabricius), which we analyzed separately due to reports that they may produce quieter wing sounds and may possess fewer modified primaries than adult birds (Johnston, 1960).

Wings were clamped at the exposed humerus to a small metal rod extending from a tripod into the working section of the wind tunnel. The tripod allowed for isolated rotations relative to flow about the vertical (sweep angle; β; where β is zero when the leading edge of the arm-wing is perpendicular to flow) and lateral (angle of attack; α; where α is zero when the line between the wrist and S1 is parallel to flow) axes. Wings were freely reoriented until they reliably produced wing sounds, which typically occurred when β was approximately 75° and α was approximately -45°. These orientations seem to most closely emulate those observed in the upstroke of similarly-sized Columbids (Crandell and Tobalske, 2015; see Discussion). Tunnel flow velocity (measured as in Clark and Mistick, 2018) was set to roughly correspond to the peak wingtip velocity of the third wingbeat cycle after take-off, as observed in free-flying Diamond Doves (*Geopelia cuneata*; 9.9±1.3ms^{-1} for 40g birds; Crandell and Tobalske, 2015).

In the Inca Dove, where modified feather morphology is superficially more subtle, we performed simple silencing experiments to determine the role that each modified feather plays in contributing to buzzing sounds. We used acid-neutral, removable painter's tape (3M Scotch-Blue^{TM} Painter's Tape #2090, 3M Corporate Headquarters, 3M Center St. Paul, MN, USA), cut to sizes that covered the middle of two adjacent feathers (i.e. between 20 and 70% of their lengths, covering the entire modified region in P7), in order to eliminate flutter in both feathers (Supplemental Video1). All adjacent pairs of feathers, from P10 to P5 (i.e. P10 and P9, P9 and P8, P8 and P7, etc.), were taped, one pair at a time, and video and audio recorded of each (see below). Using a similar method, we taped all primaries except for groups of three adjacent feathers (P10-8, P8-P6, and P7-P5), again recording audio and video. For all of these experiments, wing sound loudness was calculated relative to the sound of the wind tunnel when the wing was removed from flow (i.e. a unitless measurement of relative loudness).We performed taping experiments on three wings: one adult male, one adult female, and one juvenile (UWBM48439, UWBM80050, and UWBM48320 respectively). This particular juvenile lacked a modified P6 feather which influenced the ways we interpreted taping experiments (see Table S4). Including a juvenile in these analyses demonstrates the power of these experiments, such that, even in a juvenile bird which we expect to produce quieter wing sounds overall, taping certain feathers creates a measurable decrease in buzz loudness (see Results).

High speed video was collected using a Photron FASTCAM SA-3 camera (Photron USA Inc., San Diego, CA, USA; using PFV v.3282 Software) recording at 6000fps with a 1/15000s shutter speed to a laptop computer. Audio was recorded to the same laptop at 24-bits and sampling at 48kHz through an audio interface (Raven Pro, v.1.4, Cornell Lab of Ornithology Bioacoustics Research Program, Ithaca, NY, USA) and preamplifier (Roland QUAD-CAPTURE UA-55, Roland Corporation, Hamamatsu, Japan) using a 0.5in free-field microphone (Brüel & Kjaer 4190, Naerum, Denmark) with a turbulence-reducing nose cone (B&K UA 0386). The microphone was placed approximately 10cm downstream, but not within the wake of the wings (see Clark et al. 2013).

Wing sounds from the field

Recordings of birds in flight were acquired from XenoCanto.org and the Macaulay Library of Sound (Table S2). In total, we acquired three recordings of the Common Ground Dove, four recordings of the Inca Dove, and two recordings of the Ruddy Ground Dove. Within each recording, we identified and characterized (see below) two to seven buzz elements per wingbeat and averaged the frequency of those elements across each wingbeat. For some analyses, we collapsed these average buzz frequencies per wingbeat into an overall average for a given recording to eliminate the pseudoreplicated effect of comparing recordings with differing numbers of elements per wingbeat, and wingbeats per flight for a given individual (i.e. recording).

To characterize these wing sounds consistently and rigorously across multiple recordings from different recordists with different equipment, recording conditions, and post-processing techniques, we analyzed wing sounds using a novel, self-correcting method that utilized repeated, time-sensitive measurements. Sounds that are characterized as “buzzes” in nature are typically a series of rapidly repeating broadband elements (e.g. shuttle display buzzes in Calliope Hummingbirds, *Stellula calliope*; Clark, 2011). These elements can be described from a time-sensitive perspective that resolves individual elements, or from a frequency-sensitive perspective that instead describes the rate of element repetition (Charif et al., 2010, Appendix B for a detailed discussion). In frequency-sensitive analyses, the rate of element repetition becomes the fundamental frequency of the sound, which can be measured in Raven using the “peak frequency” function. However, for low rates of element repetition (e.g. <600Hz), other low-frequency ambient sounds common to audio recordings from the field (i.e. wind, vehicles on roadways, motors, flowing water, etc.) often overlap with the “peak frequency” of these repeating elements, making frequency-sensitive analyses unreliable (Araya-salas et al., 2017). A time-sensitive analysis allows us to visualize each broadband element as it repeats, and distinguishes tonal sounds from atonal (i.e. broadband) sounds by the breadth (i.e. height) of their frequency bands. However, at extremely time-sensitive resolutions, all sounds begin to appear broadband. Therefore, we utilized a spectrum of time-sensitive parameters specific to the rates of repetition we observed in flapping feathers in the wind tunnel (see above), effectively eliminating elements that appear broadband as an artifact of spectrogram resolution (i.e. self-corrected artifact elimination). Specifically, all spectrograms were analyzed with a DFT frequency grid size of 2048 samples and a time grid overlap of 50%, but Hann window sizes varied temporally by 20-sample increments from 70 to 150 samples. These parameters provided a spectrum of temporal sensitivity that allowed us to fully resolve broadband elements that repeat at rates of 685Hz (at 70 samples) or less. To our knowledge, an analysis routine such as this has not been performed for biological sounds in the past, and we propose that it is a valuable method for confidently characterizing buzzes from a diverse set of recordings such as those available in ever-growing online public libraries of sound and video.

P7 throughout the genus *Columbina*

We surveyed additional spread wing specimens and photographs from the Burke Museum, and University of Alaska Museum, supplemented with images of live birds in-the-hand, to roughly characterize the P7 morphologies across the genus (Table S3). For *C. picui*, and *C. squammata* P7 morphology was determined from photographs of birds in-the-hand provided by Paul Smith (http://www.faunaparaguay.com/columbina_picui.html) and Raphael Igor Dias (Amorim and Dias, 2019), respectively. For the remaining six species, P7 morphology was determined from museum specimens. All eight members of *Columbina* (excluding *C. cyanopis*, as previously mentioned) possess modified P7 feathers, so we further categorized morphologies into three groups based on the size and shape of their modified regions (Figure 1; Table S3). Using a phylogram built from trees estimated from mitochondrial and nuclear loci and published by Sweet and others (2017), we inferred the maximum likelihood of the ancestral state of P7 given the three forms that we had identified in *Columbina*. Outside of *Columbina*, P7 feathers appear to be typical, aerodynamically stereotyped shapes (except, perhaps in *Claravis mondetoura*; see Discussion) and we included fourteen such species in our analyses: eight within the subfamily of New World ground doves (Peristerinae), and six as outgroups. P7 morphology for these species was described from spread wing and feather specimens (Table S3) from the Burke Museum, Slater Museum, University of Alaska Museum, and from

Featherbase, an online digital collection of feather specimens (www.featherbase.info/), except for three species (*Uropelia campestris, Claravis mondetoura*, and *Claravis geoffroyi*) for which high quality material could not be located (see Discussion). We performed our analyses in Mesquite v.3.5 (Maddison and Maddison, 2018) and inferred the maximum likelihood of ancestral states using an Mk1 rate model (Lewis, 2001) for trait evolution.

Statistical Analyses

All statistical analyses (except ancestral state reconstructions, above) were performed in IBM SPSS Statistics v.24 (IBM Corp. Released 2016. Armonk, NY, USA) on data that did not violate assumptions of normalcy.

RESULTS

Modified remex morphologies in *Columbina*

All members of the genus *Columbina* (excluding *C. cyanopis*, as mentioned previously) appear to have P7 feathers that are modified in similar ways. Specifically, all P7 feathers show a distinct elongation and narrowing of barbs in the midregion of the trailing vane (e.g. between 20 and 70% of its length; Figure 1). In some species (see below), these modified barbs create a large “recurved lobe” (Johnston, 1961, 373) that dramatically alters the gross morphology of the feather (i.e. the feather “silhouette”), while in others, the barbs are similarly modified, yet do not dramatically alter the feather’s overall shape (Figure 1). Across all eight species surveyed, we classified P7 feathers according to the degree to which these barb modifications influenced overall feather shape. In *C. inca*, *C. squammata*, and *C. cruziana*, modified barbs generate a subtle change to the P7 gross morphology which we classified as *inca*-like (Figure 1D). In *C. talpacoti* and *C. buckleyi*, modified barbs create a dramatic recurved region, nearly doubling the width of the trailing vane at its widest point in some individuals (Figure 1F). We classified this shape as *talpacoti*-like. In *C. passerina*, *C. picui*, and *C. minuta*, P7’s overall shape is similar to the *talpacoti*-like feathers, but to a lesser extent (Figure 1E), which we classified as *passerina*-like.

In adult *C. inca* and *C. squammata*, modifications are present in both P7 and P6 (see below). All other species appear to have modifications in P7 only, with a few rarer instances of modifications also appearing in P6 in *C. talpacoti* (e.g. UWBM84051; Fig. 1B), *C. passerina,* and in other members of the genus, though reports are vague (Goodwin, 1983; Johnston, 1961).

Dried spread wings in an aeroacoustic wind tunnel

Columbina passerina specimens possess a single modified feather (P7) with a protrusion of elongated barbs (Figure 1A,E) which fluttered at 260±10Hz (Figure 2), causing the protruding region of the trailing vane of P7 to collide with P6 to produce a buzz (Video 1). *C. talpacoti* wings also have a modified P7 feather (Figure 1B,F) which fluttered at 250±30Hz (Figure 2), producing very similar sounds. For both species, there was a 1:1 match between the motion of feather flutter and the broadband acoustic signature of buzz sounds. In other words, audio and video recordings are simply different methods of observing the same physical phenomenon (Figure 2).

In *C. inca*, adult birds possess modified P7 and P6 feathers (Figure 1D) which buzzed at 350±40Hz and 340±10Hz respectively (Figure 2). This flutter appears to cause collisions between adjacent feathers (as above) to produce buzzes. To confirm this link between feather flutter and buzz sounds, we performed taping experiments (see Table S4 for a summary of taping manipulations and groupings) and determined that the relative loudness of buzzes depends on which modified feathers are fluttering (ANOVA; $F=12.59$, $df=3,24$, $p<0.01$). Specifically, wing sounds were loudest whenever P7 was freely fluttering (+P7/+P6 and +P7/-P6; Figure 3; Table S5). The sounds generated by P7 and P6 fluttering together (+P7/+P6) were not significantly louder than those produced by P7 alone (+P7/-P6; Figure 3; $p=0.76$). Wing sounds were quietest when neither P7 nor P6 (-P7/-P6) were fluttering (Figure 3; Table S5). Wing sounds produced whenever P6 but not P7 was fluttering (-P7/+P6) were of intermediate loudness (Figure 3; ANOVA and Tukey HSD post-hoc tests for all the above comparisons are summarized in Table S5).

In juvenile *C. inca* individuals, three of four specimens lacked obvious modifications in P6 and one individual lacked obvious modifications in P7 as well as P6. In juveniles that possessed a modified P7, feathers fluttered at a rate of 410±50Hz Adult birds produced significantly louder buzzes than juvenile birds relative to background tunnel noise (t=2.56, d.f.=6, p=0.04), but P7 feathers in both adults and juveniles fluttered at the same rate (t=-1.51, d.f.=5, p=0.19; mean buzz frequencies for adults and juveniles designated as * and × respectively in Figure 2).

Across all adult wings for all three species, buzz sounds were of similar loudness regardless of species or sex (two-way ANOVA; F_{sex}=0.39, d.f.=1,15, p=0.55; $F_{species}$=0.75, d.f.=1,15, p=0.50; $F_{sex*species}$=0.10, d.f.=1,15, p=0.91).

Wing sounds from the field

Recordings of *C. passerina* flights from the field contained a total of 23 wingbeats with an average of 4.1±1.2 buzz elements per wingbeat. Buzzes in wild *C. passerina* were 310±30Hz, significantly faster than the 260Hz buzzes recorded in the wind tunnel (t=5.66, d.f.=5, p=0.002; Figure 2). Buzz elements were not detected in our analyses of recordings of wild *C. talpacoti* in take-off, which instead produced loud, atonal claps that may obscure the presence of buzzes (see Discussion). Buzzes were an obvious feature of *C. inca* flights and, across all recordings, we observed 20 wingbeats with an average of 3.4±1.0 elements per wingbeat. Buzzes in wild *C. inca* flights were produced at 350±50Hz and were not significantly different from those recorded in the wind tunnel for adults alone (t=0.2, d.f.=6, p=0.83) or for adults and juveniles together (t=-1.03, d.f.=9, p=0.33; Figure 2).

Aside from recordings of *C. talpacoti*, obvious wing claps were only detected in one recording of *C. inca* (XC368476) and in no recordings of *C. passerina*. This is unusual considering that other pigeons and doves typically produce claps above- and sometimes below-the-body during vigorous take-off (Crandell and Tobalske, 2015; Murray et al., 2017; Niese and Tobalske, 2016; see Discussion).

P7 evolution throughout the genus *Columbina*

Reconstructed ancestral states of P7 shape in *Columbina* suggest that an *inca*-like or *passerina*-like morphology were equally likely to be ancestral within the genus (Figure 4) though this largely depends on how P7 morphology in *Claravis mondetoura* is defined (see below). Notably, the allopatric sister species *C. cruziana* and *C. picui* have strikingly different P7 morphologies and *C. cruziana* possesses a morphology that may in fact be unique in the genus. We coded it as *inca*-like due to its relatively small increase to vane width and its lack of a large hooked or recurved region of barbs as in *passerina*- and *talpacoti*-like feathers. Outside of the genus *Columbina*, P7 morphologies do not typically deviate from an aerodynamically stereotyped form except perhaps for *Claravis mondetoura* (see Discussion). Unfortunately, without material from *Columbina*'s sister species (*Claravis mondetoura, Claravis geoffroyi*), a confident estimation of the ancestral states of P7 at some internal nodes is impossible (grey nodes in Figure 4).

DISCUSSION

Spread wing specimens from three species of *Columbina* ground doves possess highly modified primary feathers that produced buzzing sounds in our aeroacoustic wind tunnel. These sounds varied between species but were all produced by flutter in modified P7 feathers that caused specialized elongated barbs on the trailing vane to collide with the adjacent P6 feather, producing rapid, broadband sounds on contact. These buzzes are produced in flight by several *Columbina* species and have been hypothesized to be communicative (Johnston, 1960; Johnston, 1961). Here, we confirm that these wing sounds are sonations by characterizing the intrinsic (i.e. 1:1) link between specialized P7 morphologies and buzzes. In other words, P7 feathers in *Columbina* ground doves deviate from a typical, aerodynamically constrained form because they have been coopted as specialized acoustic signaling structures, a process which has been identified in two other species of Columbids (Murray et al., 2017; Niese and Tobalske, 2016).

Gross feather shapes vary between *Columbina* species, but appear to have a similar morphological basis in modifications to barb length and width. In all three of the species we investigated in detail, barbs within the modified region of P7 are longer and more narrow at their tips (i.e. distal half) than adjacent barbs in unmodified regions of the feather (Fig. 1). The lengthening, narrowing, distal curvature, and increased density of barbs along the rachis are all developmentally linked, suggesting that one or two growth parameters may control all the variation in morphology between these species (Li et al., 2017; Prum and Williamson, 2001). These same shape parameters appear to influence P10 morphology in *Columba livia* wings

(Niese and Tobalske, 2016), where modified regions have a similar barb morphology to the modified regions of *inca*-like P7 feathers.

In *C. inca*, modified shapes are found in both P7 and P6 in adult birds. In *C. passerina* and *C. talpacoti*, modified barbs occur in P7 feathers and, more rarely (one specimen of *C. talpacoti* here, others of *C. passerina* and *C. talpacoti* in UWBM collection), in P6 as well. This variation may explain vague and conflicting reports in the literature (e.g. Goodwin, 1983; Johnston, 1961) regarding the exact number of modified feathers present in each species. Transcriptomic analyses of developing P6 feather buds in individuals that express a this "doubled" feather modification morphology, as compared to typical individuals, could help reveal the developmental and genetic pathways responsible for the evolution of feather shape (e.g. Li et al., 2017).

In all the wings we tested, adult birds regularly produced buzzing sounds as P7 flapped against P6. These sounds precisely match the wing buzzes produced by *Columbina inca* in natural take-offs, nearly match the sounds produced by *C. passerina*, but do not match the wing sounds produced by fleeing *C. talpacoti*. Buzzes produced by *C. passerina* wings in the wind tunnel were similar, but statistically different from those observed in recordings of wild birds. These differences could be due to differences between the wingtip velocities estimated in the wind tunnel and those that occur *in vivo*. In the wind tunnel, flow velocity was approximately 10 ms^{-1} which emulated the peak wingtip velocities observed in casual, horizontal flight in trained Diamond Doves (*Geopelia cuneata*), a similarly sized (about 40g), but distantly related ground dove. This estimate of wing-tip velocity for *C. passerina* could be low simply because of the slow, casual flights from which we extracted velocities for *G. cuneata*. Often, flow velocity is positively correlated with flutter frequency , and a higher flow velocity associated with a more rapid take-off event in wild *C. passerina* could account for the differences between flutter observed in the wind tunnel and *in vivo* (Clark and Prum, 2015; Clark et al., 2013a). Alternatively, differences in the wing-beat kinematics of flying *C. passerina* and *G. cuneata* could have influenced our velocity estimates. In wild *C. passerina*, audio recordings of take-off events had a wingbeat frequency (WBF) between 18 and 20Hz (18.7±0.9). In previous observations of *G. cuneata*, a species which is not known to produce communicative wing sounds, fleeing birds had a WBF between 14 and 16Hz (15.0±0.6), substantially lower than *C. passerina*. This difference in WBF may not directly translate to a difference in wing-tip velocity, however, as all recordings of *C. passerina*, along with most recordings of *C. inca,* do not contain wing claps, implying that these birds fly with a lower wingbeat amplitude (WBA) as well. Interestingly, in other species where wing sounds are communicative and involved in display flights, individuals modulate their WBF and WBA when signaling, a behavior which often coevolves with sonations (Clark, 2011). It is possible that the variation in WBF and WBA between these two similarly-sized birds could be a coevolved behavior associated with sonating in *Columbina* doves.

Recordings of *C. talpacoti* suggest that it produces prominent wing claps as it flees, and these loud, broadband sounds may occlude the subtler sounds of feathers fluttering against adjacent feathers. Additionally, this species may perform sexually selected flight displays that incorporate wing claps (Goodwin, 1983), and is the only species in the genus for which such displays have been described. Both the morphology of P7 and its function may be influenced by such locomotion-induced sexually selected sonations.

Unlike all other recordings of *C. inca* and *C. passerina*, one recording of *C. inca* (XC368476) contained loud, broadband claps, once per wing cycle similar to those that readily occur above-the-body in *Columba livia*, *Ocyphaps lophotes*, and *Geopelia cuneata* (Crandell and Tobalske, 2015; Murray et al., 2017; Niese and Tobalske, 2016). In Columbids, above-the-body claps are more common than below-the-body claps which tend to only occur during powerful, high wingbeat amplitude escape maneuvers (Hingee and Magrath, 2009a; Murray et al., 2017; Niese and Tobalske, 2016). Interestingly, in *Columbina inca* these clap-like elements occurred at the end of buzz cycles, not the beginning as would be predicted if buzzes were produced on the downstroke following an above-the-body clap. This indicates that buzzes are produced on the upstroke. This is corroborates our wind tunnel experiments in which the wings of all three species sonated best when their orientations matched the kinematics of upstroke (e.g. Crandell and Tobalske, 2015), not downstroke. The Crested Pigeon (*Ocyphaps lophotes*) also produces sonations on the upstroke and also has a modified P7 feather, though the mechanism of the sonation and the shape of the feather are different, producing tonal "whistles" in this species, not buzzes (Murray et al., 2017).

Adult *C. inca* individuals always possessed modified morphologies in both P7 and in P6 which are similar in shape and flutter at similar rates. The loudness of *C. inca* wing buzzes was primarily due to flutter in P7, and buzzes were silenced entirely when P7 and P6 were prevented from fluttering. This demonstrates a more explicit link between these modified feathers and the buzzy wing sounds of *C. inca* – a link which we have emphasized here due to the more subtle modifications (i.e. an "ambiguous morphology"; see Clark, 2018) to P7 and P6 gross morphology in this species.

Buzz sounds were significantly weaker or absent in juvenile *C. inca* individuals which often lacked the morphological modifications present in adults. This corroborates anecdotal reports in the literature (Johnston, 1960) and has intriguing implications for the function of the sonation. Juvenile individuals are typically considered less reliable signalers than more experienced adults. If an individual is unable to produce a signal until they have moulted into their adult plumage, then they may be prevented from diluting the efficacy of the signal with their unreliable responses to cues. In alarm sonations specifically, this may prevent young birds from inducing a costly predator avoidance take-off event, or it may prevent "bird who cried wolf" scenarios that degrade the value of the alarm signal (McLinn and Stephens, 2010; Murray et al., 2017).

Across the Peristerinae, unusual remex morphologies have been described in all of the outermost five primary feathers (P6-P10), but only *Columbina* has modifications to P7. There are some reports that *Claravis mondetoura* occasionally possesses a modified P7. We attempted to find images of *Claravis mondetoura* wings to clarify these reports, but only succeeded in finding one photograph of a partial wing submitted to iNaturalist.org, a citizen science database of images and observations. This image does, however, appear to corroborate Johnston's (1961) statements that P7 is modified, but it is unclear if this shape is similar to those in *Columbina*. Given that all members of this subfamily (except, perhaps *Uropelia campestris*) possess modified outer primaries in differing combinations, shapes, and locations, the Peristerinae may be an excellent candidate clade for testing the evolution of feather morphologies and their development more broadly.

Within the Columbidae as a whole, modifications to P7 are uncommon and, outside of the Peristerinae, occur only in *Ocyphaps lophotes* where they produce alarm sonations (Murray et al., 2017). A morphology similar to those described here is found in some species of green pigeon in the genus *Treron* (see Gibbs et al., 2010, p 425 for a drawings and details), though this morphology is in P8, not P7, and its function is unknown. Wing buzzes are also relatively uncommon among birds, but have been described extensively in *Stellula calliope* (Trochilidae; Clark, 2011) where they are performed during shuttle displays and may be a signal of a male's flight ability. Like the buzzes in these hummingbirds, buzzes produced by *Columbina* ground doves are intrinsically linked to locomotion and may be a reliable indicator of flight kinematics such as wingbeat frequency and amplitude, suggesting that they are capable of encoding information related to take-off power. Such information may be related to predator avoidance and/or mate fitness (the two are not mutually exclusive), though the latter has never been tested in pigeons and mutual mate choice displays are uncommon in birds.

It is possible that, in addition to acting as specialized sonating structures, these feathers could also function as visual signals or specialized aerodynamic devices, though this is unlikely. Feathers that are sexually selected visual signals are exaggerated, involved in visual displays, and sexually dimorphic. Male *Columbina* ground doves do perform a variety of wing-raising sexual or agonistic displays that might display these modifications, but across all eight species, these specialized feathers are monomorphic between the sexes. Feathers that are specialized aerodynamic devices in other species either generate unique tip vortices or leading edge vortices (KleinHeerenbrink et al., 2017; Lee et al., 2015). Modifications to *Columbina* feathers are not at the feather tips nor at the leading edge of the wing/feathers, suggesting that they likely do not play a role in generating tip or leading edge vortices. However, it is possible that they may play some undiscovered, specialized role in manipulating aerodynamic forces.

Conclusions

P7 feathers in the genus *Columbina* deviate from a stereotyped aerodynamic shape and occur in several forms, all of which appear to be specialized to produce buzzing sounds. These buzzes are sonations in *C. passerina* and *C. inca* and likely communicate predator-related information, as has been observed in other Columbids and speculated for these species in the past (Johnston, 1960; Johnston, 1961; Murray et al., 2017), and possibly performance-related information, as is more common for feather-produced sonations (Clark and Prum, 2015). Given the diversity of P7 shape in *Columbina* ground doves, and the variety of modified remiges in the Peristerinae broadly, sonation behaviors are likely a powerful force driving the diversification of remiges which are otherwise strongly constrained by the physical demands of flight.

Acknowledgements

The authors would like to thank Raphael Igor Dias and Paul Smith for providing images of birds in-the-hand, Jack Withrow for photographing spread wing specimens at the University of Alaska Museum, the recordists who generously contributed their media to the Creative Commons at Xeno-Canto.org, and Rob Faucett at the University of Washington Burke Museum for this specimen loan.

Competing interests

The authors declare no competing or financial interests.

Author contributions

RLN, CJC and BWT designed the study. RLN and CJC carried out the experiments. RLN analyzed the data and prepared the original draft. CJC and BWT shared in review and editing.

Funding

Research and equipment was funded by the National Science Foundation [CMMI 1234737 and IOS-1838688]. Travel funding was provided by a Drollinger-Dial Research Grant.

Data availability

All photographs of UWBM and PSM spread wing specimens can be accessed at

https://digitalcollections.pugetsound.edu/digital/collection/slaterwing

Feather specimens from Featherbase can be accessed at

http://www.featherbase.info/en/home

Audio recordings can be accessed via the reference links listed in Table S2

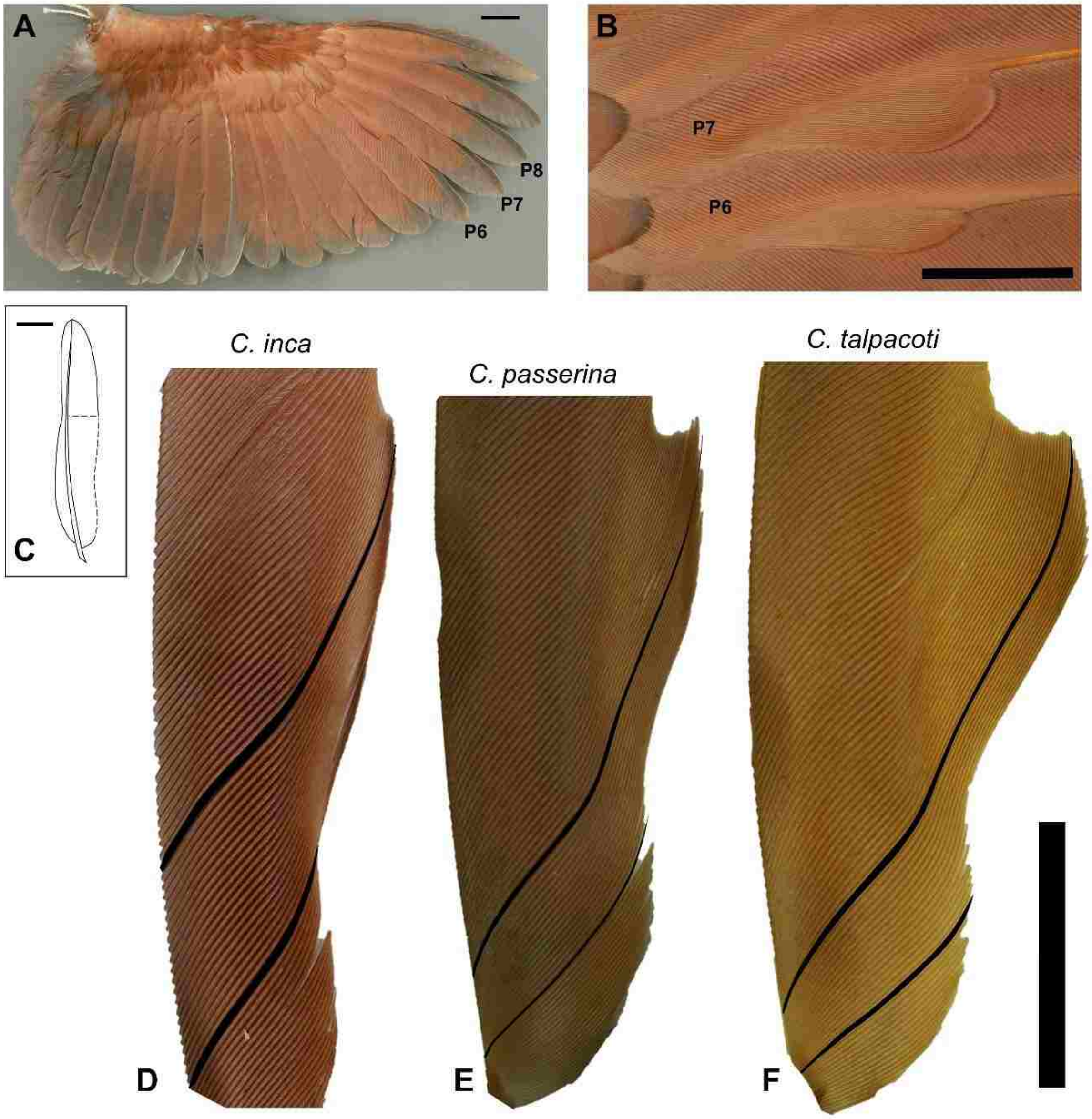

FIGURE 1. Remex morphologies in three species of Columbina ground doves. (A) A typical wing of *Columbina passerina* showing a distinct morphology in P7. Across all three species, the outermost three primary feathers (P10, P9, and P8) do not vary dramatically, but P7 and occasionally P6 show modified morphologies. (B) A magnified view of P7 and P6 in a *C. talpacoti* specimen (UWBM84051). The presence of a modified P6 feather in addition to a modified P7 was not common among the specimens surveyed in this study. (C) A simplified P7 feather

indicating the modified region of interest (dashed lines) shown in D, E, and F. For images D, E, and F, two barbs on each feather have been darkened for emphasis. The lower barb (proximal to feather insertion) is an unmodified barb and the upper barb is modified. (D) *C. inca* barb morphology of P7. Note that P6 is similarly modified in adults of this species but is not shown here (see text). (E) *C. passerina* barb morphology of P7. (F) *C. talpacoti* barb morphology of P7. High resolution image online. Scale bars indicate 10mm for all images.

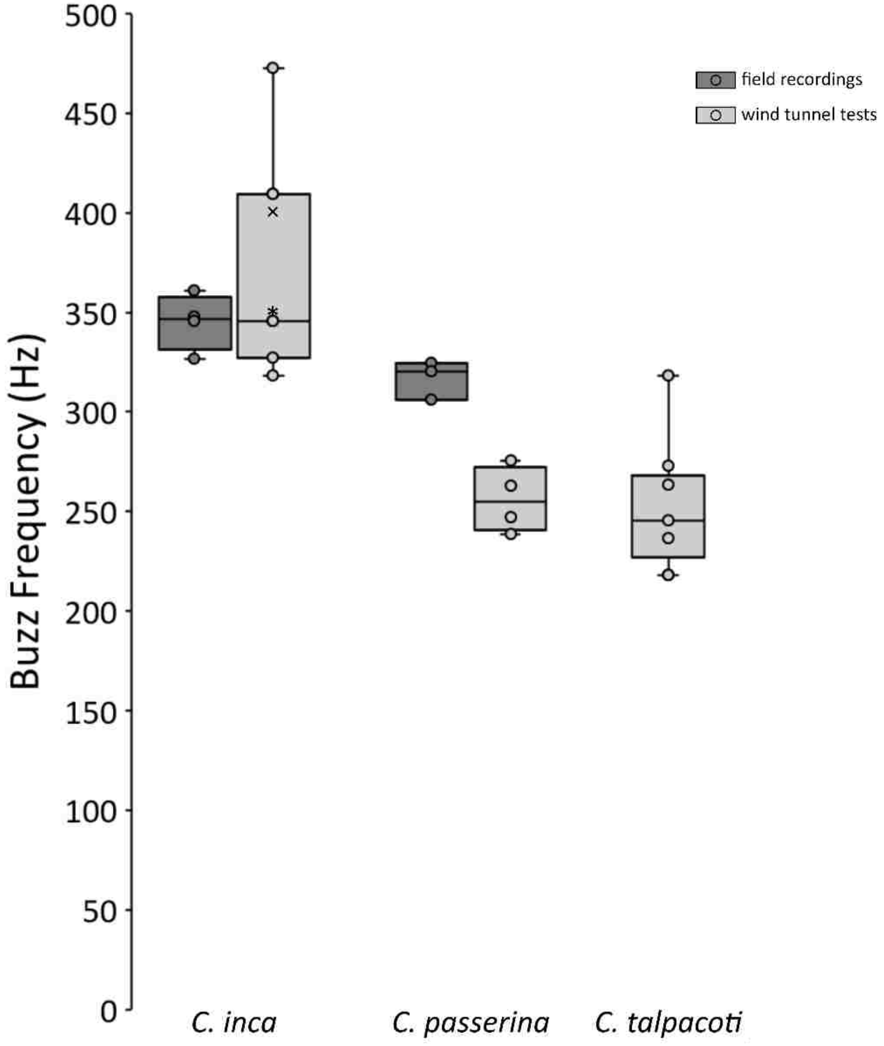

FIGURE 2. Buzz frequencies produced by birds from field recordings as compared to those recorded in the wind tunnel. Buzzes produced by *Columbina inca* during flight (N=4) matched those recorded in the wind tunnel (N=7; t=-1.03, d.f.=9, p=0.33). Wings from juvenile birds that possessed a modified P7 are included here and did not flutter at frequencies significantly different from adults (t=1.5, d.f.=5, p=0.19; average buzz frequency for adults indicated by *; average buzz frequency for juveniles indicated by ×). In *C. passerina*, buzzes produced in flight (N=3) were similar, but statistically different (t=5.66, d.f.=5, p=0.003) to those produced in the wind tunnel (N=4). Recordings of *C. talpacoti* in flight did not contain buzz elements, but the

frequencies observed in the wind tunnel (N=7) are shown. Dots show all observed buzz frequencies (some are overlapping). Each point is the averaged buzz frequency across all wingbeats across all flights in single field recording, or over 10ms of video for an individual specimen in the wind tunnel.

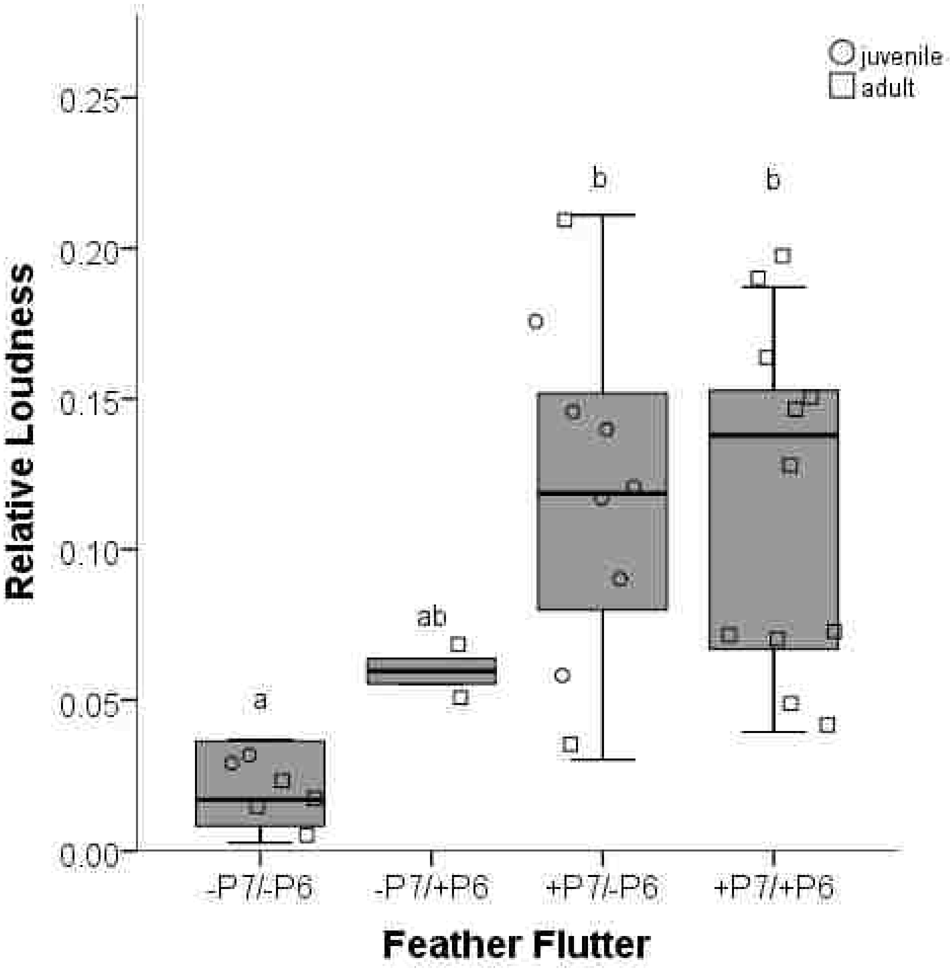

FIGURE 3. Loudness of buzz sounds relative to wind tunnel noise for a series of silencing tests in *Columbina inca* wings. Loudness relative to tunnel noise varies significantly depending on which modified feathers are fluttering (F=12.59, df=3,24, p<0.01). Wings produced the loudest buzzes whenever P7 was fluttering freely (+P7). Whenever P7 was taped (-P7), buzzes were noticeably quieter. If both P7 and P6 were not fluttering (-P7/-P6), buzzes were nearly eliminated. Statistical differences are indicated by letters above bars and are summarized in Table S5.

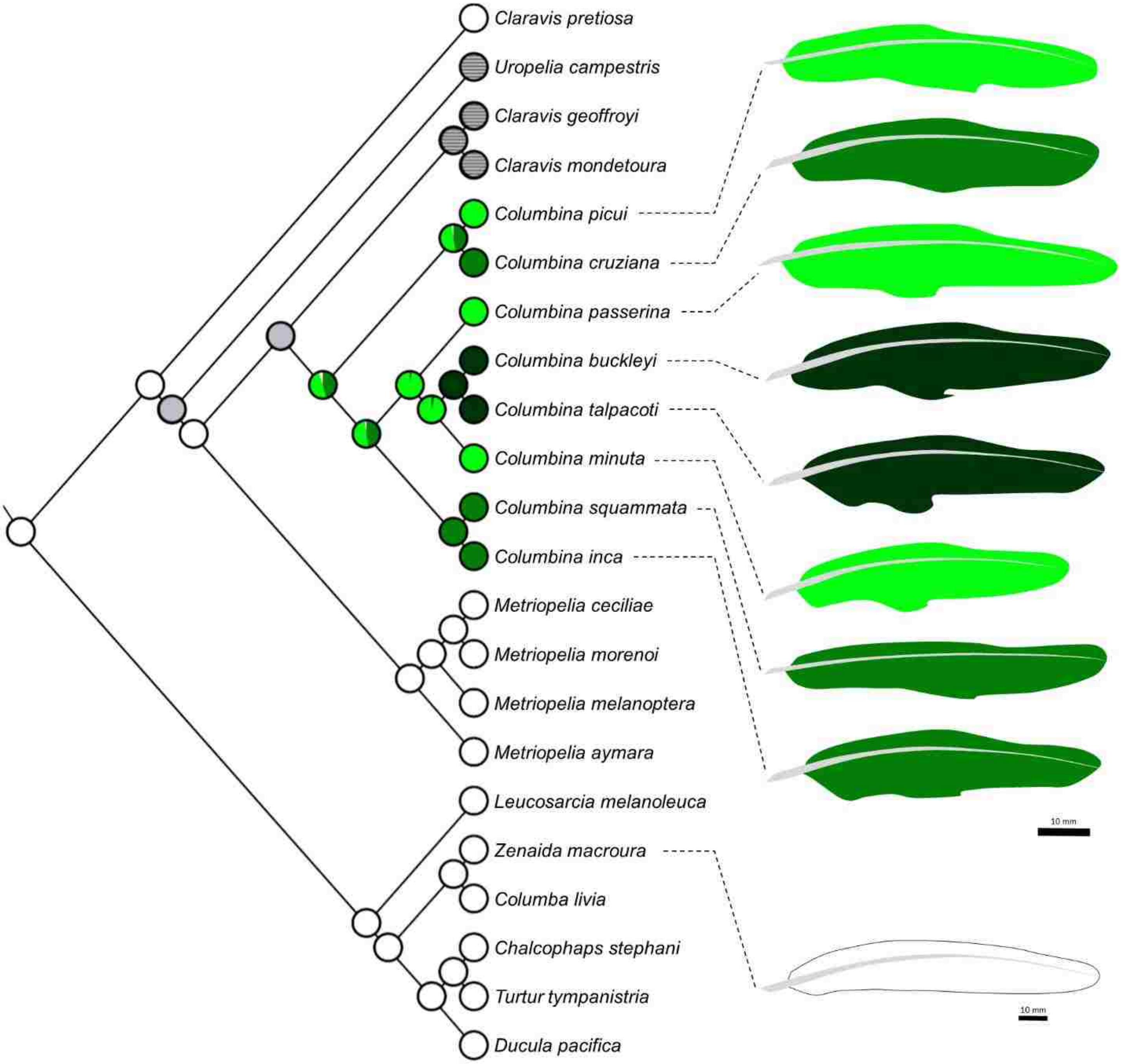

FIGURE 4. Ancestral state reconstructions of P7 morphology in *Columbina* using a maximum likelihood approach. White nodes and tips indicate a typical, aerodynamic P7 morphology such as that shown for *Zenaida macroura*. Hashed grey and black tips indicate an unknown or unconfident P7 morphology. Grey nodes indicate that ancestral states are impossible to infer. All P7 feathers are drawn to scale, except *Z.*

macroura (scale bar shown). Phylogram based on trees estimated from mitochondrial and nuclear loci and published by Sweet and others (2017) with minor changes to the outgroup.

REFERENCES

Amorim, P. S. and Dias, R. I. (2019). Non-vocal communication as an anti-predator strategy in scaled doves (Columbina squammata). *J. Ethol.* 1–9.

Araya-salas, M., Smith-vidaurre, G. and Webster, M. (2017). Assessing the effect of sound file compression and background noise on measures of acoustic signal structure. *Bioacoustics* 1–17.

Audubon, J. J. (1870). *The Birds of America, Vol. V*. New York: Lockwood and Son.

Bachmann, T., Emmerlich, J., Baumgartner, W., Schneider, J. M. and Wagner, H. (2012). Flexural stiffness of feather shafts: geometry rules over material properties. *J. Exp. Biol.* **215**, 405–415.

Bostwick, K. S., Elias, D. O., Mason, A. and Montealegre-Z, F. (2010). Resonating feathers produce courtship song. *Proc. Biol. Sci.* **277**, 835–41.

Charif, R., Waack, A. and Strickman, L. (2010). Raven Pro 1.4 User's Manual. 367.

Clark, C. J. (2011). Wing, tail, and vocal contributions to the complex acoustic signals of courting Calliope hummingbirds. *Curr. Zool.* **57**, 187–196.

Clark, C. J. (2018). Signal or cue? Locomotion-induced sounds and the evolution of communication. *Anim. Behav.* **143**, 83–91.

Clark, C. J. and Mistick, E. A. (2018). Kinematic control of male Allen's Hummingbird wing trill over a range of flight speeds. *J. Exp. Biol.* jeb.173625.

Clark, C. J. and Prum, R. O. (2015). Aeroelastic flutter of feathers, flight, and the evolution of nonvocal communication in birds. *J. Exp. Biol.* **218**, 3520–3527.

Clark, C. J., Elias, D. O. and Prum, R. O. (2013). Hummingbird feather sounds are produced by aeroelastic flutter, not vortex-induced vibration. *J. Exp. Biol.* **216**, 3395–3403.

Craig, W. (1911). The Expressions of Emotion in the Pigeons. III. The Passenger Pigeon (Ectopistes migratorius Linn.). *Auk* **28**, 408–427.

Crandell, K. E. and Tobalske, B. W. (2015). Kinematics and aerodynamics of avian upstrokes during slow flight. *J. Exp. Biol.* **218**, 2518–27.

Cuvier, G. (1817). *The animal kingdom arranged according to its organization. Vol 1. Vertebrates*.

Ennos, A. R., Hickson, J. and Roberts, A. (1995). Functional morphology of the vanes of the flight feathers of the pigeon Columba livia. *J. Exp. Biol.* **198**, 1219–1228.

Feo, T. J., Field, D. J. and Prum, R. O. (2015). Barb geometry of asymmetrical feathers reveals a transitional morphology in the evolution of avian flight. *Proc. R. Soc. B Biol. Sci.* **282**, 20142864.

Gibbs, D., Barnes, E. and Cox, J. (2010). *Pigeons and doves: A guide to the pigeons and dove of the world*. A & C Black.

Goodwin, D. (1983). *Pigeons and doves of the world*. Comstock Pub. Associates.

Heers, A. M. and Dial, K. P. (2012). From extant to extinct: Locomotor ontogeny and the evolution of avian flight. *Trends Ecol. Evol.* **27**, 296–305.

Hingee, M. and Magrath, R. D. (2009). Flights of fear: a mechanical wing whistle sounds the alarm in a flocking bird. *Proc. R. Soc. B Biol. Sci.* **276**, 4173–9.

Johnston, R. F. (1960). Behavior of the Inca dove. *Condor* **62**, 7–24.

Johnston, R. F. (1961). The genera of American ground doves. *Auk* **78**, 372–378.

KleinHeerenbrink, M., Johansson, L. C. and Hedenström, A. (2017). Multi-cored vortices support function of slotted wing tips of birds in gliding and flapping flight. *J. R. Soc. Interface* **14**, 20170099.

Lee, S., Kim, J., Park, H., Jabłoński, P. G. and Choi, H. (2015). The Function of the Alula in Avian Flight. *Sci. Rep.* **5**, 9914.

Lewis, P. O. (2001). A Likelihood Approach to Estimating Phylogeny from Discrete Morphological Character Data. *Syst. Biol.* **50**, 913–925.

Li, A., Figueroa, S., Jiang, T. X., Wu, P., Widelitz, R., Nie, Q. and Chuong, C. M. (2017). Diverse feather shape evolution enabled by coupling anisotropic signalling modules with self-organizing branching programme. *Nat. Commun.* **8**, 1–13.

Lucas, A. M. and Stettenheim, P. R. (1972). *Avian anatomy: integument*. Washington D.C.: United States Department of Agriculture; Agriculture handbook, no. 362.

Maddison, D. R. and Maddison, W. P. (2018). Mesquite: A modular system for evolutionary analysis.

Mahler, B. and Tubaro, P. L. (2001). Attenuated Outer Primaries in Pigeons and Doves: a Comparative Test Fails To Support the Flight Performance Hypothesis. *Condor* **103**, 449.

McLinn, C. M. and Stephens, D. W. (2010). An experimental analysis of receiver economics: Cost, reliability and uncertainty interact to determine a signal's value. *Oikos* **119**, 254–263.

Murray, T. G., Zeil, J. and Magrath, R. D. (2017). Sounds of Modified Flight Feathers Reliably Signal Danger in a Pigeon. *Curr. Biol.* **27**, 3520–3525.e4.

Niese, R. L. and Tobalske, B. W. (2016). Specialized primary feathers produce tonal sounds during flight in rock pigeons (Columba livia). *J. Exp. Biol.* **219**, 2173–81.

Pereira, S. L., Johnson, K. P., Clayton, D. H. and Baker, A. J. (2007). Mitochondrial and nuclear DNA sequences support a Cretaceous origin of Columbiformes and a dispersal-driven radiation in the Paleocene . *Syst. Biol.* **56**, 656–72.

Prum, R. O. and Brush, A. H. (2002). The evolutionary origin and diversification of feathers. *Q. Rev. Biol.* **78**, 275–301.

Prum, R. O. and Williamson, S. (2001). Theory of the growth and evolution of feather shape. *J. Exp. Zool.* **291**, 30–57.

Selby, P. J. (1850). The Natural History of Gallinaceous Birds: Columbidae or Pigeons. In *The Naturalist's Library: Ornithology* (ed. Jardine, W.), Lizars, W. H.), Smith, C. H.), and Stewart, J.), p. London: W. H. Lizars.

Stoddard, M. C. and Prum, R. O. (2011). How colorful are birds? Evolution of the avian plumage color gamut. *Behav. Ecol.* **22**, 1042–1052.

Swaddle, J. P., Witter, M. S., Cuthill, I. C., Budden, A. and McCowen, P. (1996). Plumage Condition Affects Flight Performance in Common Starlings: Implications for Developmental Homeostasis, Abrasion and Moult. *J. Avian Biol.* **27**, 103–111.

Swainson, W. (1825). On the characters and natural affinities of several birds from Australia; including some observations on the Colulmbidae. *Zool. J.* **1**, 463–484.

Sweet, A. D., Maddox, J. D. and Johnson, K. P. (2017). A complete molecular phylogeny of Claravis confirms its paraphyly within small New World ground-doves (Aves: Peristerinae) and implies multiple plumage state transitions. *J. Avian Biol.* **48**, 459–464.

Wetmore, A. (1920). Observations on the Habits of the White-Winged Dove. *Condor* **22**, 140–146.

Wilson, A. (1808). *American Ornithology, Vol. III*. New York: Collins & Co.

SUPPLEMENTAL MATERIAL

Audio 1. *Columbina passerina* (XC169166) wild bird producing wing buzzes in flight. This file appears to include take-off and landing. Recordist: Paul Marvin.

Video 1. *Columbina passerina* (UWBM90871) in an aeroacoustic wind tunnel. Note that P7 is fluttering and colliding with the adjacent P6 once per flutter cycle. This specimen is fluttering at a rate of approximately 260Hz.

Video S1. Compiled clips of tests of *Columbina inca* (UWBM48439) in an aeroacoustic wind tunnel. Tape is placed on various combinations of feathers to determine the source of buzzing sounds. For analysis, audio data collected from these experiments was categorized into one of four groups for each taping trial. The analysis category of each taping trial is defined in Table S4.

Table S1. Specimens used in wind tunnel experiments.

UWBM Specimen Number	Species	Sex	Age	Modified P7	Modified P6
48320	*C. inca*	female	juvenile	Yes	No
48439	*C. inca*	male	adult	Yes	Yes
63639	*C. inca*	female	adult	Yes	Yes
69076	*C. inca*	female	adult	Yes	Yes
69080	*C. inca*	male	juvenile	Yes	Yes
69162	*C. inca*	male	juvenile	No	No
80050	*C. inca*	female	adult	Yes	Yes
84002	*C. inca*	female	juvenile	Yes	No
90697	*C. passerina*	male	adult	Yes	No
90745	*C. passerina*	male	adult	Yes	No
90791	*C. passerina*	female	adult	Yes	No
90871	*C. passerina*	female	adult	Yes	No
81305	*C. talpacoti*	male	adult	Yes	No
82605	*C. talpacoti*	female	adult	Yes	No
82695	*C. talpacoti*	male	adult	Yes	No
84051	*C. talpacoti*	male	adult	Yes	Yes
84059	*C. talpacoti*	male	adult	Yes	No
84086	*C. talpacoti*	female	adult	Yes	No
90707	*C. talpacoti*	female	adult	Yes	No

Table S2. Wild bird recordings used in this study.

Recording ID	Species	Recordist	Reference
XC368476	*C. inca*	Dan Lane	https://www.xeno-canto.org/368476
XC368477	*C. inca*	Dan Lane	https://www.xeno-canto.org/368477
XC392911	*C. inca*	Jeff Norris	https://www.xeno-canto.org/392911
ML110429481	*C. inca*	Paul Marvin	https://macaulaylibrary.org/asset/110429481
XC147314	*C. passerina*	Paul Marvin	https://www.xeno-canto.org/147314
XC169165	*C. passerina*	Paul Marvin	https://www.xeno-canto.org/169165
XC169166	*C. passerina*	Paul Marvin	https://www.xeno-canto.org/169166
ML3931	*C. talpacoti*	Walter Thurber	https://macaulaylibrary.org/asset/3931
XC186147	*C. talpacoti*	Fernando Igor de Godoy	https://www.xeno-canto.org/186147

Table S3. Supplemental specimens for ancestral state reconstruction of P7 morphology.

Collection Code	Specimen Number	Species	Modified Feathers?	P7 morpho-type
UAM	20984	*Columbina minuta*	P7	intermediate, *passerina*-like
UAM	20847	*Columbina buckleyi*	P7	large, *talpacoti*-like
UAM	20974	*Columbina buckleyi*	P7	large, *talpacoti*-like
UAM	20975	*Columbina buckleyi*	P7	large, *talpacoti*-like
UAM	20977	*Columbina cruziana*	P7	subtle, *inca*-like
UAM	20978	*Columbina cruziana*	P7	subtle, *inca*-like
UAM	20979	*Columbina cruziana*	P7	subtle, *inca*-like
UAM	20985	*Metriopelia aymara*	P10, P9	typical
UAM	39363	*Metriopelia aymara*	P10, P9	typical
UWBM	54428	*Metriopelia aymara*	P10, (P9 damaged)	typical
UAM	20981	*Metriopelia ceciliae*	P10, P9?	typical
UAM	39364	*Metriopelia melanoptera*	P10	typical
UWBM	54405	*Metriopelia morenoi*	P10	typical
Featherbase	428	*Claravis pretiosa*	P10, P9, P8	typical
Featherbase	828	*Leucosarcia melanoleuca*	-	typical
PSM	24041	*Zenaida macroura*	-	typical
PSM	17193	*Columba livia*	P10	typical
UWBM	76724	*Chalcophaps stephani*	-	typical
UWBM	67089	*Turtur tympanistria*	P10	typical
UWBM	42555	*Ducula pacifica*	-	typical

Note: UAM = University of Alaska Museum; UWBM = University of Washington Burke Museum; PSM = Puget Sound Museum (Slater Museum of Natural Hisoty); Featherbase = http://www.featherbase.info/en/home. UWBM and PSM material can be viewed in the Wing and Tail Image Collection: https://digitalcollections.pugetsound.edu

Table S4. Feather taping combinations and their respective groupings as shown in Figure 3.

	-P7/-P6	**-P7/+P6**	**+P7/-P6**	**+P7/+P6**
2 adults	(P6,P7), (P5,P6,P7)	(P7,P8)	(P6,P5)	(P8,P9), (P9,P10), (P5,P9,P10), (P8,P9,P10), no tape
1 juvenile	(P6,P7), (P7,P8), (P5,P6,P7),	×	(P6,P5), (P8,P9), (P9,P10), (P5,P9,P10), (P8,P9,P10), no tape	×

×=P6 was not modified and never fluttered in this juvenile bird, regardless of which feathers were taped.

Table S5. One-way ANOVA and Tukey HSD post-hoc test results for all respective grouping comparisons as defined in Table S4 and shown in Figure 3.

ANOVA	**df**	**F**	**p**
	3,24	12.59	**<0.001**

Tukey HSD	**comparison**	**p**
	-P7/-P6 × -P7/+P6	0.076
	-P7/-P6 × +P7/-P6	**<0.001**
	-P7/-P6 × +P7/+P6	**<0.001**
	-P7/+P6 × +P7/-P6	0.742
	-P7/+P6 × +P7/+P6	0.761
	+P7/-P6 × +P7/+P6	1.00

CHAPTER 2

Pigeons and doves utilize uniquely shaped feathers to improve aerodynamic performance

Robert L. Niese and Bret W. Tobalske

Field Research Station at Fort Missoula, Division of Biological Sciences, University of Montana,
Missoula, MT 59812, USA

ABSTRACT

The feathers of the wing that power flight in birds are morphologically constrained by the demands of aerial locomotion, but peculiar morphologies exist in many taxa in spite of these constraints. In the family Columbidae (pigeons and doves), we identified 56 species and at least 16 independent evolutionary origins of a highly-attenuated outermost primary feather (P10) whose function is unknown and has been the subject of two centuries of speculation. We sought to test two prevailing hypotheses – that this morphology is specialized either to (1) produce acoustic signals or (2) to improve aerodynamic performance. We measured whether the specialized columbid P10 feather is necessary and sufficient to produce sonations in live birds, spread wings, and isolated feathers, and concluded that it may influence sound production, but is not specialized to do so. We conducted aerodynamic tests using dried, spread wings in preparations that emulated gliding flight in a wind tunnel and downstroke at low advance ratios (slow flight speeds) using a propeller model. We determined that the specialized P10 feather improves aerodynamic performance by reducing drag in emulated

gliding and flapping. At low angular velocities and moderate angles of attack (20-30 deg), wings with the specialized P10 dramatically outperformed wings without P10, exhibiting greater ratios of Lift : Drag. This effect was an order of magnitude greater in emulated slow flapping flight than in gliding flight for some individuals. We hypothesize that P10 is a specialized aerodynamic device similar to the slotted primaries or the alula of passerines.

INTRODUCTION

Feathers are the most phenotypically diverse (Prum and Brush, 2002; Stoddard and Prum, 2011) and structurally complex (Feo et al., 2015; Prum and Williamson, 2001) integumentary structures in vertebrates. They vary in size, shape, color, structure, and chemical composition between species, between locations on the body, and even within a single feather follicle across an individual's lifetime (Lucas and Stettenheim, 1972). Not all feathers vary to the same degree across species, however. Remiges (flight feathers of the wing), for example, are remarkably morphologically conserved and show little variation across disparate taxa, individual lifespans, and evolutionary time. These feathers, which make up the majority of the surface area of a wing, are morphologically constrained by the physical demands of flight (Fig. 1 A, B). This presumed selection for morphology driven by capacity for flight has shaped the avian Bauplan since the Jurassic, and paleornithologists have used the presence of these specialized, asymmetrical feathers to define the origins of flight in the fossil record (e.g. Feduccia and Tordoff, 1979; Heers and Dial, 2012). In modern birds, these stereotyped feathers are required for effective and efficient flight (Hedenström, 2003), and birds go to great lengths to compensate for, and recover from the impacts of a reduction in overall wing surface area caused by feather damage or loss (DesRochers et al., 2009; Echeverry-Galvis and Hau, 2013; Hedenström, 2003; Swaddle et al., 1996).

Yet, in spite of this morphological and functional stereotyping for flight ability, some species do possess remiges that deviate from typical aerodynamic forms (e.g. slotted primaries in *Buteo* hawks, Tucker, 1993; shortened first secondary (S1) in phasianids such as grouse and pheasants, Drovetski, 1996). Historically, this variation in remex morphology has been attributed to unique aerodynamic specializations of the wing such as those that increase soaring efficiency or take-off efficacy (Averill, 1927; Drovetski, 1996; Tucker, 1993), and, recently, the hypothesis that emarginated primaries improve the aerodynamics of the wingtip vortex received empirical support (KleinHeerenbrink et al., 2017). These morphologies are rarely considered "extreme" and can be found in hundreds of disparate taxa (Klaassen van Oorschot et al., 2017).

In a substantially less common phenomenon, birds can also possess morphologies that are extreme, sexually dimorphic, and, often, unique to a species or clade (e.g. outermost primary feather shape in male Scissor-tailed Flycatchers, *Tyrannus forficatus*; Clark and Prum, 2015). Recent research suggests that these particular morphologies are the result of selection for locomotion-induced acoustic signals, or sonations, that are produced in sexually selected displays (Clark and Prum, 2015). In some species, however, conspicuous atypical remex morphologies exist in both sexes and do not appear to play an obvious role in sexually-selected displays (e.g. outermost primaries with "hooked" tips in the Monk Parakeet, *Myiopsitta monachus*). These morphologies are not subtle and have captured the attention of naturalists for centuries (Cuvier, 1817a; Selby, 1850; Swainson, 1825), and yet, outside of the present study, only one such feather has been rigorously tested to determine the function of its unusual morphology (Murray et al., 2017).

Among pigeons and doves (Fig. 1 C, D, E, F), a peculiar morphology in the outermost primary (P10; Fig. 1 C, F) has been the subject of much interest and speculation due to its extreme morphology and apparent abundance within the clade. This remex was first described in an Australian fruit pigeon in the genus *Ptilinopus* by William Swainson (1825) where he noted that it occurred in species found in Australasia and South America and suggested it likely influenced the “powers of loco-motion” and thus deserve our attention (473). Subsequent authors speculated that the morphology might improve flight maneuverability in enclosed habitats (Goodwin, 1983) or take-off performance while fleeing a predator (Mahler and Tubaro, 2001), but, to date, these aerodynamic hypotheses have not been tested.

Alternatively, as in other clades, the presence of an extreme remex morphology in the wing may be associated with sonation behaviors such as those in sexually selected displays or in signaling alarm (Clark and Prum, 2015; Murray et al., 2017). A similar P10 morphology exists in several species where it is sexually dimorphic and used in displays to produce sonations (e.g. Scissor-tailed Flycatcher, Black Scoter). It is also possible, as with the outermost tail feathers in swallows (Rowe et al., 2001), that the morphology provides an aerodynamic benefit to some extent while simultaneously receiving a co-opted benefit related to signaling. In order to determine which selective forces drove the shape of the columbid remex to deviate from a stereotyped form, we tested the feather’s ability to produce sonations (the aeroacoustic hypothesis) and to improve flight performance (the aerodynamic hypothesis) in a single species, the diamond dove (*Geopelia cuneata*; Fig. 1 F), and then evaluated its evolution across the entire clade.

According to the aeroacoustic hypothesis, remiges that are specialized to produce sonations have co-opted naturally occurring sound-generating phenomena, the most common and widespread of which are tonal sounds produced by aeroelastic flutter (Clark and Prum, 2015). To test this hypothesis, we must determine if the feather of interest is necessary for normal sound production and if the feather can sufficiently replicate the sound on its own under the appropriate flow conditions. In evaluating the evolution of such a morphology across the clade, we expect the appearance of the trait to be associated with behavioral traits such as group living (required for sonations of alarm) or sexually selected displays, or with morphological traits indicative of a history of strong sexual selection.

According to the aerodynamic hypothesis, feathers are specialized to produce lift or reduce drag via mechanisms that manipulate the flow over upper surface of the wing or the vortices shed at the tip of the wing. Such specialized devices function either to prevent stall (i.e. maintain/promote lift) during take-off or landing (Lee et al., 2015; Muijres et al., 2012), or to improve span efficiency and, thereby, reduce induced drag (KleinHeerenbrink et al., 2017). We tested the wing's overall lift and drag characteristics with and without P10 using preparations that emulated gliding (a fixed wing in a wind tunnel) and flapping at low advance ratio (slow flight speeds such as immediately after take-off or before landing). Our evaluation of the evolutionary histories of P10 will vary depending on the types of aerodynamic benefits they confer. If the feather helps prevent stall, we expect the morphology to be associated with ecological traits such as terrestriality, frequent take-off and landing, and, perhaps, the presence of terrestrial predators. If the feather improves span efficiency, we expect the trait to be particularly associated with ecological or biogeographic factors such as long or frequent daily or seasonal migrations.

RESULTS AND DISCUSSION

Aeroacoustic Signaling Hypothesis

Diamond Doves (*Geopelia cuneata*) that engaged in takeoff and vigorous short-distance flights (≤ 6 m in distance) produced tonal wing sounds at 4800±250Hz. In eight laboratory animals, across 120 total flights that varied in urgency, take-off trajectory, and duration, tonal wing sounds were produced in 75 trials (63%), but were only produced by five (63%) of the birds. Among these five individuals, two birds produced tones consistently in all flights, while the remaining three tended to only produce tones during what appeared to be maximal-effort events. These inconsistencies across individuals could be due to the age or sex of each bird (this information was unavailable), undetected differences in the physical state of the remiges, or it may indicate that the sounds are spurious and non-communicative (Clark, 2018). For the two birds that consistently produced tones with fully intact wings, P10 removal altered tonal sound production , but did not eliminate it (N=2).

The sounds produced by isolated P10 feathers in our test preparations that emulated flapping and gliding flight never matched those recorded *in vivo*, and were variable in pitch, but never exceeded 1300Hz (Fig. 2). In addition to P10, we tested the sound-producing abilities of the adjacent P9 which possesses a stereotyped morphology. This feather was similarly insufficient to reproduce the 4800Hz tones observed in live birds, never producing tones greater than 1400Hz. As such, we were unable to determine that *in vivo* flight tones were produced by a single feather source, and instead we hypothesize that multiple feathers interact (Clark and Mistick, 2018b; Clark et al., 2011a) to produce the 4800Hz tones. However, tests of whole spread wings in our flapping-flight (spinning) model were also unable to replicate the tones produced *in vivo*, regardless of angular velocity (ω; rad s^{-1}) of the wing or angle of attack (α, Fig. 2). Instead, whole wings (i.e. "+P10" in Figure 2) typically produced tones around 3600Hz, but these tones were produced inconsistently (38% of the time; N=27/71) across a range of α (0-60°) and ω (89, 120, and 131 rad s^{-1}). After the P10 feather had been removed (i.e. "-P10" in Figure 2), wings produced tones significantly less frequently (24%; N=20/85; χ^2=3.86, df=1, p=0.049) and with a lower pitch (p=0.09 at 89 rad s^{-1}; p<0.01 at 120 and 131 rad s^{-1}; Fig. 2).

Together, these experiments suggest that, while P10 influences sound production, it is not necessary or sufficient to produce *in vivo* tones. If the atypical morphology displayed by this P10 feather in diamond doves was the result of an aeroacoustic specialization for sonations, we would expect it to reliably reproduce tones under the appropriate experimental flow conditions, or to consistently eliminate tones in removal experiments (Clark, 2018; Clark and Prum, 2015). This was not the case, and as such, we cannot conclude that this peculiar morphology is aeroacoustically specialized.

Aerodynamic Performance Hypothesis

Wings (n = 5) mounted to emulate gliding flight in a wind tunnel with and without P10 indicated that P10 enhanced aerodynamic performance of the wing (Fig. 3). Across a range of α (-30 to 100°) P10 reduced drag coefficients (C_D; χ^2 = 156, df = 1, p < 0.001; Fig. 3B). This effect was pronounced in all but one wing (80%) when $-10 \leq \alpha \leq 50°$, which are values of α relevant to flapping flight. The effect of P10 removal on lift production (C_L) varied among wings and α, but, overall, this change in lift producing ability was not significantly different from zero (χ^2 = 1.93, df = 1, p = 0.16; Fig. 3A). Wings with P10 exhibited higher lift:drag ratios (C_L:C_D) during emulated gliding compared with wings where P10 had been removed (Fig. 3C). These results are consistent with the aerodynamic effects of slotted primaries in other birds, which act to decrease induced drag, thus increasing C_L:C_D. Polar curves showing the coefficients of lift and drag at every α for each wing before and after the removal of P10 summarize these differences (Fig. 4).

In emulated flapping flight using a propeller model, wings (n = 5) with and without P10 behaved differently at intermediate α (20-30°) than they did at higher or lower α, a relationship which was not observed in our emulated gliding flight (Fig. 5). Specifically, at intermediate α (20 - 30°) wings that possessed P10 had higher C_L, but below 20° and above 30° this relationship inverted (Fig. 5A). Similarly, at 20°, C_D was higher in wings with P10 than in wings without P10, but was lower at α below 20° and above 30° (Fig. 5B). At 30° α, the effect of P10 varied between wings, where some wings had higher C_D when P10 was present, while others had lower C_D. Consequently, intact wings that had lower C_D at 20 and 30° α exhibited dramatically higher peak C_L:C_D than wings with P10 removed (Fig. 5C). Across all wings and speeds, peak C_L:C_D was significantly larger in wings with P10 than in wings without P10 (W=19, Z=2.33, p=0.018). This effect was greatest at ω = 89 and 120 rad s^{-1}, where C_L:C_D was, on average, twice as large in wings with P10 than in wings without P10. The effect of P10 in increasing C_L and decreasing C_D at $\alpha = 20 – 30^o$ in emulated flapping flight suggests that the feather is functioning in a manner similar to the alula, controlling flow separation over the upper surface of the wing via vortices shed from the tip of the feather (Lee et al. 2015).

Overall, the aerodynamic function of P10 varied in emulated gliding versus flapping flight, and also varied with α. In flapping, but not in gliding, wings had higher C_L at $20° \geq \alpha \geq 30°$

when P10 was present. In both emulated gliding and flapping, C_D was consistently lower in wings with P10 at high α (>30°) and at α = 0°, but in emulated flapping C_D was higher in wings with P10 at intermediate α (20 - 30°). This variable way in which P10 influences aerodynamic performance at a given α in flapping versus gliding suggests that P10 functions in two different aerodynamically specialized ways – , one specific to low advance ratio flight and one specific to gliding or cruising flight. This could be interpreted as P10 acting like a slotted primary in gliding (KleinHeerenbrink et al., 2017), but acting like the alula in take-off or landing (Lee et al., 2015; see Conclusions).

P10 Evolution Across Columbidae

Our ancestral state reconstruction analyses indicated that P10 likely evolved at least 16 times independently across the clade where it is present in 56 species, and has likely only been lost in one species, *Ptilinopus dohertyi* (Fig. 6). The evolution of this morphology did not appear to depend on the terrestrial or arboreal foraging habits of a species (p=0.98; Pagel, 1994) as has been hypothesized in the past (Goodwin, 1983; Mahler and Tubaro, 2001), though our analyses did indicate that the transition from terrestrial to arboreal foraging habits may depend on P10 morphology (p=0.01). This trend is driven by the *Ptilinopus-Ducula* clade which is almost exclusively arboreal and one of the largest clades in the family. This group features 36 of the 56 (64%) columbid species with a specialized P10 and 96 of the 135 (71%) species that forage arboreally. This pattern of foraging habit and P10 morphology, where arboreality evolved once in the clade and a specialized P10 evolved multiple times, is an example of an unreplicated burst – a form of pseudoreplication to which Pagel's phylogenetic tests of trait independence are often susceptible (Maddison and Fitzjohn, 2015). Given that the remaining 20 species with a specialized P10 are not arboreal, we conclude that the significance of arboreality's dependence on P10 morphology is overestimated.

Conclusions

The morphologically atypical P10 feathers found in 56 species of columbids are likely specialized for aerodynamic performance and not sonation. In other species, similarly-shaped P10 feathers appear to function in signaling, producing sounds during flight to communicate alarm or to display to potential mates. Comparing wing sounds in free-flying diamond doves with those produced by isolated feathers and dried, spead, whole-wing prepartions revealed that P10 influences wing sounds but is not its source and is not required for sound production to occur. Instead, P10 improved whole-wing aerodynamic performance in emulated gliding and flapping flight. Specifically, P10 decreased the coefficient of drag (C_D) during emulated gliding across all angles of attack (α). In emulated flapping, P10 had an aerodynamically beneficial effect at moderate α ($20\text{-}30^o$) where it increased coefficient of lift (C_L) and decreased C_D, dramatically improving performance. The aerodynamic mechanisms responsible for the effects of P10 remain to be revealed, but we hypothesize that P10 generates a tip vortex that interacts with adjacent slotted primaries to improve span efficiency and reduce induced drag during gliding or cruising flight at low wingbeat amplitude (KleinHeerenbrink et al., 2017) or is shed over the surface of a vigorously flapping wings at $\alpha = 20\text{-}30^o$ to increase lift like the alula, as described in passerines engaged in flight at low advance ratios (Lee et al., 2015). This unique P10 feather in pigeons and doves appears to be a specialized aerodynamic device that, like other morphologically atypical flight feathers (e.g. tail feathers in Hirundines; Rowe et al., 2001), may influence signaling but, in this case, is not specialized to do so.

MATERIALS AND METHODS

Study animals and *in vivo* sound production

Six Diamond Doves (*Geopelia cuneata*) were purchased from commercial providers and allowed to breed, eat, and drink ad libitum in a small aviary (2 x 2 x 2.3m). Two additional birds sired by these original six were included in this study after they had molted into their adult plumage. All eight birds performed between 3 and 20 flights motivated by a pursuing researcher, where they flew vertically in a narrow, high-ceilinged room, horizontally in a long, low-ceilinged flight corridor, and/or haphazardly in an open space. Each bird performed at least one vertical and one horizontal flight. For two individuals that reliably produced tones during all control flights, we proceeded to remove the outermost primary feather (P10) on each wing and recorded a new set of three flights for each bird. For all birds, flight tests were only performed if the individual possessed fully intact outermost primaries (P10, P9, and P8). For all flights, audio was recorded to computer at 16-bits sampling at 44.1kHz through an audio interface (Raven Pro, v.1.4, Cornell Lab of Ornithology Bioacoustics Research Program, Ithaca, NY, USA) and preamplifier (Roland QUAD-CAPTURE UA-55, Roland Corporation, Hamamatsu, Japan) using a Sennheiser ME67 shotgun microphone (Sennheiser Electronic, Wedemark, Germany) set approximately two meters away from the point of take-off. Audio analyses are described below.

All experiments and protocols were approved by the University of Montana Institutional Animal Care and Use Committee (AUP: 049-16BTDBS-080316).

Emulating flapping flight

Five of the above doves, for which *in vivo* tonal wing sounds had already been recorded, died of natural causes or were euthanized (using approved protocols, see above), and one wing from each individual was removed at the humerus and dried in a spread position approximating mid-downstroke. P10 and P9 feathers were removed from the opposite wing of three of these deceased birds. Both wings and feathers were mounted on brass rods and spun using a brushless DC motor (BL3056 Series Motor, BPMC Technology Ltd., Tsuen Wan, Hong Kong) controlled using a Luminary Micro Stellaris BLDC Motor Control Module (MDL-BLDC, Luminary Micro/Texas Instruments, Austin, TX, USA) as described by Niese and Tobalske (2016). Wings were then spun at three angular velocities (ω) and seven angles of attack (α; every ten degrees from 0 to 60°; measured at rest) to emulate flapping flight (Usherwood, 2009). Angles of attack were referenced to be parallel to the line between the wrist and the tip of the first secondary feather (S1) for all wings. Feathers were spun at 0° as measured at rest and referenced to the proximal 1/3 of the inner vane (Niese and Tobalske, 2016). Angular velocities were calculated from high speed video of doves in take-off as described by Provini and others (2012), and correspond to the average downstroke velocity of the wingtip (*v*) during the first six wingbeats (10.6 m s^{-1}), peak downstroke velocity of wingbeat three (15.7 m s^{-1}), and peak downstroke velocity of wingbeat four (14.4 m s^{-1}) where wing sounds regularly occurred. For spinning wings, which were all similar in length, these linear velocities correspond to angular velocities of 89, 131, and 120 rad s^{-1} respectively. Feathers were spun at angular velocities to match the tip velocities measured *in vivo* and corresponded to 100-209 rad s^{-1} depending on their lengths. The sounds produced by spinning feathers and wings were recorded using the shotgun microphone, preamplifier, and audio software described above and analyzed in Raven (see below).

To measure the aerodynamic forces produced by wings in emulated flapping flight, spinning wings were mounted on a custom-built force plate (15x15 cm, Bertec Corp., Columbus, OH, USA) where we measured vertical force due to lift along the y-axis and torque about the z-axis due to drag as described by Crandell and Tobalske (2011) and Usherwood and Ellington (2002). In short, vertical and horizontal absolute forces (N) were converted to coefficients of vertical and horizontal force which depend on air density (1.07 kg m^{-3} for Missoula, MT, USA), angular velocity (ω), and the second and third moments of area of a given wing (Crandell and Tobalske, 2011, eq. 1 and 2, respectively). The surface area, and subsequently the second and third moments of area, were calculated from photographs of individual wings using ImageJ (v1.43u, National Institutes of Health, Bethesda, MA, USA). Coefficients of vertical and horizontal force were subsequently converted to dimensionless coefficients of lift (C_L) and drag (C_D) using estimates of the local angle of induced velocities along each wing (Crandell and Tobalske, eq. 3 and 4, respectively). These coefficients are directly comparable to those calculated from forces measured in the wind tunnel emulating gliding flight (below).

Following force measurements in the wind tunnel (see below), the P10 feather of each wing was removed (plucked) and wings were re-tested to measure their sound- and force-production at the same three ω and the same seven α. New photographs and calculations of the first, second, and third moments of area were acquired for each wing, but the overall length of wings was not altered by the removal of P10.

Emulating gliding flight

Force production was measured in a custom built wind tunnel (Hedrick et al., 2002) where all five wings were flown at a translational flight speed of 8 m s^{-1} and rotated through a broad range of α to emulate gliding flight. Wings were mounted to the abovementioned force plate via a stepper motor (NEMA 23, 23W108D-LW8, Anaheim Automation, Inc., Anaheim, CA, USA) which rotated wings every 3 degrees from approximately -30 to 100°. Both the force plate and stepper motor were placed outside the working section of the wind tunnel so as not to interact with flow. Angle of attack was *a posteriori* set to be 0° at the orientation at which vertical forces were closest to zero for a given wing. Absolute measurements of vertical and horizontal force were converted to dimensionless coefficients of lift and drag given the air density, tunnel flow velocity (8 m s^{-1}) and surface area of each wing.

Following force measurements and acoustic data collection from intact wings, P10 was removed from each specimen and all wings were re-tested to measure their force- and sound-production as described above for intact specimens. The surface area of each wing was recalculated following feather removal.

Wing sounds could not be recorded in this wind tunnel, but individual feathers were recorded in an aeroacoustic wind tunnel (Clark and Mistick, 2018a) at velocities between approximately 12.5 and 15.5 m s^{-1} and angles of attack between approximately -90 and 90° to determine the orientations and speeds at which the strongest tones were produced.

Data processing and statistical analyses

Audio analyses were conducted in Raven software (see above). For recordings of live birds in flight, we visualized spectrograms using the Hann window function with a window size of 1300 samples and a 2048-sample FFT frequency grid, and we measured the tonality and frequency of flight sounds using the average entropy and peak frequency functions, respectively, on data selections of similar bandwidth and duration (Niese and Tobalske, 2016). For spinning wings and feathers, spectrograms were visualized with a Hann window size of 10,000 samples (Niese and Tobalske, 2016), and as in live bird flights, we measured the peak frequency and average entropy of selections of similar bandwidth and duration.

Statistical analyses were conducted in SPSS (v.24, IBM, Armonk, NY, USA) and Excel (v.16, Microsoft Corporation, Redmond, WA, USA) software. Three paired t-tests were used to compare the tonal content of sounds produced by wings spun across all α, within a given ω, before and after P10 removal (with a Bonferroni adjusted p-value of 0.017). A chi-squared comparison was used to determine whether the rate at which wings produced tones changed before and after feather removal. For wings in the wind tunnel, we calculated the pair-wise change in force coefficients before and after P10 removal and determined whether or not the distribution of those changes in force coefficients was statistically different from 0 using a chi-squared analysis. Furthermore, we tested whether peak coefficients of force (as well as peak C_L:C_D) were different or peaked at a different angle in intact wings compared to wings without P10 (six paired t-tests; Supplemental Data). For spinning wings, we compared peak C_L:C_D before and after feather removal across all three angular velocities using a Wilcoxon signed rank sum test.

Supplementally, for spinning wings we also calculated the pair-wise change in force coefficients before and after P10 removal, then evaluated the regression model that best explained how the change in force coefficients changed with angle of attack to determine if this relationship was statistically variable or invariable. We expect this relationship to be invariable (i.e. linear) if wings simply decreased their force-producing ability. This polynomial regression model selection was performed for all angular velocities and both coefficient of forces, and a quadratic non-linear regression model was the best model that fit every relationship (model selection summary Supplemental Table 1).

Ancestral state reconstructions and trait dependencies

In order to better understand the evolutionary history of this unique morphology, we compiled data (Baptista et al., 2019; Mahler and Tubaro, 2001) regarding 282 of the approximately 350 species of pigeons and doves and reconstructed the ancestral states of their P10 feathers. Using nuclear and mitochondrial nucleotide phylogenies published by Cibois et al. (2014; 2017), Johnson and Weckstein (2011), Johnson et al. (2001), Moyle et al. (2013), Pereira et al. (2007), and Sweet et al. (2017), we constructed a phylogram for the entire Columbidae. This phylogram includes polytomies where the abovementioned trees disagreed or were uncertain, such as those in *Ducula* (reflecting uncertainties discussed by Cibois and others; 2017) or in the clade of Australasian ground doves that includes *Gymnophaps* and *Geopelia* (which reflects a common disagreement among the above phylogenies). Additionally, some species for which no genetic data exists have been added based on assumed relations (Baptista et al., 2019) if they possess a modified P10 or are in a clade where the morphology is particularly variable. These species include *Ducula poliocephala* which is considered conspecific with *D. forsteni*, *D. carola* which is thought to be sister to the *D. poliocephala* group (a polytomic node), *Ptilinopus fischeri* which is closely allied to *P. occipitalis*, *P. dohertyi* and *P. alligator* which appear to be closely related to *P. cinctus* and *P. porphyreus* (polytomic), and *Columbina cyanopis* which has been included in a large polytomic node that is unresolved (Sweet et al., 2017). For simplicity, some species were removed and are represented by a single member (*Treron*, *Reinwardtoena*, *Turacoena*, *Goura*) or a few members (*Streptopelia*, *Columba*, *Patagioenas*) of their well-supported clades if they lack the P10 morphology investigated here and their removal did not alter the reconstructed ancestral states of nearby nodes (215 remaining species). We determined the ancestral state of P10 using a maximum likelihood approach with an Mk1 rate model with all branch lengths set to be equal. In a comparative dataset where branch lengths were proportional and ultrametric (see below) but included fewer species (N=153), identical nodes (where the number and branching relationships between species were the same) only showed a slight change (<10%) in likelihoods. Thus, there are only two groups of nodes that might be strongly influenced by the inclusion of proportional branch lengths: the two basal-most nodes in the *Ptilinopus solomonensis-P. viridis* clade, and the three basal-most nodes (one which is polytomic) of the *Claravis-Metriopelia* clade.

Given the broad distribution of the specialized P10 feather across the Columbidae, and evidence that it improves aerodynamic performance in flapping (see Results and Discussion), we attempted to determine whether the feather's morphology was dependent on a species' foraging habits. We categorized species as terrestrial if they regularly or sometimes foraged on the ground (N=107), and categorized species as strictly arboreal if they rarely foraged on the ground (N=46; Baptista et al., 2019). Using an ultrametric tree estimated from Bayesian analyses of six mitochondrial and three nuclear genes for 153 species (alignments from Lapiedra et al., 2013), we assessed the independence of P10 morphology and foraging habits using a modified version of Pagel's method (1994) for comparing the evolution of binary traits (Midford and Maddison, 2006). This method does not account for the pseudoreplicative effect of correlating synapomorphic traits across multiple species that could instead be ascribed to single correlated evolutionary event for the clade (Maddison and Fitzjohn, 2015). Significance was estimated from 1000 Monte Carlo simulations of the observed likelihood ratios estimated from 50 search iterations each. Significant results were assessed for potential pseudoreplicated events (see Results and Discussion).

All reconstruction analyses and tests of trait independence were performed in Mesquite (v.3.6; Maddison and Maddison, 2018). The phylogram used in ancestral state reconstruction analyses was manually constructed in Mesquite. The ultrametric phylogenetic tree used to compare with the phylogram and to assess trait independence was generated using BEAUti and the BEAST (v.1.10.4; Drummond et al., 2012). This ultrametric tree was estimated according to Lapiedra and others (2013) where analyses were run four times for $1\text{x}10^7$ generations each, sampling every 10,000 generations (excluding the first 10% of generations as burn-in) and combined using LogCombiner v.1.10.4 (included in the BEAST package). The branching topology of the final tree did not differ from expected patterns (Lapiedra et al., 2013).

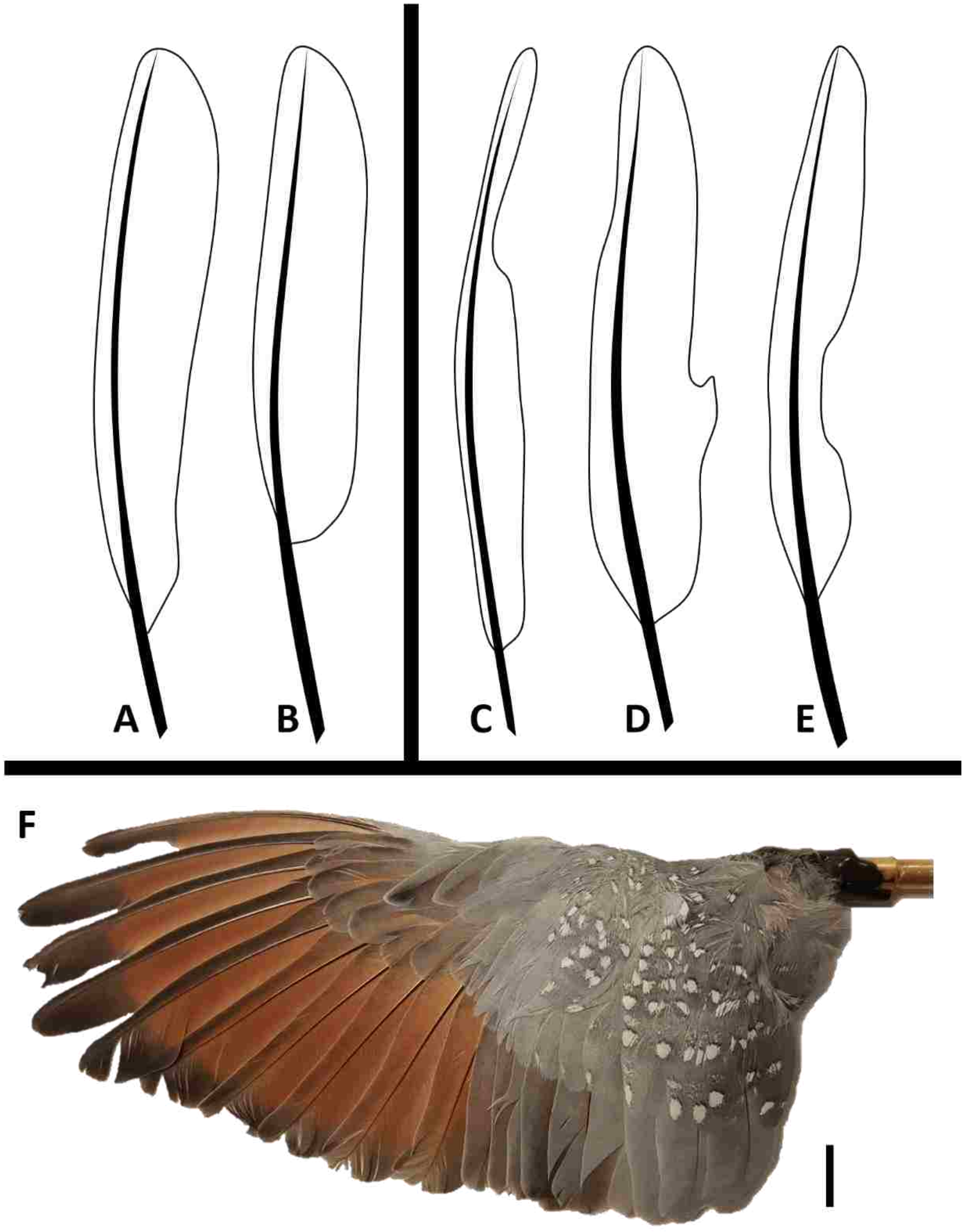

FIGURE 1. Primary feathers can be aerodynamically stereotyped (A, B), but occasionally display unique morphologies (C, D, E, F). (A) P6 feather in the House Finch (*Haemorhous mexicanus*; Passeriformes, Fringillidae). (B) P6 feather in the Trumpeter Swan (*Cygnus buccinator*; Anseriformes, Anatidae). (C) P10 feather in the Yungas Dove (*Leptotila megalura*; Columbiformes, Columbidae). (D) P7 feather in the Common Ground Dove (*Columbina passerina*; Columbiformes, Columbidae). (E) P8 feather in the Pink-necked Green Pigeon (*Treron verans*; Columbiformes, Columbidae). (F) Diamond Doves (*Geopelia cuneata*; Columbiformes,

Columbidae) wings possess a unique P10 feather like that in C. Scale bar for F is 10mm. All feathers (A-E) scaled to be similar heights.

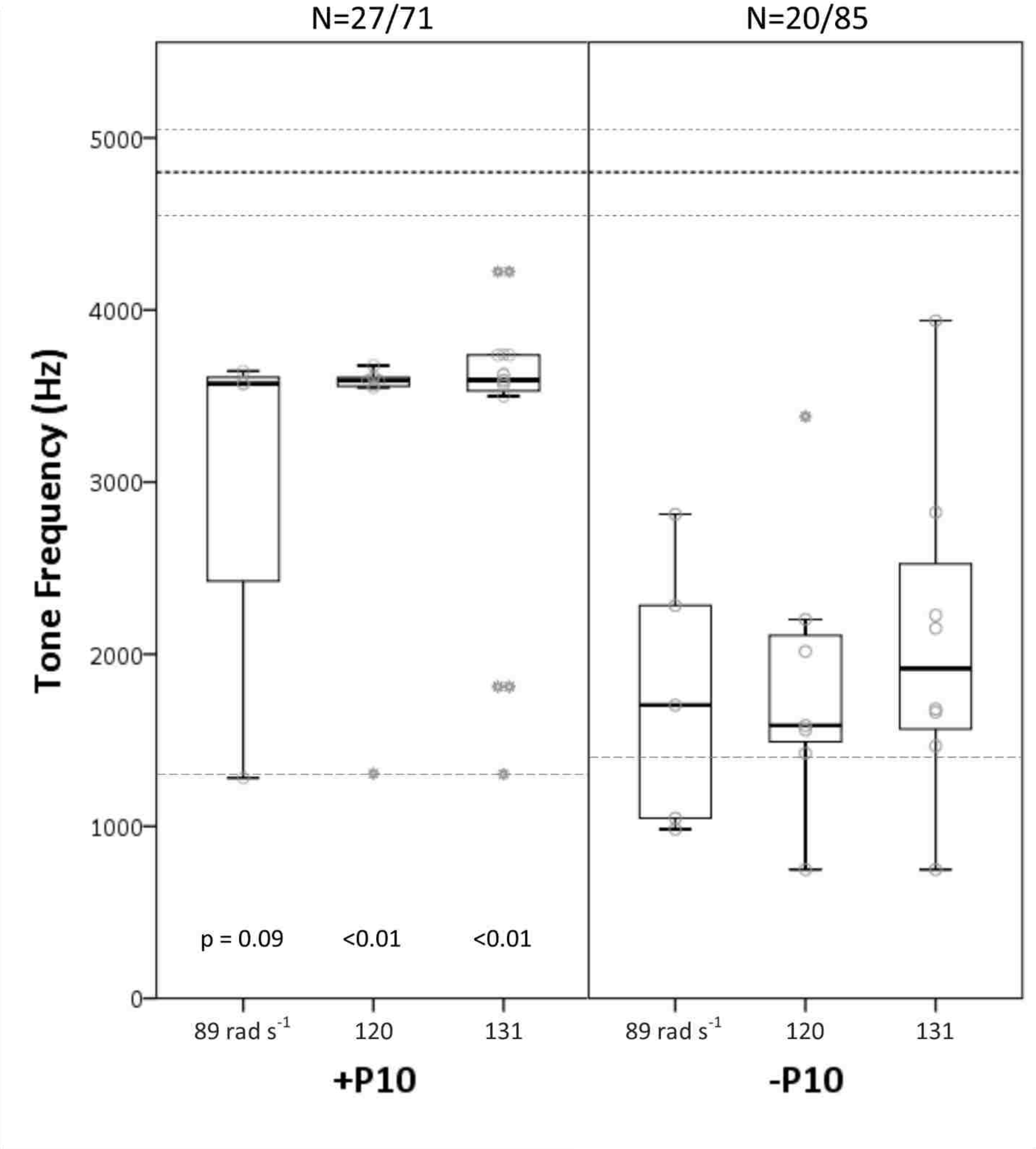

FIGURE 2. Distributions of tones produced by spinning wings at three different angular velocities with and without P10. Dashed lines at 4800±250 Hz indicates the tones produced *in vivo*. Dashed lines at 1300Hz and 1400Hz indicate tones produced by P10 feathers individually and P9 feathers individually (respectively). P-values indicate the significance of pairwise

changes in the mean tone frequency produced by spinning wings after P10 feathers had been removed.

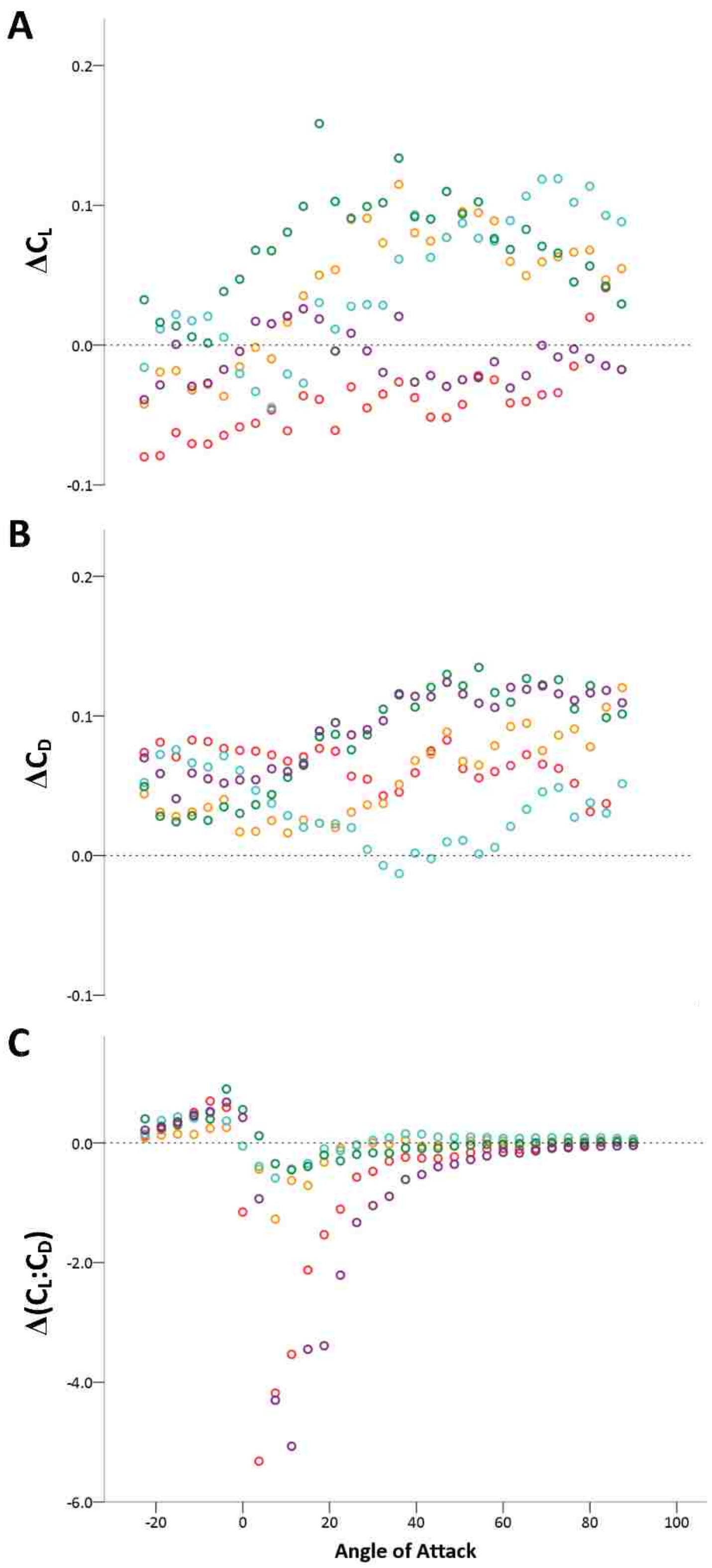

FIGURE 3. **Coefficients of lift and drag (C_L and C_D) as a function of angle of attack (α) obtained from dried, spread diamond dove wings (n = 5) during emulated gliding flight.** A) Difference in C_L obtained by subtracting the value of C_L from an intact wing from the value of C_L after P10 was removed from the wing. B) Difference in C_D obtained by subtracting the value of C_D from an intact wing from the value of C_D after P10 was removed from the wing. . C) Difference in the ratio of C_L:C_D due to P10 removal. All points color-coded for individual birds as in Figure 4. For all panels, positive values indicate the dependent variable was greater after P10 was removed.

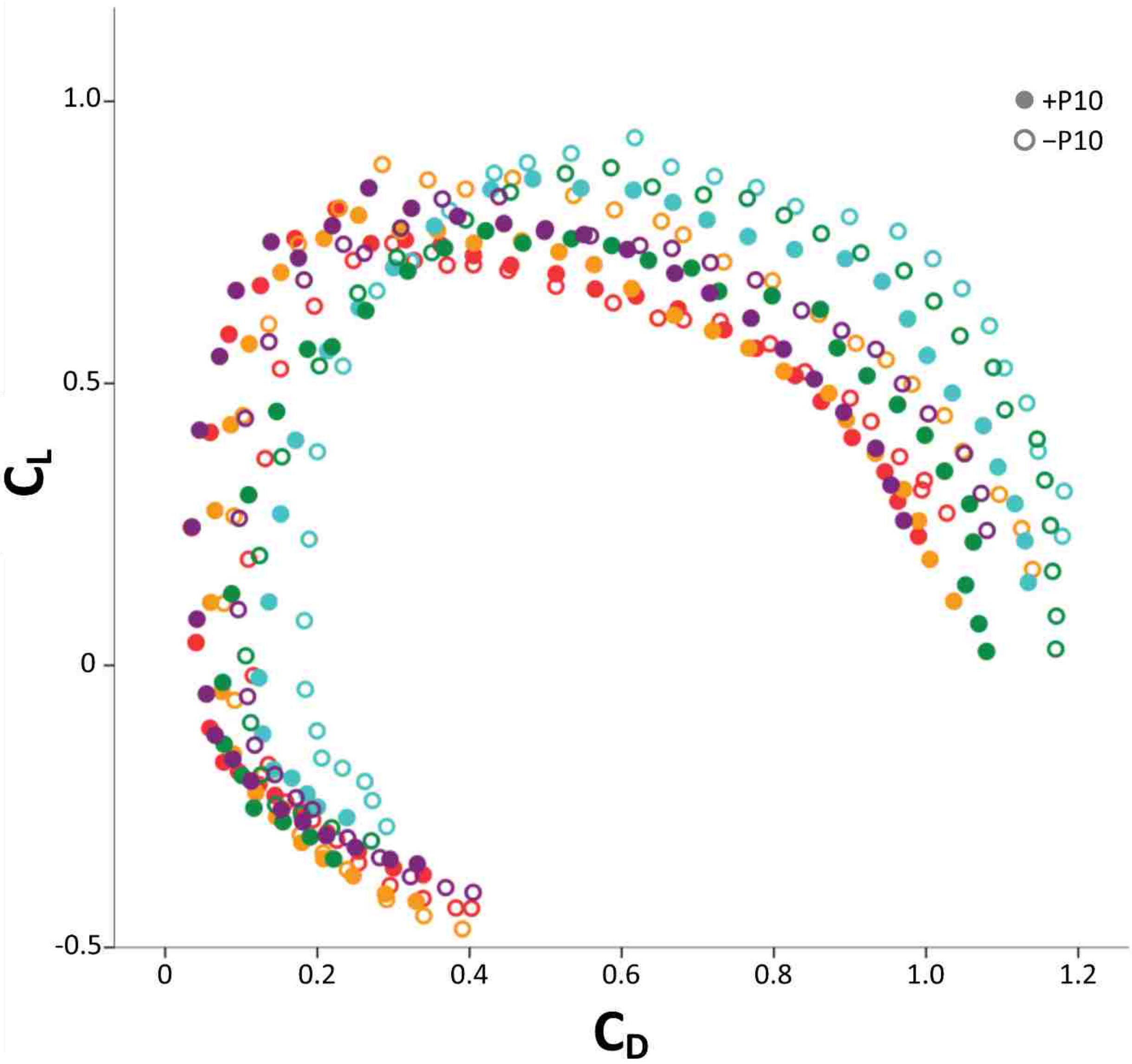

FIGURE 4. Lift-drag (C_L and C_D) polar curves obtained from dried, spread diamond dove wings (n = 5) during emulated gliding flight. Closed points indicate measurements from intact wings (+P10). Open circles indicate measurements from wings after P10 had been removed (-P10). Colors represent the same individuals as in Figure 3.

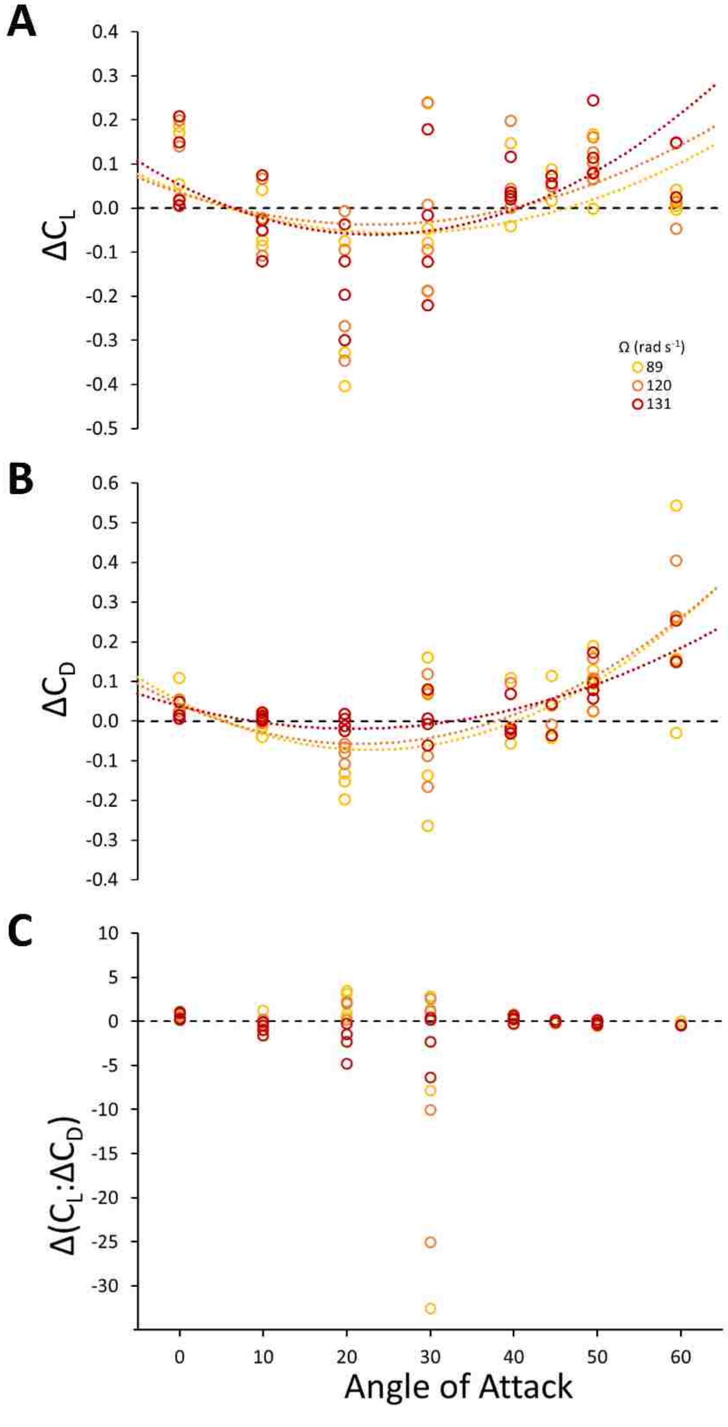

FIGURE 5. Coefficients of lift and drag (C_L and C_D) as a function of angle of attack (α) and angular velocity (w) obtained from dried, spread diamond dove wings (n = 5) during emulated flapping flight. A) Difference in C_L obtained by subtracting the value of C_L from an intact wing from the value of C_L after P10 was removed from the wing. B) Difference in C_D obtained by subtracting the value of C_D from an intact wing from the value of C_D after P10 was removed from the wing. C) Difference in the ratio of C_L:C_D due to P10 removal. All points color-coded for angular velocity (ω). In A, B, and C, positive values indicate the dependent variable was greater in the modified (P10 removed) wing.


P10
P10
unknown
Ptilinopus viridis
Ptilinopus eugeniae
Ptilinopus iozonus
Ptilinopus ornatus
Ptilinopus aurantiifrons
Ptilinopus wallacii
Ptilinopus perlatus
Ptilinopus hyogastrus
Ptilinopus tannensis
Ptilinopus dupetithouarsii
Ptilinopus mercierii
Ptilinopus perousii
Ptilinopus huttoni
Ptilinopus insularis
Ptilinopus chalcurus
Ptilinopus coralensis
Ptilinopus purpuratus chrysogaster
Ptilinopus rarotongensis
Ptilinopus purpuratus purpuratus
Ptilinopus purpuratus frater
Ptilinopus greyi
Ptilinopus porphyraceus
Ptilinopus pelewensis
Ptilinopus richardsii
Ptilinopus roseicapilla
Ptilinopus coronulatus
Ptilinopus regina
Ptilinopus monacha
Ptilinopus pulchellus
Ptilinopus superbus
Ptilinopus rivoli
Ptilinopus solomonensis
Ptilinopus porphyreus
Ptilinopus dohertyi
Ptilinopus cinctus
Ptilinopus melanospilus
Ptilinopus nainus
Ptilinopus luteovirens
Ptilinopus layardi
Ptilinopus victor
Drepanoptila holosericea
Alectroenas sganzini
Alectroenas nitidissima
Alectroenas madagascariensis
Alectroenas pulcherrimus
Ptilinopus leclancheri
Ptilinopus subgularis
Ptilinopus jambu
Ptilinopus fischeri
Ptilinopus occipitalis
Ptilinopus merrilli
Ptilinopus marchei
Ptilinopus bernsteinii
Ptilinopus magnificus
Gymnophaps albertisii
Lopholaimus antarcticus
Hemiphaga novaeseelandiae
Ducula rufigaster
Ducula chalconota
Ducula finschii
Ducula basilica
Ducula cineracea
Ducula lacernulata
Ducula badia
Ducula carola
Ducula radiata
Ducula mindorensis
Ducula poliocephala
Ducula forsteni
Ducula galeata
Ducula oceanica
Ducula aurorae
Ducula pacifica
Ducula myristicivora
Ducula rubricera
Ducula pistrinaria
Ducula whartoni
Ducula rosacea
Ducula pickeringii
Ducula perspicillata
Ducula concinna
Ducula aenea
Ducula zoeae
Ducula latrans
Ducula goliath
Ducula pinon
Ducula melanochroa
Ducula bakeri
Ducula mullerii
Ducula brenchleyi
Ducula luctuosa
Ducula bicolor
Ducula spilorrhoa
Phapitreron amethystina
Chalcophaps stephani
Turtur brehmeri
Oena capensis
Turtur tympanistria
Turtur afer
Turtur abyssinicus
Turtur chalcospilos
Treron calvus
Trugon terrestris
Goura victoria
Henicophaps albifrons
Gallicolumba sanctaecrucis
Claravis pretiosa
Metriopelia aymara
Streptopelia decaocto
Geotrygon chiriquensis

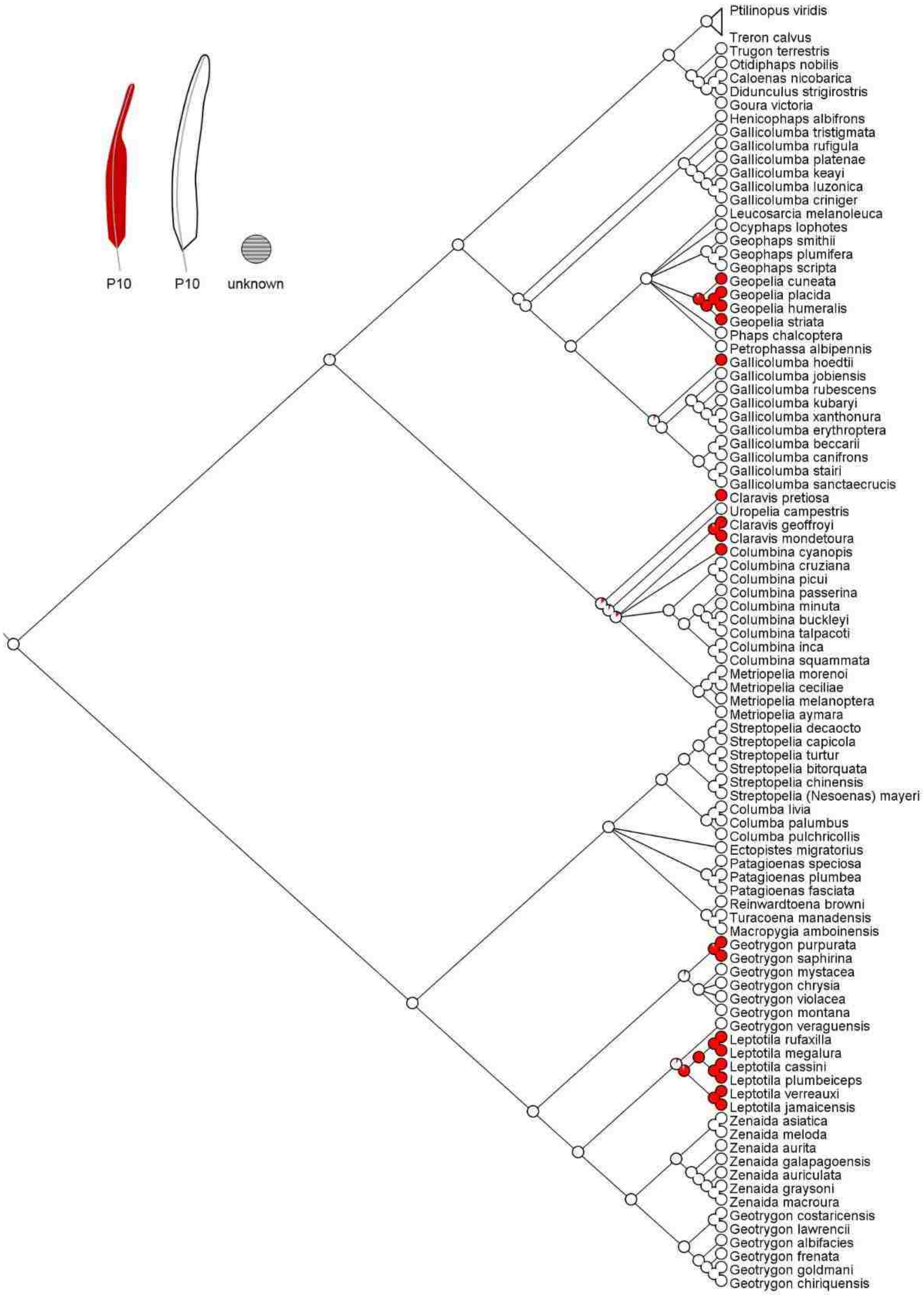

FIGURE 6. Ancestral state reconstructions of P10 morphology across Columbidae. Tree based on the combined nuclear and mitochondrial nucleotide phylogenies published by Cibois et al. (2014; 2017), Johnson and Weckstein (2011), Johnson et al. (2001), Moyle et al. (2013), Pereira

et al. (2007), and Sweet et al. (2017). Maximum likelihood ancestral state reconstructions of the specialized P10 feather indicate that this morphology has independently evolved at least 16 times and has only been lost once (*Ptilinopus dohertyi*). For visual simplicity, some species have been collapsed to be represented only at the genus-level if their clade lacks P10 specializations, but were included in analyses (see text).

SUPPLEMENTAL TABLE 1. Polynomial regression model selection values

ΔC_F	ω	Model	R^2	F	df	p
ΔC_L	89 rad s^{-1}	Variable $\Delta C_F \propto \alpha$	0.136	2.13	2,27	0.0655
ΔC_L	120 rad s^{-1}	Variable $\Delta C_F \propto \alpha$	0.151	2.32	2,26	0.0833
ΔC_L	131 rad s^{-1}	Variable $\Delta C_F \propto \alpha$	0.312	5.68	2,25	0.0064
ΔC_L	All	Variable $\Delta C_F \propto \alpha$	0.178	9.08	2,84	0.0003
ΔC_D	89 rad s^{-1}	Variable $\Delta C_F \propto \alpha$	0.447	10.9	2,27	0.0010
ΔC_D	120 rad s^{-1}	Variable $\Delta C_F \propto \alpha$	0.656	24.8	2,26	0.0000
ΔC_D	131 rad s^{-1}	Variable $\Delta C_F \propto \alpha$	0.618	20.2	2,25	0.0001
ΔC_D	All	Variable $\Delta C_F \propto \alpha$	0.510	43.7	2,84	0.0000
ΔC_L	89 rad s^{-1}	Invariable $\Delta C_F \propto \alpha$	0.019	0.53	1,28	0.4723
ΔC_L	120 rad s^{-1}	Invariable $\Delta C_F \propto \alpha$	0.045	1.28	1,27	0.2678
ΔC_L	131 rad s^{-1}	Invariable $\Delta C_F \propto \alpha$	0.069	1.91	1,26	0.1783
ΔC_L	All	Invariable $\Delta C_F \propto \alpha$	0.039	3.44	1,85	0.0671
ΔC_D	89 rad s^{-1}	Invariable $\Delta C_F \propto \alpha$	0.170	5.75	1,28	0.0234
ΔC_D	120 rad s^{-1}	Invariable $\Delta C_F \propto \alpha$	0.278	10.4	1,27	0.0033
ΔC_D	131 rad s^{-1}	Invariable $\Delta C_F \propto \alpha$	0.259	9.11	1,26	0.0056
ΔC_D	All	Invariable $\Delta C_F \propto \alpha$	0.204	21.7	1,85	0.0000

REFERENCES

Averill, C. K. (1927). Emargination of the Long Primaries in Relation to Power of Flight and Migration. *Condor* **29**, 17–18.

Baptista, L. F., Trail, P. and Horblit, H. M. (2019). Family Columbidae (Pigeons and Doves). *Handb. Birds World Alive*.

Cibois, A., Thibault, J.-C., Bonillo, C., Filardi, C. E., Watling, D. and Pasquet, E. (2014). Phylogeny and biogeography of the fruit doves (Aves: Columbidae). *Mol. Phylogenet. Evol.* **70**, 442–53.

Cibois, A., Thibault, J. C., Bonillo, C., Filardi, C. E. and Pasquet, E. (2017). Phylogeny and biogeography of the imperial pigeons (Aves: Columbidae) in the Pacific Ocean. *Mol. Phylogenet. Evol.* **110**, 19–26.

Clark, C. J. (2018). Signal or cue? Locomotion-induced sounds and the evolution of communication. *Anim. Behav.* **143**, 83–91.

Clark, C. J. and Mistick, E. A. (2018a). Strategic Acoustic Control of a Hummingbird Courtship Dive. *Curr. Biol.* **28**, 1257–1264.e6.

Clark, C. J. and Mistick, E. A. (2018b). Kinematic control of male Allen's Hummingbird wing trill over a range of flight speeds. *J. Exp. Biol.* jeb.173625.

Clark, C. J. and Prum, R. O. (2015). Aeroelastic flutter of feathers, flight, and the evolution of nonvocal communication in birds. *J. Exp. Biol.* **218**, 3520–3527.

Clark, C. J., Elias, D. and Prum, R. O. (2011). Aeroelastic flutter produces hummingbird feather songs. *Science (80-.).* 1430–1433.

Cuvier, G. (1817). *The Animal Kingdom: Arranged According to Its Organisation*. Paris: Wm. S. Orr and Company.

DesRochers, D. W., Reed, J. M., Awerman, J., Kluge, J. A., Wilkinson, J., van Griethuijsen, L. I., Aman, J. and Romero, L. M. (2009). Exogenous and endogenous corticosterone alter feather quality. *Comp. Biochem. Physiol. - A Mol. Integr. Physiol.* **152**, 46–52.

Drovetski, S. (1996). Influence of the trailing-edge notch on flight performance of galliforms. *Auk* **113**, 802–810.

Drummond, A. J., Suchard, M. A., Xie, D. and Rambaut, A. (2012). Bayesian Phylogenetics with BEAUti and the BEAST 1.7. *Mol. Biol. Evol.* **29**, 1969–1973.

Echeverry-Galvis, M. A. and Hau, M. (2013). Flight Performance and Feather Quality: Paying the Price of Overlapping Moult and Breeding in a Tropical Highland Bird. *PLoS One* **8**,.

Feduccia, A. and Tordoff, H. B. (1979). Feathers of archaeopteryx: Asymmetric vanes indicate aerodynamic function. *Science (80-.).* **203**, 1021–1022.

Feo, T. J., Field, D. J. and Prum, R. O. (2015). Barb geometry of asymmetrical feathers reveals a transitional morphology in the evolution of avian flight. *Proc. R. Soc. B Biol. Sci.* **282**, 20142864.

Goodwin, D. (1983). *Pigeons and doves of the world*. Comstock Pub. Associates.

Hedenström, A. (2003). Flying with holey wings. *J. Avian Biol.* **34**, 324–327.

Hedrick, T. L., Tobalske, B. W. and Biewener, A. a (2002). Estimates of circulation and gait change based on a three-dimensional kinematic analysis of flight in cockatiels (Nymphicus hollandicus) and ringed turtle-doves (Streptopelia risoria). *J. Exp. Biol.* **205**, 1389–409.

Heers, A. M. and Dial, K. P. (2012). From extant to extinct: Locomotor ontogeny and the evolution of avian flight. *Trends Ecol. Evol.* **27**, 296–305.

Johnson, K. P. and Weckstein, J. D. (2011). The Central American land bridge as an engine of diversification in New World doves. *J. Biogeogr.* **38**, 1069–1076.

Johnson, K. P., de Kort, S., Dinwoodey, K., Mateman, A. C., ten Cate, C., Lessells, C. M. and Clayton, D. H. (2001). a Molecular Phylogeny of the Dove Genera Streptopelia and Columba. *Auk* **118**, 874.

Klaassen van Oorschot, B., Tang, H. K. and Tobalske, B. W. (2017). Phylogenetics and ecomorphology of emarginate primary feathers. *J. Morphol.* **278**, 936–947.

KleinHeerenbrink, M., Johansson, L. C. and Hedenström, A. (2017). Multi-cored vortices support function of slotted wing tips of birds in gliding and flapping flight. *J. R. Soc. Interface* **14**, 20170099.

Lapiedra, O., Sol, D., Carranza, S. and Beaulieu, J. M. (2013). Behavioural changes and the adaptive diversification of pigeons and doves. *Proc. R. Soc. B* **50**, 20122893.

Lee, S., Kim, J., Park, H., Jabłoński, P. G. and Choi, H. (2015). The Function of the Alula in Avian Flight. *Sci. Rep.* **5**, 9914.

Lucas, A. M. and Stettenheim, P. R. (1972). *Avian anatomy: integument*. Washington D.C.: United States Department of Agriculture; Agriculture handbook, no. 362.

Maddison, W. P. and Fitzjohn, R. G. (2015). The unsolved challenge to phylogenetic correlation tests for categorical characters. *Syst. Biol.* **64**, 127–136.

Maddison, D. R. and Maddison, W. P. (2018). Mesquite: A modular system for evolutionary analysis.

Mahler, B. and Tubaro, P. L. (2001). Attenuated Outer Primaries in Pigeons and Doves: a Comparative Test Fails To Support the Flight Performance Hypothesis. *Condor* **103**, 449.

Midford, P. and Maddison, W. P. (2006). Pagel94 Analysis Module for Mesquite.

Moyle, R. G., Jones, R. M. and Andersen, M. J. (2013). A reconsideration of Gallicolumba (Aves: Columbidae) relationships using fresh source material reveals pseudogenes, chimeras, and a novel phylogenetic hypothesis. *Mol. Phylogenet. Evol.* **66**, 1060–6.

Muijres, F. T., Johansson, L. C. and Hedenstrom, a. (2012). Leading edge vortex in a slow-flying passerine. *Biol. Lett.* **8**, 554–557.

Murray, T. G., Zeil, J. and Magrath, R. D. (2017). Sounds of Modified Flight Feathers Reliably Signal Danger in a Pigeon. *Curr. Biol.* **27**, 3520–3525.e4.

Niese, R. L. and Tobalske, B. W. (2016). Specialized primary feathers produce tonal sounds during flight in rock pigeons (Columba livia). *J. Exp. Biol.* **219**, 2173–81.

Pagel, M. D. (1994). Detecting correlated evolution on phylogenies: a general method for the comparative analysis of discrete characters. *Proc. R. Soc. London. Ser. B Biol. Sci.* **255**, 37–45.

Pereira, S. L., Johnson, K. P., Clayton, D. H. and Baker, A. J. (2007). Mitochondrial and nuclear DNA sequences support a Cretaceous origin of Columbiformes and a dispersal-driven radiation in the Paleocene . *Syst. Biol.* **56**, 656–72.

Provini, P., Tobalske, B. W., Crandell, K. E. and Abourachid, A. (2012). Transition from leg to wing forces during take-off in birds. *J. Exp. Biol.* 4115–4124.

Prum, R. O. and Brush, A. H. (2002). The evolutionary origin and diversification of feathers. *Q. Rev. Biol.* **78**, 275–301.

Prum, R. O. and Williamson, S. (2001). Theory of the growth and evolution of feather shape. *J. Exp. Zool.* **291**, 30–57.

Rowe, L. V., Evans, M. R. and Buchanan, K. L. (2001). The function and evolution of the tail streamer in hirundines. *Behav. Ecol.* **12**, 157–163.

Selby, P. J. (1850). The Natural History of Gallinaceous Birds: Columbidae or Pigeons. In *The Naturalist's Library: Ornithology* (ed. Jardine, W.), Lizars, W. H.), Smith, C. H.), and Stewart, J.), p. London: W. H. Lizars.

Stoddard, M. C. and Prum, R. O. (2011). How colorful are birds? Evolution of the avian plumage color gamut. *Behav. Ecol.* **22**, 1042–1052.

Swaddle, J. P., Witter, M. S., Cuthill, I. C., Budden, A. and McCowen, P. (1996). Plumage Condition Affects Flight Performance in Common Starlings: Implications for Developmental Homeostasis, Abrasion and Moult. *J. Avian Biol.* **27**, 103–111.

Swainson, W. (1825). On the characters and natural affinities of several birds from Australia; including some observations on the Colulmbidae. *Zool. J.* **1**, 463–484.

Sweet, A. D., Maddox, J. D. and Johnson, K. P. (2017). A complete molecular phylogeny of Claravis confirms its paraphyly within small New World ground-doves (Aves: Peristerinae) and implies multiple plumage state transitions. *J. Avian Biol.* **48**, 459–464.

Tucker, V. (1993). Gliding birds: reduction of induced drag by wing tip slots between the primary feathers. *J. Exp. Biol.* **180**, 285–310.

Usherwood, J. R. (2009). The aerodynamic forces and pressure distribution of a revolving pigeon wing. *Exp. Fluids* **46**, 991–1003.

Usherwood, J. R. and Ellington, C. P. (2002). The aerodynamics of revolving wings I. Model hawkmoth wings. *J. Exp. Biol.* **205**, 1547–1564.

CHAPTER 3

Specialized primary feathers produce tonal sounds during flight in rock pigeons (*Columba livia*)

Robert L. Niese and Bret W. Tobalske

Field Research Station at Fort Missoula, Division of Biological Sciences, University of Montana, Missoula, MT 59812, USA

ABSTRACT

For centuries, naturalists have suggested that the tonal elements of pigeon wing sounds may be sonations (non-vocal acoustic signals) of alarm. However, spurious tonal sounds are produced passively by the flight feathers of almost all birds when they aeroelastically flutter. Using mechanistic criteria emerging from recent work on sonations, we sought to: 1) identify characteristics of rock pigeon flight feathers that might be adapted for sound production rather than flight, and 2) provide evidence that this morphology is necessary for *in vivo* sound production and is entirely sufficient to replicate *in vivo* sounds. Our investigations revealed that birds produce tonal sounds (700±50Hz) during the latter 2/3 of downstroke during take-off. These tones are produced when a small region of long, curved barbs on the inner vane of the outermost primary feather (P10) begins to flutter. Tones were silenced in live birds when we experimentally increased the stiffness of this region, thus preventing flutter. Isolated P10 feathers were sufficient to reproduce *in vivo* sounds when spun at the peak angular velocity of

downstroke (53.9-60.3 rad s^{-1}), but did not produce tones at the average velocity (31.8 rad s^{-1}), while P9 and P1 feathers never produced tones. Furthermore, P10 feathers had significantly lower coefficients of resultant force (C_R) when spun at peak angular velocity than at average angular velocity. P9 and P1 feathers did not show this difference in C_R. These mechanistic results suggest that the tonal sounds produced by P10 feathers are not purely incidental and may be communicatively significant.

INTRODUCTION

Sound is an intrinsic byproduct of all motion in the natural world. Perceptible motion-induced sound plays a critical role in the lives of all multicellular organisms including plants (Appel and Cocroft, 2014) and perhaps even single-celled eukaryotes (Kolle-Kralik and Ruff, 1967). Motion-induced sound can act as a record of any biotic or abiotic movement, thus making it inherently informative (i.e. a cue). Nearly all animals possess the ability to detect this sound (Budelmann, 1989; Budelmann, 1992; Fay, 2009; Horch, 1971), and many may go to great lengths to mask their own locomotion-induced sounds (Conner, 2014; Graham, 1934; Roche et al., 1999). Conversely, however, many species have also developed remarkable ways to amplify and otherwise modulate these motion-induced sounds for communicative purposes (Bostwick, 2006; Darwin, 1871).

Arguably, all aural communication – from the relatively simple sounds produced by stridulating insects (Darwin, 1871, 10), to the vast complexity of human language (Larsson, 2014) – can trace its origins to incidental, motion-induced sounds. This evolutionary link between incidental sounds and communicative signals is perhaps most easily explored in birds where motion-induced sounds associated with courtship behaviors can become the subject of novel female preferences, exaggerating them into complex signals (e.g. strut displays in Greater Sage Grouse, wing-snapping displays in Manakins; Prum, 1998). These non-vocal acoustic signals, or sonations, are common among birds, perhaps due to the inherently noisy nature of feathers, wings, and flight (Fournier et al., 2013; Wei et al., 2013).

Incidental sounds produced during flight are ubiquitous among volant birds (except perhaps owls: Graham, 1934) and are, in part, due to the natural propensity of all stiff, light airfoils (e.g.

feathers) to aeroelastically flutter under certain flow conditions (Clark et al., 2011b; Clark et al., 2013b; Clark et al., 2013a). Specifically, aerodynamic energy input from flow over an airfoil excites one or more resonance frequencies within the airfoil. Above a certain threshold (critical velocity, U*), energy input from the airflow exceeds the structural damping of the airfoil (inertial and elastic forces), causing it to enter stable oscillations (Clark et al., 2011b; Clark et al., 2013b; Clark et al., 2013a). Feathers that enter these aeroelastic oscillations produce tones whose pitch, amplitude, and harmonic content are dependent on complex interactions between flow conditions and the structural, resonance properties of a given feather (Clark et al., 2013b; Clark et al., 2013a). In addition to aeroelastic, tonal sounds, feathers and wings can also produce atonal sounds as turbulence is shed in their wake (Blake, 1986; Wei et al., 2013) or as flutter causes collisions between adjacent feathers (Clark, 2011). Together, these passive mechanisms of tonal and atonal sound production make flight an inherently noisy mode of locomotion, suggesting that feather sonations could evolve easily and repeatedly among birds. The ways in which aeroelastically fluttering feathers have been evolutionarily co-opted for communication have been thoroughly described in two taxa (Pipridae: Bostwick and Prum, 2003; Bostwick et al., 2010; Prum, 1994; Prum, 1998; and Trochilidae: Clark, 2008; Clark and Feo, 2010; Clark et al., 2011; Hunter, 2008) and have been implicated in many others (Bostwick, 2006).

In many of these sonating species, selection for specific behaviors and sounds may have led to the evolution of feather morphologies specialized for sound-production, particularly in sexually-selected displays (Clark and Feo, 2010). While the link between particular morphologies and their sound-producing abilities is tenuous, ornithologists have nevertheless hypothesized a direct connection between unique shape and sound in many species (Bahr, 1907; Craig, 1984; Hingee and Magrath, 2009b; Johnston, 1960; Wetmore, 1926), while, in many others, sounds are produced in the complete absence of obvious feather morphologies (Clark, 2008; Coleman, 2008; Lebret, 1958).

Historically, no group has received quite as much attention in this regard as the pigeons and doves whose wing sounds and unique feather morphologies have intrigued naturalists for nearly three centuries (Audubon, 1831; Craig, 1911b; Cuvier, 1817a; Darwin, 1871; Edwards, 1743; Edwards, 1760; Selby, 1850; Wilson, 1808). In spite of this impressive record of observations, the wing sounds and feather morphologies of these species have never been experimentally linked. Others (Barrera et al., 2011; Coleman, 2008; Hingee and Magrath, 2009b) have attempted to link wing sounds to anti-predator behaviors, claiming that sounds produced by the wings during alarmed take-off (specifically tonal elements of wing sounds, i.e. “whistles”) are signals of alarm (Barrera et al., 2011; Hingee and Magrath, 2009b). But the sounds of wings flapping are inherently informative (i.e. cues) because they are intrinsically linked to locomotion, and we expect all listeners to have evolved some response to them (Maynard Smith and Harper, 2003). The fact that these wing sounds contain tonal elements is not sufficient evidence to conclude that they are an evolved signal because all flight feathers possess the ability to produce tonal sounds through aeroelastic flutter. It is premature, therefore, to consider tonal wing sounds as signals, unless we can experimentally arrive at two conclusions: first, that these elements are critical for conveying alarm-related information (see Hingee and Magrath, 2009) and, second, that those elements are produced by feathers that are specialized (i.e. co-opted) specifically for this purpose. While this first line of evidence must be purely behavioral in origin, the second will largely rely on morphological and mechanistic investigations of feather structure and function which we have attempted to elucidate in this study.

In order to better understand the role that tonal wing sounds could play in communication, we investigated the link between unique feather morphologies and tonal sound production in the primary feathers of both male and female Rock Pigeons (*Columba livia*). First, we quantified variation in gross feather shape between male and female rock pigeons to determine whether or not a link between sexually-selected displays and sound-production could exist, as is common among other species (Prum, 1998). We then examined several characteristics of feather barbs which are known to influence feather shape and stiffness (Feo and Prum, 2014; Feo et al., 2015), two characteristics which are associated with aeroelastic flutter and sound-production (Clark et al., 2013b; Clark et al., 2013a). Finally, we experimentally tested the necessity of particular feather morphologies for natural, *in vivo* sound production, and the sufficiency of individual feathers to reproduce *in vivo* sounds in laboratory simulations of flapping wings.

MATERIALS AND METHODS

Feather morphology

The five outermost primary feathers (P10-P6; Fig. 1a) in 10 male and 10 female study skins from the Burke and Slater Museums of Natural History were photographed and digitally measured (Bachmann, et al. 2007) using tpsDig software (v.2.17, Rohlf, 2013). For each feather, the depth of the outer and inner vanes was measured every tenth percent of the vane length (Fig. 1b). Measurements of vane depth were normalized by the length of the vane for each feather (as per Bachmann et al., 2007).

In five additional birds (see Testing Sufficiency below), two primary feathers (P10 and P09) were removed from the wing and photographed. For each of these feathers, the barb length, distal barb angle, and proximal barb angle on the inner vane were digitally measured (as above) at six points along the rachis (Fig 1c). Measurements of barb length were also normalized by the length of the feather vane (as per Bachmann et al., 2007).

Testing Necessity: feather manipulations on live birds

Five birds were tested in outdoor aviaries for their sound-producing abilities. Birds were video and audio recorded during a single release flight as they returned to flock-mates 10m away at the opposing end of an aviary with dimensions 6m x 6m x 15m. High speed video was collected using a Photron FASTCAM SA-3 camera (Photron USA Inc., San Diego, CA, USA; using PFV v.3282 Software) recording at 1000fps with a 1/6000s shutter speed. Audio was recorded to desktop computer at 24-bits and sampling at 96kHz through an audio interface (Raven Pro, v.1.4, Cornell Lab of Ornithology Bioacoustics Research Program, Ithaca, NY, USA) and preamplifier (Roland QUAD-CAPTURE UA-55, Roland Corporation, Hamamatsu, Japan) using a

Sennheiser ME67 shotgun microphone (Sennheiser Electronic, Wedemark, Germany). High speed video and audio were trigger-synchronized using an ART AVDirect converter box (Applied Research and Technology, Inc., Rochester, NY, USA) to convert a TTL (transistor-transistor logic) trigger pulse input into an audio signal which was recorded on a second channel using the previously-mentioned recording set-up. This trigger-synchronization process creates a repeatable 3.9ms delay in the audio signal, which, along with a minor sound lag due to distance, was accounted for in our analyses. Birds were then recaptured and released individually into a separate aviary (of the same dimensions as above) where they were audio recorded during 6-18 consecutive escape flights motivated by a pursuing researcher. Audio recordings of these escape flights were collected continuously using the abovementioned microphone and a portable 24-bit Marantz PMD661 field recorder (Marantz America, Inc., Mahwah, NJ, USA) sampling at 96kHz and were analyzed using Raven Pro software (as above).

Birds were then recaptured and an aerosol plastic polymer fixative (i.e. hairspray; TRESemmé TRES Two® Freeze Hold Hair Spray, Godefroy Manufacturing Company, St. Louis, MO, USA) was applied to a 5cm-long region on P10 (identified in feather morphology analyses mentioned above) on both wings. The fixative was allowed to dry for approximately 5 minutes. Each treated bird was then video and audio recorded during a single flight (as above). Treated birds were then recaptured and released into a solitary aviary and audio recorded (as above) during 9-14 consecutive escape flights motivated by a pursuing researcher.

Testing Sufficiency: laboratory experiments on isolated feathers

Three primary feathers (P10, P9 and P1) were removed from five deceased rock pigeons (donated salvage from MT, OR, WA) and spun on a brushless DC motor (BL3056 Series Motor, BPMC Technology Ltd., Tsuen Wan, Hong Kong) using a Luminary Micro Stellaris BLDC Motor Control Module (MDL-BLDC, Luminary Micro/Texas Instruments, Austin, TX, USA). High speed video of spinning feathers was collected using a Photron FASTCAM SA-3 camera recording at 3000 fps with a 1/6000s shutter speed. Audio was recorded from a distance of 2m using the previously mentioned microphone to a desktop computer and pre-amplifier, as above, at 24-bits and sampling at 96kHz.

Feathers were spun at 0° angle of attack (α) at two biologically relevant velocities that were calculated from high speed video of a single bird in a controlled, horizontal flight from perch to perch motivated by a pursuing researcher (Crandell and Tobalske, 2011). Average wing-tip velocity (11.4 m s^{-1}) and peak wing-tip velocity (16.2 m s^{-1}) were calculated from the dowstroke of the third wing-beat after take-off as per methods detailed in Crandell and Tobalske (2011). Wing-tip velocities were then converted into average and peak angular velocities (38.1 rad s^{-1} and 53.9 rad s^{-1}, respectively), and rotational frequencies (r.p.m.) were calculated for each feather given its length. This flapping wing model assumes that each feather is placed at the tip and leading edge of the wing during downstroke in spite of the fact that P10 and occasionally P9 (when P10 molts) are the only feathers that occur in this position *in vivo*. Feathers were tested at low rotational frequencies first (i.e. average wing-tip velocity before peak wing-tip velocity) to avoid potential hysteresis complications from feather flutter at higher frequencies. P10 feathers that did not flutter (i.e. activate) at peak wing-tip velocities were then spun faster until activation occurred. These activation velocities (U*) were within 10-12% of the peak wing-tip velocities – a difference which can easily be accounted for by biologically relevant variation in flight motivation (life-threatening take-off vs. casual take-off), wing span, and/or body mass (Berg and Biewener, 2010).

Spinning feathers were mounted on a custom-built force plate (15x15 cm, Bertec Corp., Columbus, OH, USA) to measure vertical force along the y-axis and torque about the z-axis due to drag (Crandell and Tobalske, 2011; Usherwood, 2009). The voltage output from the force plate was amplified (10x digital gain, Bertec amplifier, model M6810) before being converted with an ADInstruments PowerLab 8SP A/D converter sampling at 1000Hz and imported to a desktop computer using LabChart v5.2 software with a 1Hz low-pass digital filter (ADInstruments Inc., Colorado Springs, CO, USA) as per methods detailed in Crandell and Tobalske (2011). Data from the force plate were converted into dimensionless coefficients of vertical (C_v) and horizontal (C_h) forces following Crandell and Tobalske (2011) and Usherwood and Ellington (2002) assuming an air density of 1.07kgm^{-3} (for Missoula, MT, USA), and were expressed together as the resultant coefficient of force (C_R; C_v+C_h=C_R).

Statistical Analyses

Statistical analyses were performed using SPSS (v.17.0, Polar Engineering and Consulting, Nikiski, AK, USA) and Excel (v.14.0, Microsoft Corporation, Redmond, WA, USA) software. To test for differences in vane depths between male and female rock pigeons we used two-way ANOVAs to determine the effects of sex at a given position along the rachis for each vane on each feather. To test for differences between barb angles (distal and proximal angles separately) between feathers we used two-way ANOVAs to determine the effects between feathers and positions along the rachis. Independent samples t-tests were used to analyze specific differences between feathers at a given position along the rachis. To test for differences between coefficients of resultant force between angular velocities in different feathers, we used paired samples t-tests. Herein we report means ±s.d.

RESULTS

Feather Morphology

Across the five outermost primary feathers (P10-P6; Fig 1a) in 10 male and 10 female Rock Pigeons, there were no significant differences in vane depths (Fig 1b) at any point along any feather between males and females (Fig 2; all $p>0.5$). The inner vane (IV) of all P10 feathers showed slight attenuation around 60% of the vane length (Fig 2). This was consistent with analyses performed by Bachmann et al. (2007). Barb measurements (Fig 1b, c) from the IV of P10 showed that this area of attenuation possesses barbs that are between 14% and 30% longer than barbs in adjacent regions of the same feather, in spite of the fact that vane depths exhibit a distinct narrowing in this region (Fig 3). Analyses of barb angles revealed that this increase in barb length concurrent with a narrowing of vane depth is due to significant changes in the distal barb angle but not in the proximal barb angle (Fig 4) within the attenuated region. Specifically, P10 possesses barbs with a distal angle that is significantly more acute (i.e. more parallel to the rachis) at 40%, 50%, and 60% (all $p<0.05$) and significantly more obtuse (i.e. more perpendicular to the rachis) at 70% ($p=0.01$) than barbs in the same region on P9. In contrast, P10 and P9 feathers have similar distal barb angles at other points along the rachis (20% and 80%; both $p>0.5$).

Testing the necessity of P10 for sound production in live birds

Upon determining that P10 feathers possess unique barb morphology in their IV, we tested the necessity of this region of the feather for natural wing-sound production in live birds. Three of five birds produced tonal sounds in 100% of flights (N = 18, 14, and 12 flights per bird) prior to feather manipulations. Two other birds produced tonal sounds in 83 and 31% of flights (N =

6, 13 flights per bird, respectively) prior to manipulations. Following the application of an aerosol plastic polymer fixative (i.e. hairspray, see Methods) to the small target region of P10 (see Feather Morphology), the tonal aspect of wing-sounds was eliminated in 100% of flights (Fig 5) in four birds (N = 14, 13, 10, 9 flights per bird; supplementary material Audio 1). The remaining individual produced slightly fewer wing sounds with tonal elements (83%; N = 12 flights) but see Discussion.

Qualitative comparisons of high speed video of test flights pre- and post-manipulation suggested that the application of the fixative to the small region of the IV on P10 did not significantly alter the birds' flight kinematics. High speed video synchronized with audio recordings revealed that the tonal aspect of unmanipulated flight sounds occurs throughout the latter 2/3 of downstroke, and not during the upstroke (Fig 6). Analysis of synchronized video and audio also revealed that the broadband "clap" aspect of pre- and post-manipulation flight sounds occurs at the end of the upstroke and is caused by dorsal wing-to-wing contact (Crandell and Tobalske, 2015; Fig 6).

Testing the sufficiency of individual feathers to replicate *in vivo* tones

Using measurements gathered from high speed video recordings of birds with unmanipulated wings, we spun feathers on a motor to simulate the angular velocities experienced by individual feathers during downstroke. P10 feathers that were spun at the average angular velocity of downstroke (38.1 rad s^{-1}) never produced tonal sounds and never fluttered. Three of the five P10 feathers we tested produced tonal sounds and fluttered at peak angular velocities (53.9 rad s^{-1}). The remaining two P10 feathers produced tonal sounds and fluttered when spun at a biologically plausible speed 10-12% faster than peak angular velocity (up to 60.3 rad s^{-1}). All tones produced by P10 feathers had a fundamental frequency of approximately 500Hz (480±20Hz; N = 5), while *in vivo* wing sounds (from the abovementioned captive birds) had frequencies between 650 and 750Hz (700±50Hz; N = 24). Flutter in all P10 feathers occurred in the region of the IV identified in the abovementioned morphological investigations, but also occurred, at comparatively smaller amplitudes, more proximally on the IV (supplementary material Video 1).

P9 feathers never produced tones and never fluttered when spun at average or peak angular velocities. Additionally, P1 feathers never produced pure tonal sounds, but consistently fluttered at peak angular velocities and occasionally and sporadically at average velocities. Flutter in P1 feathers was always chaotic (i.e. non-limit cycle) and often resulted in barb separation at one or multiple points in both the IV and OV.

In order to determine how flutter influences the aerodynamic performance of a feather, we measured the vertical and horizontal forces produced by individual, spinning feathers at average angular velocities and at the velocity required for flutter to activate in P10 (i.e. activation velocity for P10; U*). The activation velocity for three of five P10 feathers was at or slightly below the calculated peak angular velocity, as previously mentioned. Two P10 feathers, required higher-than-peak angular velocities to activate (within 12% of peak; up to 60.3 rad s^{-1}). Activated P10 feathers had significantly lower coefficients of resultant force (C_R) than inactive (i.e. not fluttering; at average angular velocity) P10 feathers (t=9.12, df=4, p=0.001; Fig 7). This difference in force production was not observed in P9 and P1 feathers when spun at average angular velocity and peak or U* velocity (P9: t=0.92, df=4, p=0.63; P1: t=-0.11, df=4, p=0.92; Fig 7).

DISCUSSION

Morphological investigations of the outer primaries on Rock Pigeons revealed one region of the outermost feather (P10) that may be specialized for sound production in both sexes (Figs. 2-4). This small, 5-cm-long region of P10 (between 50 and 70% of IV length) has barb characteristics that decrease its stiffness and promote aeroelastic flutter, which is necessary for the production of tonal sounds during flight. P10 feathers that were stiffened with a temporary fixative (i.e. hairspray) were effectively silenced (Fig. 5) in all the birds we tested except one which had accidentally crimped its feather during the drying process. This crimped feather produced tones, but with fewer or no harmonics and at a different frequency than all the other individuals we tested. Preliminary tests of hairsprayed and unmanipulated feathers in an aeroacoustic wind tunnel revealed that the fixative successfully prevents flutter in the target region of P10, but allows flutter elsewhere in the vane, providing further support for our conclusion that this region has been co-opted to promote flutter (supplementary material Video 2).

Flutter in this specialized region of P10 is sufficient on its own to nearly replicate the tonal sounds produced *in vivo*. We determined that the velocity at which flutter activates (U*) in P10 occurs at or around (i.e. within 12%) the peak velocity of wing-tips during downstroke in take-off in live birds. This is corroborated by synchronized kinematic and audio data which suggests that tonal wing sounds only occur during downstroke (latter 2/3) and during take-off (Fig. 6), when wing-tip velocity is above U*, and not during steady, level flight. The wing-tip velocities we modeled in these experiments are somewhat higher than those reported in other kinematic investigations of rock pigeon take-off (Crandell and Tobalske, 2011), which is reasonable considering that preliminary observations of behavior and tonal sound production in wild rock pigeons suggested that tones were most commonly produced during high-speed take-off events and less commonly during casual flight (R.L. Niese, unpublished). The two P10 feathers that required slightly higher than peak angular velocities to activate (up to 60.3 rad s^{-1}; wing-tip velocities up to 18.1 m s^{-1}) are still well within biologically relevant boundaries for rock pigeons (Berg and Biewener, 2010). These same peak and average angular velocities were insufficient to produce tones in the other feathers we tested, suggesting that P10 is more susceptible to aeroelastic flutter – a trait that we attribute to the barb characteristics of its inner vane. Because of this intrinsic link to high-powered downstroke, tonal wing sounds could be a cue for discerning different forms of take-off (e.g. alarmed or non-alarmed) as has been shown for crested pigeons (*Ocyphaps lophotes*) in Australia (Hingee and Magrath, 2009b).

The tones produced by individual P10 feathers under laboratory conditions had a peak fundamental frequency around 500Hz while *in vivo* tonal sounds had peak fundamental frequencies around 700Hz. These differences in frequencies could easily be explained by differences in spectrogram window size between time-invariant laboratory recordings (larger sample window) and temporally variable *in vivo* flights (smaller sample window). Alternatively, the adjacent P9 may either aerodynamically or structurally couple to P10 to modify its sound production (Clark, 2014).

Our laboratory experiments on individual feathers also revealed that flutter in P10 significantly reduces the coefficient of resultant forces (C_R) of the feather in both the horizontal (C_h) and vertical (C_v; Fig. 7). At these same velocities, P9 and P1 feathers showed no significant change in C_R from average velocities. This suggests that, while P10 may more easily enter stable oscillations, those oscillations may reduce the overall aerodynamic activity of the feather. This reduction in aerodynamic activity could suggest that P10 feathers have been co-opted for sound production at the cost of aerodynamic performance. Further research is needed to fully understand how flutter influences aerodynamic performance and whether or not this cost to take-off efficiency is evolutionarily viable in the context of alarm signals that are produced by fleeing.

Our morphological and functional investigations of primary feathers in rock pigeons revealed a subtle, yet critically important morphology for the production of tonal wing sounds during high-speed take-off. These types of wing sounds have been implicated as signals of alarm in the past (Barrera et al., 2011; Hingee and Magrath, 2009b; Townsend, 1915), but discerning them from incidentally produced sounds of locomotion has proven difficult and consequently has impeded many conclusions about their function as signals. Providing a link between a morphology that is apparently specialized for sound-production at the expense of aerodynamic performance allows us to conclude that tonal wing-sounds could indeed be non-incidental. The significance of these tones, while possibly linked to alarm, has yet to be experimentally investigated in this species.

Acknowledgments

We thank Heather Labbe for assistance with animal care and use, the Slater Museum for donating pigeon specimens for destructive sampling, and Peter Wimberger for supporting the feather morphology portion of this research.

Competing interests

The authors declare no competing or financial interests.

Author contributions

Both authors were involved in the research design, interpretation of findings and preparation of the manuscript. R.L.N. additionally analyzed the data.

Funding

Morphological studies funded by the University of Puget Sound Undergraduate Research Grant. Remainder funded by the National Science Foundation [IOS-0919799, CMMI 1234737].

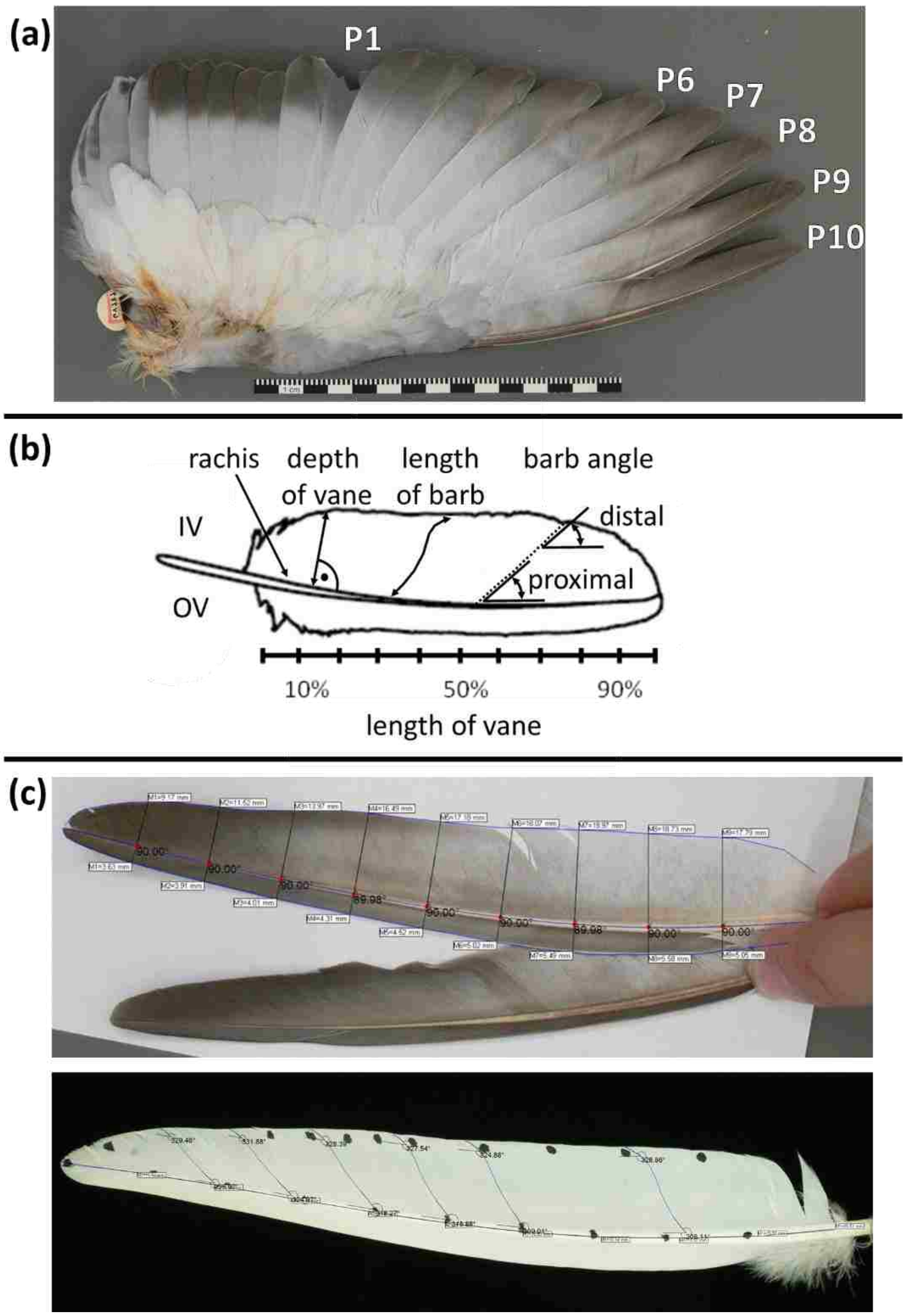

FIGURE 1. Feather location on the wing and measurements taken on each feather. (a) A typical wing of *Columba livia*. The six sampled feathers are indicated. (b) Summary of the types of measurements taken in feathers. OV = outer vane; IV = inner vane. Vane depths were measured on both the OV and the IV, while barb measurements were only taken from the IV.

Distal barb angles are measured relative to the rachis, as in proximal barb angles. (c) Example digital measurements of P9 feathers. Top = vane depths; bottom = barb measurements.

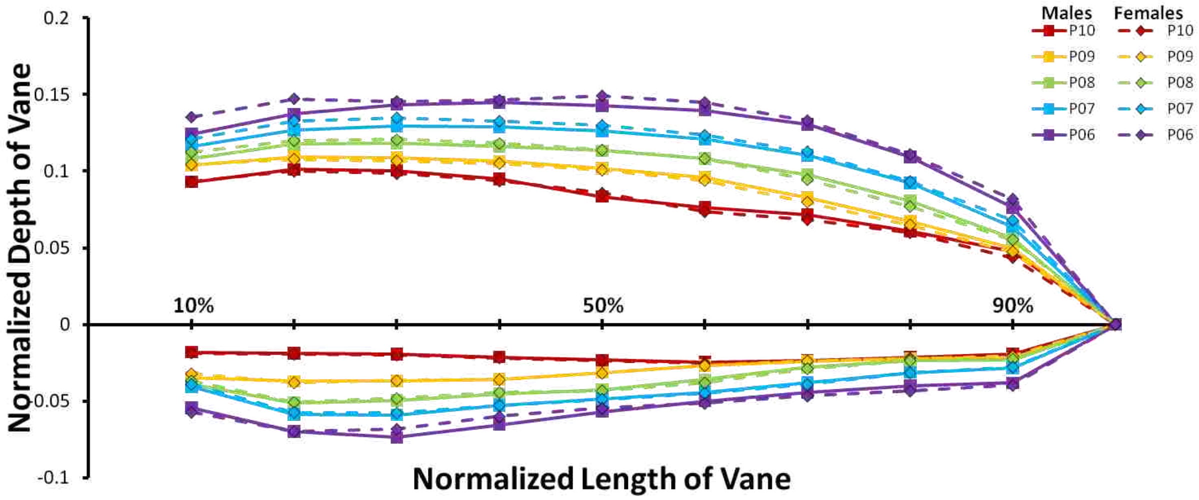

FIGURE 2. Mean normalized vane depth at every 10% of vane length for five feathers (P10-P6) of male and female Rock Pigeons. The x-axis represents the rachis (calamus towards the origin; feather tip at 100%) with measurements every 10% of the vane. Positive values are inner vane (IV) depths. Negative values are outer vane (OV) depths. Dashed lines and diamonds represent females. Solid lines and squares represent males. N=10 for each point. Error bars removed for clarity. Vane depths are not significantly different between males and females at any point in any feather (all p>0.5).

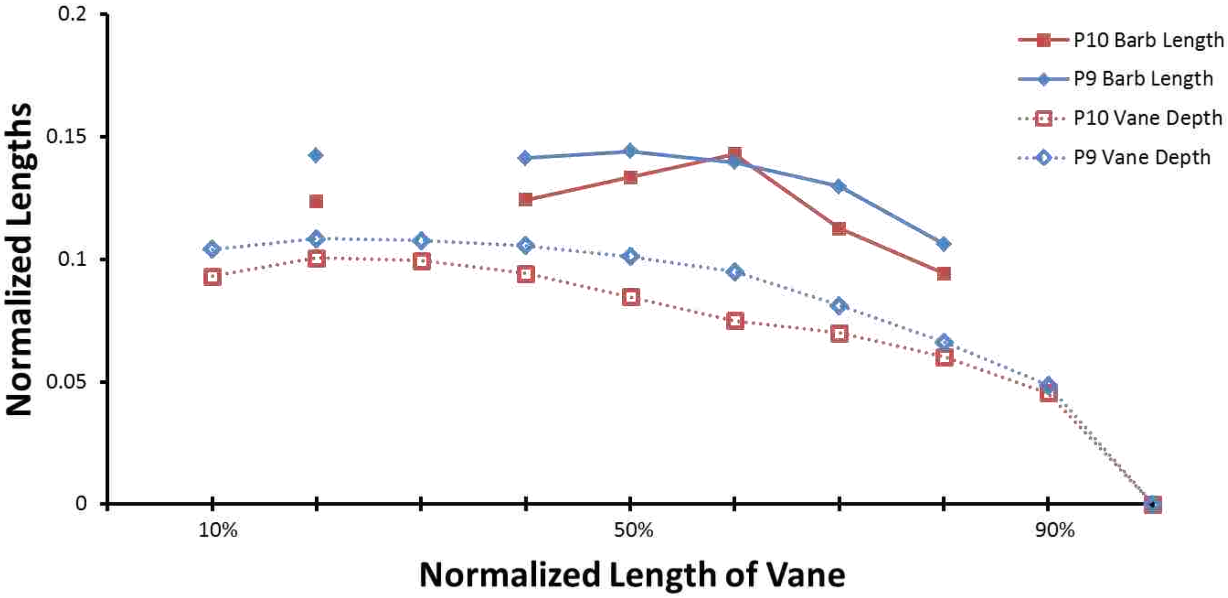

FIGURE 3. Vane depths (dashed lines, open markers) in P10 and P9 as compared to their barb lengths (solid lines, closed markers). Red squares are P10 feathers; blue diamonds are P9 feathers. For vane depths, N=20 for each point. For barb lengths, N=5 for each point. All measurements are normalized by the length of the vane. At the point of attenuation in P10 (at 60% of the vane length), barbs are 15% longer than more proximal barbs (at 40% of the vane length) and 30% longer than more distal barbs (at 70% of the vane length). In the same region on P9, barbs are approximately the same length as more proximal barbs, and 8% longer than more distal barbs.

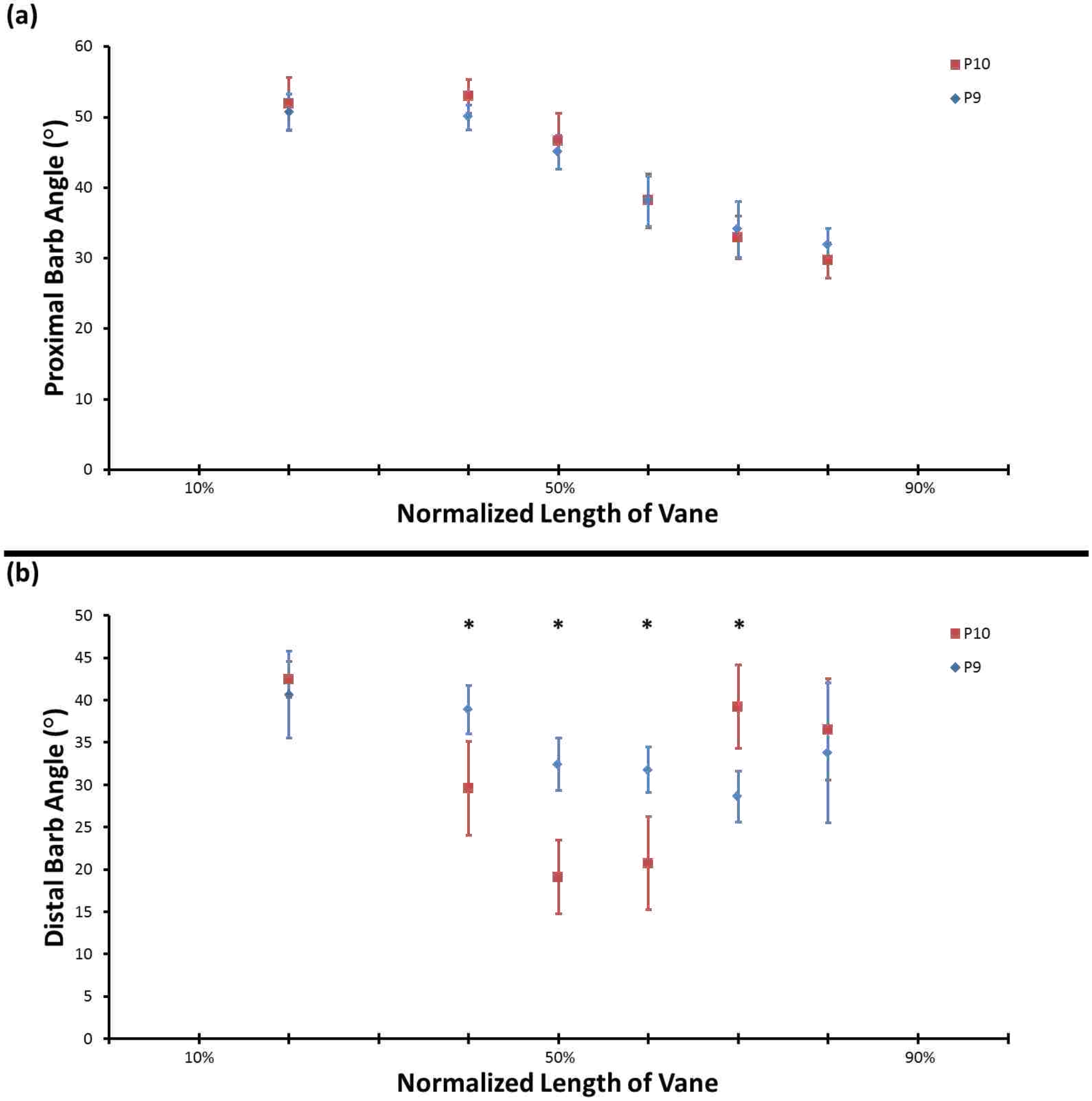

FIGURE 4. Barb angles measured proximally (a) and distally (b) to the rachis. Red squares are P10 feathers; blue diamonds are P9 feathers. N=5 for each point, ±s.d. (a) Proximal barb angles vary significantly at different points along any given feather (F=66.9, df=5,47, p<0.001), but, between P10 and P9 feathers, proximal angles are statistically similar (F=0.19,df=1,47, p=0.66) and vary along the rachis in similar ways (F=0.73, df=5,47, p=0.60). (b) The way that distal barb

angles vary at different points along the rachis is different between P10 and P9 (F=7.44, df=5,47, p<0.001). Distal barb angles are significantly more acute (more parallel to the rachis) in P10 than in P9 at 40%, 50%, and 60% of the vane length (indicated by asterisks; all p<0.05). Distal barb angles are significantly more obtuse (more perpendicular to the rachis) in P10 than in P9 at 70% of the vane length (indicated by an asterisk; t=3.32, df= 7, p=0.01). Distal barb angles at 20% and 80% of the vane length are not significantly different between P10 and P9 (all p>0.5).

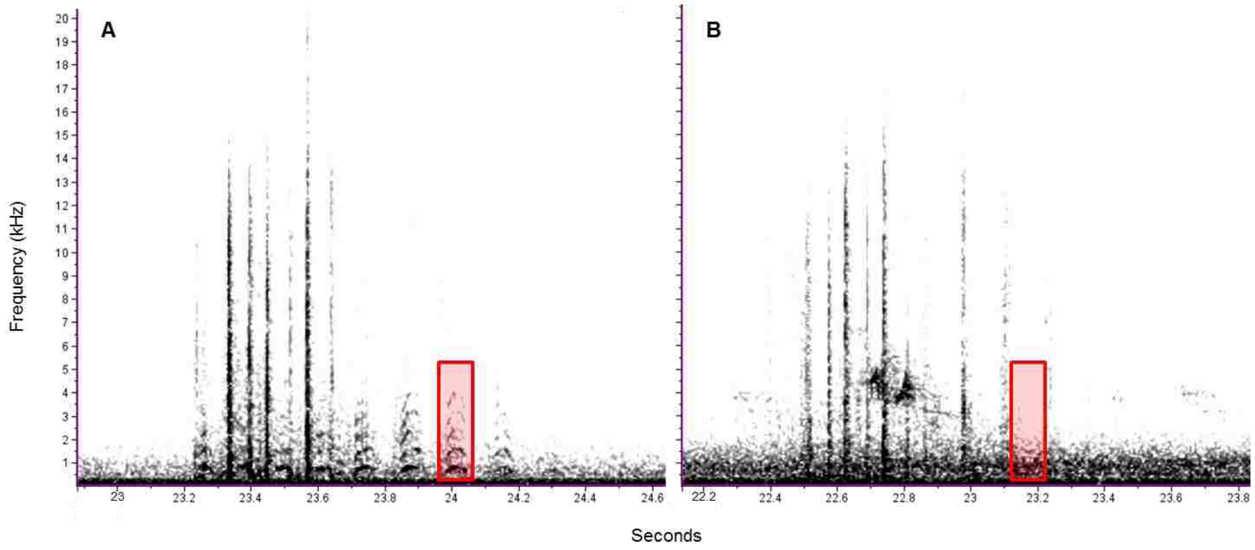

FIGURE 5. Take-off flights of a captive Rock Pigeon (Columba livia) in response to a pursuing researcher before (A) and after (B) a fixative was applied to the outermost primary feather (P10). Red highlighted region notes the presence of tonal elements in wing sounds prior to manipulation and the absence of tonal elements after manipulation. Tonal elements in A have a fundamental frequency around 0.65 kHz and up to five harmonics. Vertical, broadband sounds are wing claps in both A and B. In B, the 4.5 kHz tonal sound between 22.7 and 22.9s is a House Sparrow (*Passer domesticus*) call, not a tonal element of Rock Pigeon wing sounds. See supplementary material Audio 1.

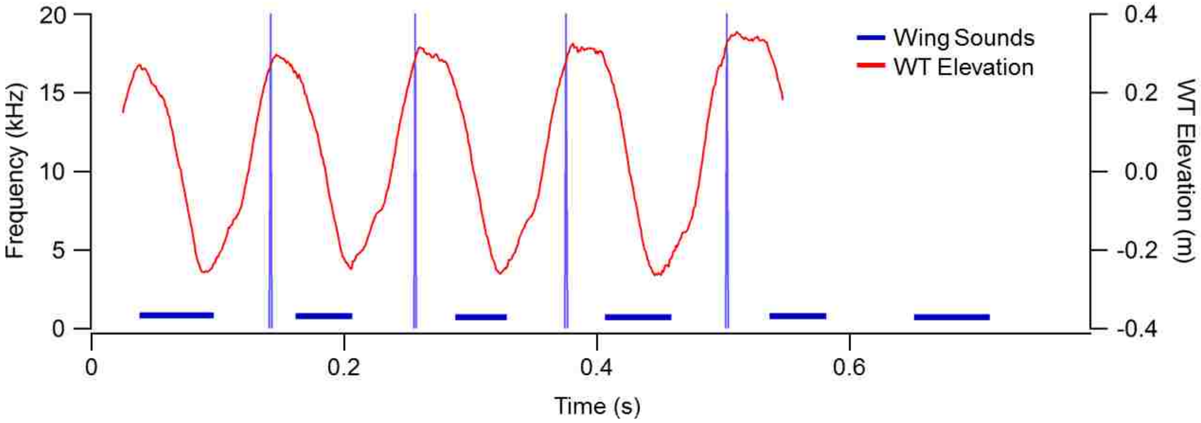

FIGURE 6. Synchronized audio and high speed video recordings of a Rock Pigeon (Columba livia) during the first six wingbeats following alarmed take-off from a perch. Atonal, broadband elements of wing sounds (blue vertical lines) occur at the end of the upstroke and tonal elements of wing sounds (blue horizontal lines) occur throughout the downstroke. Wing-tip elevation indicated by red lines. Wing sounds indicated by blue lines. Tonal elements of wing sounds have a fundamental frequency around 0.7 kHz with up to three harmonics. Harmonics removed for clarity.

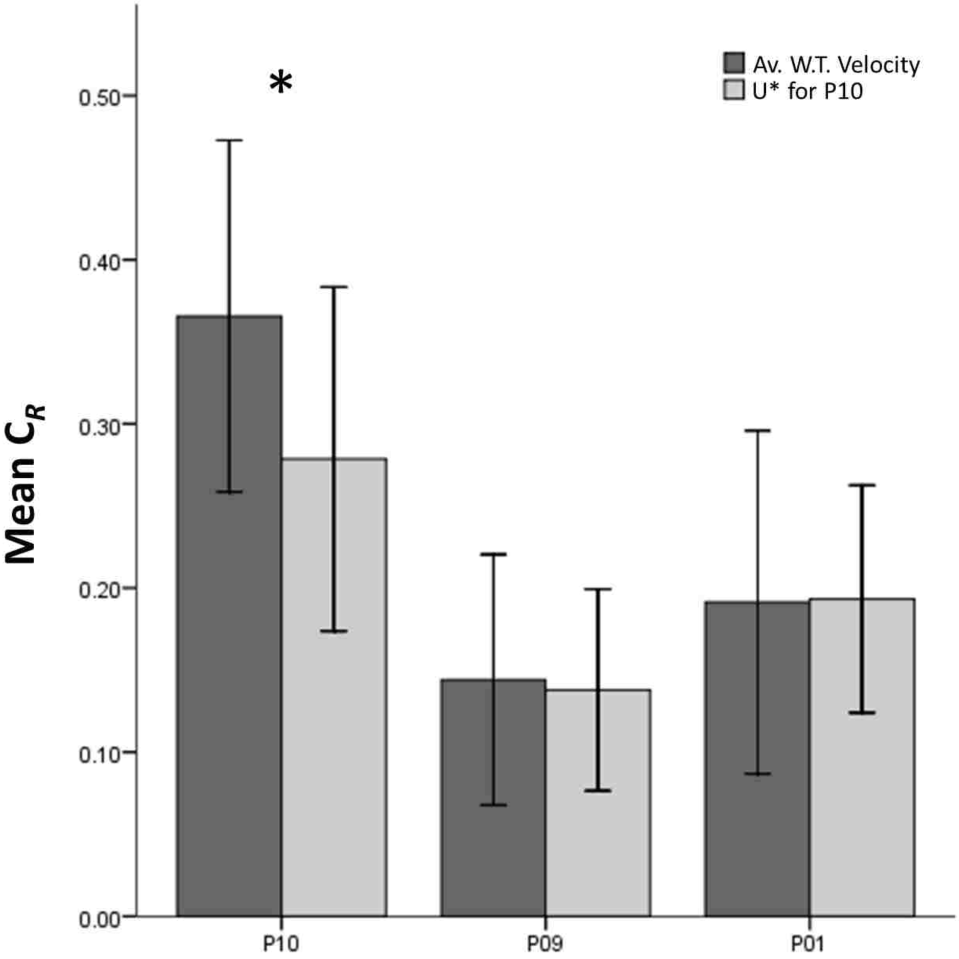

FIGURE 7. Mean coefficient of resultant aerodynamic force (CR) production of spinning Rock Pigeon (Columba livia) feathers at two velocities. Dark bars represent C_R values for feathers spun at average angular velocity (38.1 rad s^{-1}) and light bars represent C_R values for feathers spun at the angular velocity at which P10 begins to flutter (i.e. U*; between 53.9 rad s^{-1} and 60.3 rad s^{-1}). P10 has significantly lower C_R values at U* than at average angular velocities (indicated by an asterisk; t=9.12, df=4, p=0.001). P9 and P1 feathers showed no significant change in C_R between the two velocities (t=0.92, df=4, p=0.63; t=-0.11, df=4, p=0.92; respectively). N = 5 for each bar ± s.d.

SUPPLEMENTAL MEDIA FILES:

Video 1. P10 feathers do not flutter or produce tones at the average angular velocity of downstroke (38.1 rad s^{-1}). (Filmed at 3000 frames per second; audio played-back real time; video on loop). P10 feathers begin to flutter and produce tones at or slightly above the peak angular velocity of downstroke (53.9-60.3 rad s^{-1}). (Filmed at 3000 frames per second; audio played-back real time; tone frequency of 500Hz; video on loop). P9 feathers never produced tones.

Captions:

"Rock Pigeon P10 feathers do not flutter or produce tones at the average angular velocity of downstroke (38.1 rad s^{-1})"

"filmed at 3000 frames per second; audio played-back real time; (video on loop)"

"P10 feathers begin to flutter and produce tones at or slightly above the peak angular velocity of downstroke (53.9-60.3 rad s^{-1})"

"filmed at 3000 frames per second; audio played-back real time; tone frequency of 500Hz; (video on loop)"

Video 2. P10 in a wind tunnel where flow velocities mimic the average wing-tip velocity of downstroke (11.4 m s^{-1}) and peak wing-tip velocity of downstroke (16.2 m s^{-1}) both before and after the application of an aerosol fixative. Flutter occurs primarily in the region of P10 identified in our morphological investigations (see text) between 50 and 70% of the inner vane length. The feather tip is just out of view in the bottom left corner of each video. Video recorded at 6000 fps in four conditions: 11.4 m s^{-1} without hairspray (no flutter; no tones); 16.2 m s^{-1} without hairspray (flutter and tones); 11.4 m s^{-1} with hairspray (no flutter; no tones); 16.2 m s^{-1} with hairspray (no flutter; no tones).

Captions:

"P10 in a wind tunnel where flow velocities mimic the average wing-tip velocity of downstroke (11.4 m s^{-1}) and peak wing-tip velocity of downstroke (16.2 m s^{-1}) both before and after the application of an aerosol fixative."

"Flutter occurs primarily in the region of P10 identified in our morphological investigations (see text) between 50 and 70% of the inner vane length. The feather tip is just out of view in the bottom left corner of each video. Video recorded at 6000 fps."

"11.4 m s^{-1} without hairspray; (no flutter; no tones)"

"16.2 m s^{-1} without hairspray; (flutter and tones!)"

“11.4 m s^{-1} with hairspray; (no flutter; no tones)”

“16.2 m s^{-1} with hairspray; (no flutter; no tones)”

Audio 1. (Audio corresponds to Figure 5 of the text)

REFERENCES

Appel, H. M. and Cocroft, R. B. (2014). Plants respond to leaf vibrations caused by insect herbivore chewing. *Oecologia* 1257–1266.

Audubon, J. J. (1831). *Ornithological Biography: An Account of the Habits of the Birds of the United States of America*. Philadelphia, PA: Carey and Hart.

Bachmann, T., Klän, S., Baumgartner, W., Klaas, M., Schröder, W. and Wagner, H. (2007). Morphometric characterisation of wing feathers of the barn owl *Tyto alba pratincola* and the pigeon *Columba livia*. *Front. Zool.* **4**, 23.

Bahr, P. H. (1907). On the "Bleating" or "Drumming" of the Snipe (*Gallinago cœlestis*). *Proc. Zool. Soc. London* **77**, 12–35.

Barrera, J. P., Chong, L., Judy, K. N. and Blumstein, D. T. (2011). Reliability of public information: Predators provide more information about risk than conspecifics. *Anim. Behav.* **81**, 779–787.

Berg, A. M. and Biewener, A. A. (2010). Wing and body kinematics of takeoff and landing flight in the pigeon (*Columba livia*). *J. Exp. Biol.* **213**, 1651–1658.

Blake, W. (1986). *Mechanics of flow-induced sound and vibration*. New York, NY: Academic Press.

Bostwick, K. S. (2006). Mechanisms of feather sonation in Aves: unanticipated levels of diversity. *Acta Zool. Sin.* 68–71.

Bostwick, K. S. and Prum, R. O. (2003). High-speed video analysis of wing-snapping in two manakin clades (Pipridae: Aves). *J. Exp. Biol.* **206**, 3693–3706.

Bostwick, K. S., Elias, D. O., Mason, A. and Montealegre-Z, F. (2010). Resonating feathers produce courtship song. *Proc. Biol. Sci.* **277**, 835–41.

Budelmann, B.-U. (1989). Hydrodynamic Receptor Systems in Invertebrates. In *The Mechanosensory Lateral Line* (ed. Coombs, S., Görner, P., and Münz, H.), pp. 607–631. New York, NY: Springer New York.

Budelmann, B. U. (1992). Hearing in Nonarthropod Invertebrates. In *The Evolutionary Biology of Hearing* (ed. Webster, D. B., Popper, A. N., and Fay, R. R.), pp. 141–155. New York, NY: Springer New York.

Clark, C. J. (2008). Fluttering wing feathers produce the flight sounds of male streamertail hummingbirds. *Biol. Lett.* **4**, 341–4.

Clark, C. J. (2011). Wing, tail, and vocal contributions to the complex acoustic signals of courting Calliope hummingbirds. *Curr. Zool.* **57**, 187–196.

Clark, C. J. (2014). Harmonic hopping, and both punctuated and gradual evolution of acoustic characters in *Selasphorus* hummingbird tail-feathers. *PLoS One* **9**, e93829.

Clark, C. J. and Feo, T. J. (2010). Why do Calypte hummingbirds "sing" with both their tail and their syrinx? An apparent example of sexual sensory bias. *Am. Nat.* **175**, 27–37.

Clark, C. J., Elias, D. O. and Prum, R. O. (2011). Aeroelastic flutter produces hummingbird feather songs. *Science (80-.).* **333**, 1430–1433.

Clark, C. J., Elias, D. O., Girard, M. B. and Prum, R. O. (2013a). Structural resonance and mode of flutter of hummingbird tail feathers. *J. Exp. Biol.* **216**, 3404–3413.

Clark, C. J., Elias, D. O. and Prum, R. O. (2013b). Hummingbird feather sounds are produced by aeroelastic flutter, not vortex-induced vibration. *J. Exp. Biol.* **216**, 3395–3403.

Coleman, S. W. (2008). Mourning dove (*Zenaida macroura*) wing-whistles may contain threat-related information for con- and hetero-specifics. *Naturwissenschaften* **95**, 981–6.

Conner, W. E. (2014). Adaptive sounds and silences: Acoustic anti-predator strategies in insects. In *Insect Hearing and Acoustic Communication* (ed. Hedwig, B.), pp. 65–79. Berlin, Heidelberg: Springer Berlin Heidelberg.

Craig, W. (1911). The Expressions of Emotion in the Pigeons. II. The Mourning Dove (*Zenaidura macroura* Linn.). *Auk* **28**, 398–407.

Craig, J. L. (1984). Wing noises, wing slots, and aggression in New Zealand honeyeaters (Aves: Meliphagidae). *New Zeal. J. Zool.* **11**, 195–199.

Crandell, K. E. and Tobalske, B. W. (2011). Aerodynamics of tip-reversal upstroke in a revolving pigeon wing. *J. Exp. Biol.* **214**, 1867–1873.

Crandell, K. E. and Tobalske, B. W. (2015). Kinematics and aerodynamics of avian upstrokes during slow flight. *J. Exp. Biol.* **218**, 2518–27.

Cuvier, G. (1817). *The Animal Kingdom: Arranged According to Its Organisation*. Paris: Wm. S. Orr and Company.

Darwin, C. (1871). *The Descent of Man and Selection in Relation to Sex*. London: John Murray.

Edwards, G. (1743). *A natural history of uncommon birds, and of some other rare and undescribed animals*. London: the Author, at the Royal College of Physicians.

Edwards, G. (1760). *Gleanings of Natural History, Part I*. London: the Author, at the Royal College of Physicians.

Fay, R. (2009). Soundscapes and the sense of hearing of fishes. *Integr. Zool.* **4**, 26–32.

Feo, T. J. and Prum, R. O. (2014). Theoretical morphology and development of flight feather vane asymmetry with experimental tests in parrots. *J. Exp. Zool. Part B Mol. Dev. Evol.* **322**, 240–255.

Feo, T. J., Field, D. J. and Prum, R. O. (2015). Barb geometry of asymmetrical feathers reveals a transitional morphology in the evolution of avian flight. *Proc. R. Soc. B Biol. Sci.* **282**, 20142864.

Fournier, J. P., Dawson, J. W., Mikhail, a and Yack, J. E. (2013). If a bird flies in the forest, does an insect hear it? *Biol. Lett.* **9**, 20130319.

Graham, R. (1934). The silent flight of owls. *J. R. Aeronaut. Soc.* **38**, 837–843.

Hingee, M. and Magrath, R. D. (2009). Flights of fear: a mechanical wing whistle sounds the alarm in a flocking bird. *Proc. R. Soc. B Biol. Sci.* **276**, 4173–9.

Horch, K. (1971). An organ for hearing and vibration sense in the ghost crab *Ocypode*. *Z. Vgl. Physiol.* **73**, 1–21.

Hunter, T. A. (2008). On the Role of Wing Sounds in Hummingbird Communication. *Auk* **125**, 532–541.

Johnston, R. F. (1960). Behavior of the Inca dove. *Condor* **62**, 7–24.

Kolle-Kralik, U. and Ruff, P. (1967). Vibrotaxis von *Amoeba proteus* (Pallas) im Vergleich mit der Zilienschlagfrequenz der Beutetiere. *Protistologica* **3**, 319–325.

Larsson, M. (2014). Self-generated sounds of locomotion and ventilation and the evolution of human rhythmic abilities. *Anim. Cogn.* **17**, 1–14.

Lebret, L. (1958). The "Jump-flight" of the Mallard, *Anas platyrhynchos* L., the Teal, *Anas crecca* L., and the Shoveler, *Spatula clypeata* L. *Ardea* **1**, 68–72.

Maynard Smith, J. and Harper, D. (2003). *Animal Signals*. New York: Oxford University Press.

Prum, R. O. (1994). Phylogenetic analysis of the evolution of alternative social behavior in the manakins (Aves: Pipridae). *Evolution (N. Y).* **48**, 1657–1675.

Prum, R. O. (1998). Sexual selection and the evolution of mechanical sound production in manakins (Aves: Pipridae). *Anim. Behav.* **55**, 977–94.

Roche, B. E., Schulte-Hostedde, A. I. and Brooks, R. J. (1999). Route Choice by Deer Mice (*Peromyscus maniculatus*): Reducing the Risk of Auditory Detection by Predators. *Am. Midl. Nat.* **142**, 194–197.

Rohlf, F. J. (2013). tpsDig v.2.17, digitize landmarks and outlines. Department of Ecology and Evolution, State University of New York at Stony Brook, NY.

Selby, P. J. (1850). The Natural History of Gallinaceous Birds: Columbidae or Pigeons. In *The Naturalist's Library: Ornithology* (ed. Jardine, W., Lizars, W. H., Smith, C. H., and Stewart, J.), London: W. H. Lizars.

Townsend, C. W. (1915). Notes on the Rock Dove (*Columba domestica*). *Auk* **32**, 306–316.

Usherwood, J. R. (2009). The aerodynamic forces and pressure distribution of a revolving pigeon wing. *Exp. Fluids* **46**, 991–1003.

Usherwood, J. R. and Ellington, C. P. (2002). The aerodynamics of revolving wings I. Model hawkmoth wings. *J. Exp. Biol.* **205**, 1547–1564.

Wei, Q., Zhong, S. and Huang, X. (2013). Experimental evaluation of flow-induced noise in level flight of the pigeon (*Columba livia*). *J. Acoust. Soc. Am.* **134**, EL57–63.

Wetmore, A. (1926). Observations on the birds of Argentina, Paraguay, Uruguay, and Chile. *U.S. Natl. Museum Bull.* **133**, 448.

Wilson, A. (1808). *American Ornithology, Vol. III*. New York: Collins & Co.

APPENDIX A

Feather morphologies across Columbidae

The family Columbidae is a diverse clade of approximately 300 species which diverged from a common ancestor and radiated in the late cretaceous (Pereira et al., 2007). Some of the first attempts at taxonomically organizing the clade suggested utilizing the presence of certain kinds of peculiar feathers in the wings (Swainson, 1825), and that trend persisted well into the 20th century (Goodwin, 1983). Here, using modern phylogenetic approaches, I attempt to assess the ancestral states of columbid remex morphologies based on a categorizations that group morphologies based on their presumed developmental and evolutionary bases. Category A includes outermost primary feathers that are relatively long (i.e. higher aspect ratio wings; Fig. 1 A1), that can be pointed (i.e. feather slotting; Fig. 1 A2), or dramatically narrowed/pointed in sonating species (Fig. 1. A3). Category B includes outermost primary feathers that are obviously curved and relatively short (i.e. low aspect ratio wings; Fig. 1 B1), where the outermost (P10) may be substantially shorter than adjacent feathers (P9; Fig. 1 B2) or may be modified as a specialized aerodynamic device (Fig. 1 B3). Lastly, Category C includes modifications to barb morphology such that feathers may possess barbs that are distally curved towards the feather tip and elongated in the trailing vane of some outermost primaries (Fig. 1 C2) or dramatically elongated to produce a distinct protrusion of recurved barbs (Fig. 1 C3). This category also includes feathers that display the inverse of this morphology (i.e. a dramatic shortening of barbs in the same region; Fig. 1 C4) which co-occur in populations of some species of green pigeon (*Treron*), where some individuals have a protrusion and others have a gap, suggesting that the two morphologies my be mediated by similar developmental or genetic pathways.

All of these morphologies are represented in the remiges of birds outside the Columbidae as well, which may inform hypotheses as to their evolution and function. The dramatic narrowing of the tip of an inner primary is seen in the P8 of Crested Pigeons (*Ocyphaps lophotes*; Fig. 1 A3) and in the P9 of male *Mionectes* flycatchers (Kennedy et al., 2018) and the P8 or P7 of *Phoenocircus* cotingas (Clark and Prum, 2015). Attenuated outermost primaries (P10) such as those common in the genus *Ptilinopus* (Fig. 1 B3) and discussed in detail in Chapter 2 are also found in the male Scissor-tailed Flycatcher (*Tyrannus forficatus*; Clark and Prum, 2015), the male Black Scoter (*Melanitta americana*; Doran and Wimberger, unpublished data), and the Lesser Florican (*Sypheotides indicus*; Clark and Prum 2015). Enlarged regions of the trailing vane of inner primaries, such as those in *Columbina* (Fig. 1 C3) and discussed in detail in Chapter 1, can also be found in the P6 of the male Cape Sugarbird (Promerops cafer; Clark, 2018) and in the P7 of the Little Bustard (*Tetrax tetrax*; Clark and Prum, 2015). Indentations in the trailing vane of inner primaries similar to those in the green pigeons (*Treron spp.*; Fig. 1 C4) are also found in the Tui (*Prosthemadera novaeseelandiae*; Craig, 1984).

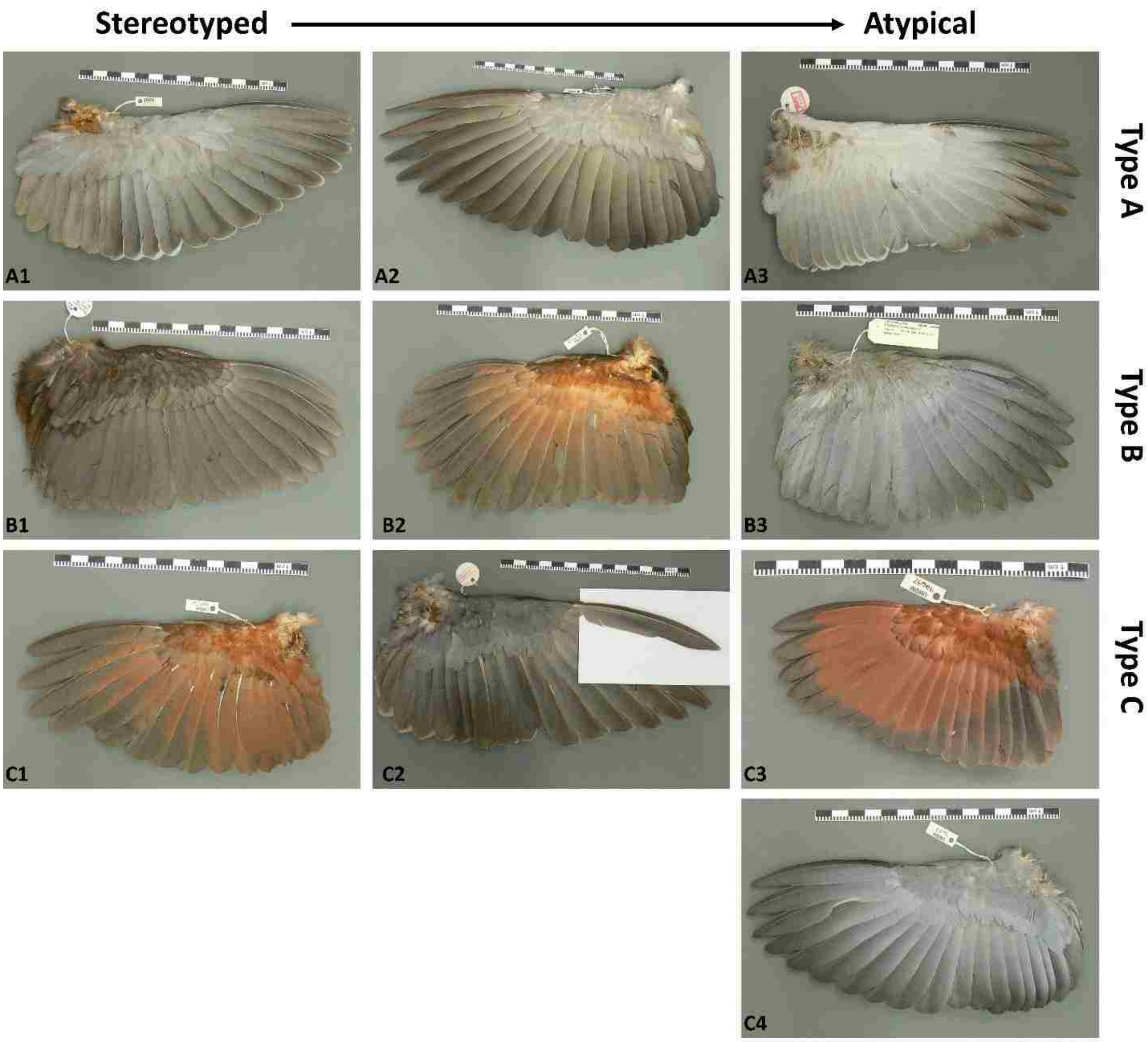

FIGURE 1. Wing specimens representative of various morphotypes. Wings on the left are considered typical, possessing aerodynamically stereotyped morphologies only. Wings on the right are considered atypical, possessing morphologies that may function as specialized aerodynamic devices or as sonation-producing structures. Morphotype numbers do not necessarily imply evolutionary or functional hierarchy, but modified morphologies within a letter category share specific modifications (e.g. tip narrowing in A). Individual feathers are not categorized into multiple morphotypes, but a single species can possess two different atypical

feathers. All stereotyped wings (the first column) are given the same categorical distinction in analyses. (A1) White-winged Dove (*Zenaida asiatica*) outer primaries equal in length, not pointed, and not strongly curved; a stereotyped shape with a relatively high aspect ratio. (A2) Red-knobbed Imperial Pigeon (*Ducula rubricera*) outer primaries pointed or emarginated. (A3) Crested Pigeon (*Ocyphaps lophotes*) inner primaries pointed. (B1) Buff-fronted Quail-dove (*Zentrygon costaricensis*) outer primary somewhat curved; a stereotyped shape with a relatively low aspect ratio wing. (B2) Olive-backed quail dove (*Leptotrygon veraguensis*) outermost primary shortened and curved. (B3) Rarotonga Fruit-dove (*Ptilinopus rarotongensis*) outermost primary shortened and modified in shape. (C1) MacKinlay's Cuckoo-dove (*Macropygia mackinlayi*) outer primaries equal in length, not pointed, and not strongly curved; a stereotyped shape. (C2) Oriental Turtle-dove (*Streptapelia orientalis*) outermost primary with a small region of trailing edge barbs that are elongated and curved. An index card has been inserted between P10 and P9 to view the morphology more clearly. (C3) Common Ground Dove (*Columbina passerina*) inner primaries (P6 to P9) with trailing edge barbs that are elongated and curved. (C4) Pink-necked Green Pigeon (*Treron verans*) inner primaries with trailing edge barbs that are shortened and curved.


P10
P10
unknown
Ptilinopus viridis
Ptilinopus eugeniae
Ptilinopus iozonus
Ptilinopus ornatus
Ptilinopus aurantiifrons
Ptilinopus wallacii
Ptilinopus perlatus
Ptilinopus hyogastrus
Ptilinopus tannensis
Ptilinopus dupetithouarsii
Ptilinopus mercierii
Ptilinopus perousii
Ptilinopus huttoni
Ptilinopus insularis
Ptilinopus chalcurus
Ptilinopus coralensis
Ptilinopus purpuratus chrysogaster
Ptilinopus rarotongensis
Ptilinopus purpuratus purpuratus
Ptilinopus purpuratus frater
Ptilinopus greyi
Ptilinopus porphyraceus
Ptilinopus pelewensis
Ptilinopus richardsii
Ptilinopus roseicapilla
Ptilinopus coronulatus
Ptilinopus regina
Ptilinopus monacha
Ptilinopus pulchellus
Ptilinopus superbus
Ptilinopus rivoli
Ptilinopus solomonensis
Ptilinopus porphyreus
Ptilinopus dohertyi
Ptilinopus cinctus
Ptilinopus melanospilus
Ptilinopus nainus
Ptilinopus luteovirens
Ptilinopus layardi
Ptilinopus victor
Drepanoptila holosericea
Alectroenas sganzini
Alectroenas nitidissima
Alectroenas madagascariensis
Alectroenas pulcherrimus
Ptilinopus leclancheri
Ptilinopus subgularis
Ptilinopus jambu
Ptilinopus fischeri
Ptilinopus occipitalis
Ptilinopus merrilli
Ptilinopus marchei
Ptilinopus bernsteinii
Ptilinopus magnificus
Gymnophaps albertisii
Lopholaimus antarcticus
Hemiphaga novaeseelandiae
Ducula rufigaster
Ducula chalconota
Ducula finschii
Ducula basilica
Ducula cineracea
Ducula lacernulata
Ducula badia
Ducula carola
Ducula radiata
Ducula mindorensis
Ducula poliocephala
Ducula forsteni
Ducula galeata
Ducula oceanica
Ducula aurorae
Ducula pacifica
Ducula myristicivora
Ducula rubricera
Ducula pistrinaria
Ducula whartoni
Ducula rosacea
Ducula pickeringii
Ducula perspicillata
Ducula concinna
Ducula aenea
Ducula zoeae
Ducula latrans
Ducula goliath
Ducula pinon
Ducula melanochroa
Ducula bakeri
Ducula mullerii
Ducula brenchleyi
Ducula luctuosa
Ducula bicolor
Ducula spilorrhoa
Phapitreron amethystina
Chalcophaps stephani
Turtur brehmeri
Oena capensis
Turtur tympanistria
Turtur afer
Turtur abyssinicus
Turtur chalcospilos
Treron calvus
Trugon terrestris
Goura victoria
Henicophaps albifrons
Gallicolumba sanctaecrucis
Claravis pretiosa
Metriopelia aymara
Streptopelia decaocto
Geotrygon chiriquensis

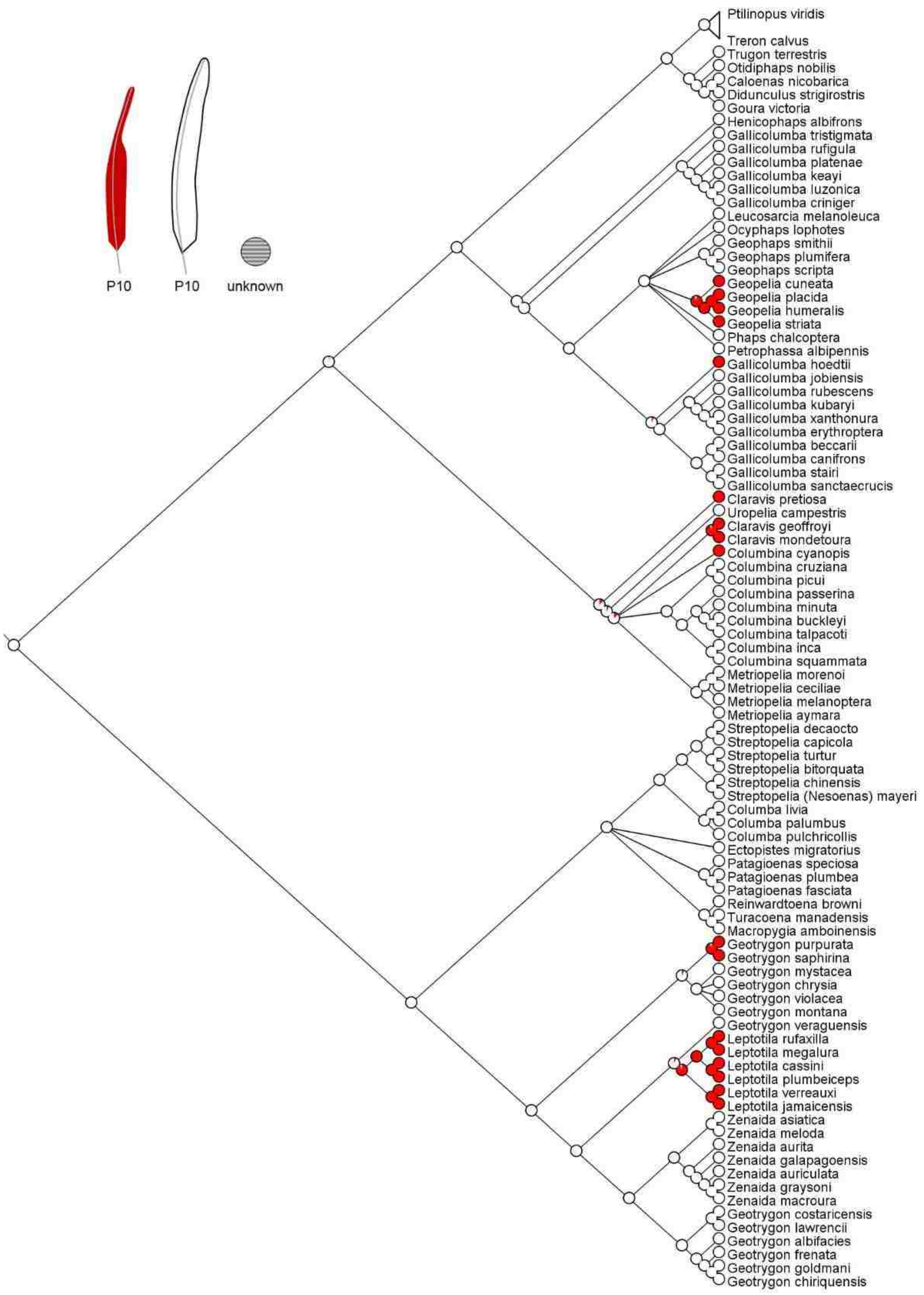

FIGURE 2. Ancestral state reconstructions of the B3 outermost remex morphology across Columbidae. Tree based on the combined nuclear and mitochondrial nucleotide phylogenies published by Cibois et al. (2014; 2017), Johnson and Weckstein (2011), Johnson et al. (2001),

Moyle et al. (2013), Pereira et al. (2007), and Sweet et al. (2017). Maximum likelihood ancestral state reconstructions of the B3 morphotype (atypical P10 morphology) indicate that this morphology has independently evolved at least 16 times and has been lost only once (*Ptilinopus dohertyi*).

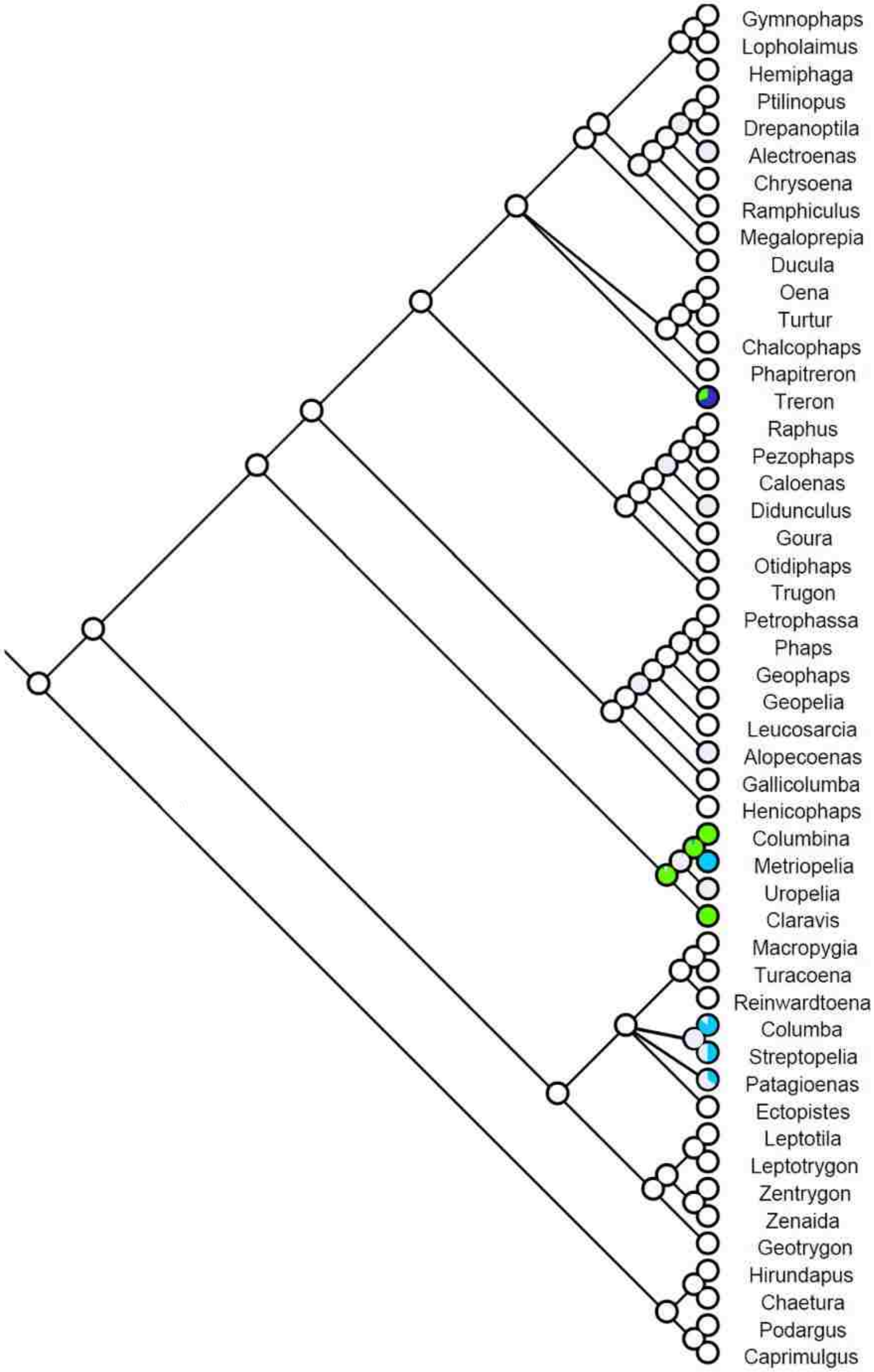

FIGURE 3. Ancestral state reconstructions of Type C barb morphologies among genera in Columbidae. Type C2 is present in *Columba*, *Streptopelia*, *Patagioenas*, and *Metriopelia* (blue).

Type C3 is present in *Columbina*, *Claravis*, and some populations of *Treron* (green). Type C4 is only present in members of the genus *Treron* (purple). Nodes are colored proportionally to represent the likelihood of a given morphology as the ancestral state. Tips are colored proportionally according to the number of species in a genus that possess a given morphology.

REFERENCES

Clark, C. J. (2018). Signal or cue? Locomotion-induced sounds and the evolution of communication. *Anim. Behav.* **143**, 83–91.

Clark, C. J. and Prum, R. O. (2015). Aeroelastic flutter of feathers, flight, and the evolution of nonvocal communication in birds. *J. Exp. Biol.* **218**, 3520–3527.

Craig, J. L. (1984). Wing noises, wing slots, and aggression in New Zealand honeyeaters (Aves: Meliphagidae). *New Zeal. J. Zool.* **11**, 195–199.

Goodwin, D. (1983). *Pigeons and doves of the world*. Comstock Pub. Associates.

Kennedy, J. J., Heavyside, J., Jankowski, J. E., Scholer, M. N., Biological, C. W., Building, S., Tg, A. and Vt, B. C. (2018). Molt patterns and sexing and aging criteria for ten species of high elevation landbirds from Southeastern Peru. *Ornitol. Neotrop.* **29**, 63–74.

Pereira, S. L., Johnson, K. P., Clayton, D. H. and Baker, A. J. (2007). Mitochondrial and nuclear DNA sequences support a Cretaceous origin of Columbiformes and a dispersal-driven radiation in the Paleocene . *Syst. Biol.* **56**, 656–72.

Swainson, W. (1825). On the characters and natural affinities of several birds from Australia; including some observations on the Colulmbidae. *Zool. J.* **1**, 463–484.